Temperature Responsive Polymeric Gels Modified with Gold Nanoparticles

by

Ewa Anna Kazimierska

A Dissertation submitted to the Graduate Faculty in Chemistry in partial fulfillment of the requirements for the degree of Doctor of Philosophy, The City University of New York

2006

This manuscript has been read and accepted for the Graduate Faculty in Chemistry in satisfaction of the dissertation requirements for the degree of Doctor of Philosophy.

04-25-2006	PROFESSOR MALGORZATA CISZKOWSKA
Date	Chair of Examining Committee
04-25-2006	PROFESSOR GERALD KOEPPL
Date	Executive Officer

PROFESSOR RONALD BIRKE

PROFESSOR MICHA TOMKIEWICZ

Supervisory Committee

The City University of New York

Abstract

Temperature Responsive Polymeric Gels Modified with Gold Nanoparticles

by

Ewa Anna Kazimierska

Adviser: Professor Malgorzata Ciszkowska

Preparation and characterization of temperature-responsive N-isopropyl-acrylamide (NIPA) polymeric gels, modified with colloidal gold nanoparticles are described. New methodology for incorporation of gold nanoparticles into gel matrixes to obtain three-dimensional crosslinked polymeric phases with uniformly distributed gold particles was developed. Gold particles of various sizes were synthesized and introduced to NIPA-gels during the free radical polymerization. These modified gels combine characteristics of gold nanoparticles and thermoresponsive polymeric gels. They undergo discontinuous volume phase transition at approximately 32 °C that results in a release of up to 97% of a solvent from the polymeric matrix; this temperature is independent of the presence of gold nanoparticles. These gels exhibit surface plasmon resonance characteristic for colloidal gold particles.

Characterization of gold modified NIPA polymeric gels was performed using electroanalytical methods supported by spectroscopic and optical techniques. Available potential window was determined and transport properties of the gels were studied in terms of diffusion of molecular probes. Main experimental approaches were steady state voltammetry and chronoamperometry with microelectrodes and cyclic voltammetry with regular size electrodes. The UV-vis spectroscopy and transmission electron microscopy were used to determine the size and size distribution of incorporated gold nanoparticles.

Diffusion coefficients of 1,1'-ferrocenedimethanol in swollen gels with and without gold nanoparticles were identical within an experimental error; they were lower than those in solutions without polymeric network. They decreased when an increased weight percentage of a polymer in a gel. These two observations were explained in terms of the "obstruction" and "hydration" effects.

Effects of the volume phase transition of the diffusion properties of the gels and the composition of released liquids were investigated. The diffusion coefficient of 1,1'-ferrocenedimethanol was up to 600 times lower in a collapsed phase than that in a swollen gel. The concentration of the 1,1'-ferrocenedimethanol probe in expelled solutions was up to 30 % smaller than that in swollen gels; the NIPA gel matrix specifically retained this organic probe.

The influence of ionic strength on temperature of the volume phase transition and transport properties of the gels were also investigated.

I dedicate this thesis to my fiancé, Enrico. He has made this experience and all the others in my life something worth doing. He always encouraged me when I was confused and he was so understanding when I was running out of time. With his optimism and faith in me it was easier to finish this work. I hope I can someday reciprocate that patience and perseverance to him.

Acknowledgements:

I would like to extend my thanks to Professor Malgorzata Ciszkowska who has been the guide and advisor throughout my graduate career. I am extremely thankful for her understanding and patience she showed me throughout all the years we worked together. I would also like to thank the members of my committee: Professor Ronald Birke and Professor Micha Tomkiewicz for their time and valuable instruction during my time at Graduate Center.

Many thanks go to Michal with whom I spent long hours in our lab and out of it. I greatly appreciate all the helpful scientific conversations shared with him almost as much as the nonscientific conversations. He was my guide through the secrets of living in New York. I also want to thank Yasemin for her great personality and ability to make me laugh and comfort in difficult moments. Her friendship means a lot to me.

I owe a deep gratitude to my parents for their guidance and constant support throughout my life. They were behind me at every point in my life, even when I didn't really know where I was going and helped to show me where I should always find my direction. And I need to thank my sister Anula, who kept the eye on me when my parents were far.

Table of Contents

List of Tables

List of Figures

I. INTRODUCTION

I. 1. Historical Background

Gold Nanoparticles

The history of colloidal gold nanoparticles can be traced back to 5th century B.C. when it was used to color glasses ("ruby glass") and ceramics. The oldest and perhaps the most famous object containing gold nanoparticles is the Lycurgus Chalice, glass vessel that appears opaque green in reflected light and a wine-red when the light passes through it. [1] Many new developments in applications of gold colloids for the production of dyes for glass and fabrics can be seen presently.

Colloidal gold was found in treatments in alternative medicine Ayurveda (the traditional medical system of India), described in the Vedas, the sacred text of India that is believed to be the oldest writings in the world. [2] Alcohol solutions of colloidal gold were also used as tonics and elixirs. The "soluble" (colloidal) gold in Middle Ages was mainly known as a fabulous cure for such diseases as heart and venereal problems, dysentery, epilepsy, and tumors, and for diagnosis of syphilis. Nowadays colloidal gold is still applied to treat arthritis. [3] Other accounts of colloidal gold are its uses in alchemy by Paracelsus around 1600. [4]

The beginning of the chemistry of gold colloids can be dated to the middle of the nineteenth century, when Michael Faraday reported the formation of deep red solutions of colloidal gold as a result of the reduction of an aqueous solution of chloroaurate ions ($AuCl_4^-$) by white phosphorus in CS_2. [5] The term "colloid" (from the French, *colle*) was introduced shortly thereafter by Graham, in 1861. [6] At the beginning of the 20th century it was Wilhelm Ostwald who first pointed out that the properties of metal particles in the

nanometer range are predominantly determined by surface atoms and he concluded that those nanoparticles, should exhibit novel properties with respect to bulk particles. [7]

Polymeric Gels

The first polymeric hydrogel network was developed by Wichterle and Lim in Czechoslovakia in 1954. [8] It was a copolymer of 2-hydroxyethyl methacrylate (HEMA) and ethylene dimethacrylate (EDMA) and it was designed for use as contact lenses. Due to the lack of interest and support from the appropriate authorities, no success was achieved. Wichterle and Lim, however, continued to work on their development and it was not until the 1960s when the versatility of synthetic polymeric hydrogels was visualised from a commercial point of view.

Gels that swell or contract gradually over time had been known already in 50'. But the history of polymeric hydrogels showing discontinuous volume phase transition can be dated back to 1975, when Tanaka described first synthesis of cross-linked gels that can absorb enough solvent to swell. [9] Soon after that the same group discovered that a small change in solvent concentration or temperature could cause copolymer gel of acrylamide and acrylate to abruptly swell to many times its original size – or collapse into a compact mass. It was a big surprise since the volume phase transition predicted theoretically in 1968 by Dusek and Patterson was believed to never happen. [10] The impossibility of this transformation was due to unreastically high cross-link density in the polymer network required for the volume phase transition as concluded based on modified Flory-Huggins model. [11]

Recently, the unique properties of the gels reacting to external stimuli in a manner reminiscent of living organisms, attracted the attention of chemists and chemical engineers for their potential applications from medicine to robotics.

I. 2. Colloidal Gold Nanoparticles

Colloidal gold nanoparticles has been known and used for centuries but it is only presently that the enormous interest in nanogold particles is observed in the fields of nanotechnology and nanoscale material science. The reason for this renewed interest is due to their ease-of synthesis, chemical and thermal stability and novel properties originating from their quantum scale dimensions. Gold nanoparticles can be classified as intermediates between molecules and bulk material and as that they have properties that are characteristic only at the nanoscale regime. The miniaturization of gold to the nanometer range has dramatic consequences for its physical and chemical properties. Gold colloids are seemingly homogenous mixtures of otherwise immiscible substances. They consist of metal particles that are so tiny that they remain suspended in a liquid phase. Within the years of use, the term ‘‘colloid’’ has been mostly substituted by ‘‘nanoparticle’’, “nanocrystal”, or ‘‘nanocluster’’ however these expressions are not very precise and there seems to be no clear definitions. [12] These terms simply mean that a particle consists of an assembly of atoms, from a few up to several hundred thousands or millions, in the size range between 1 and usually not more than 50 nm. The term “nanocluster” is most often used for particles smaller than 4 nm and “nanocrystals” when the “nanoclusters” have very well defined crystalline cores. The word “nanoparticle” is used for particles spanning the whole nanometer length scale.

Like bulk gold, nanoparticles larger than 10 nm adopts the face centered cubic (fcc) crystal structure and the particles exhibit the cubic, octahedral or rhombohedral crystal forms associated with the fcc structure, [13] however, the other characteristics of such particles are different from that of the bulk. Gold nanoparticles with diameter less than 10 nm show a dramatic decrease of melting point. [14] Colloidal gold nanoparticles show attractive combination of optical properties, which depends on the electronic properties rather than molecular structure, and the facile functionalization of this material with a variety of molecules including biomolecules.

Physicists and chemists predicted that nanoparticles in the diameter range intermediate between the size of small molecules and that of bulk metal would display electronic properties strongly dependent on the particle size, interparticle distance, nature of the protecting organic shell, and shape of the nanoparticles. [15] The few "last metallic electrons" are used for tunneling processes between neighboring particles. The quantum size effect is involved when the de Broglie wavelength of the valence electrons is of the same order as the size of the particle itself. Then, the particles behave electronically as zero-dimensional quantum dots (or quantum boxes). Freely mobile surface electrons trapped in such metal boxes give rise to particle plasmon called also surface plasmon resonance (SPR). SPR is due to collective oscillation of these surface electrons induced by visible light and it results in light scattering and absorption by noble metal colloids. For 5-20 nm gold particles SPR is observed around 520 nm and it is responsible for the specific red color of such suspensions.

Unlike in bulk metals, in nanoparticles, there is a gap between the valence band and the conduction band. The size-induced metal-insulator transition, described in 1988,

is observed if the metal particle is small enough (about 20 nm) that size-dependent quantization effects occur. [1]

Gold nanoparticles show high affinity to thiols, phosphines, and amines that can be easily chemisorbed on the surface to form self-assembled monolayers. The pioneering work by Schmid and co-workers on well-defined phosphine-stabilized gold clusters showed the properties of quantum-dot particles for the first time. [16]

The use of nanosized colloidal Au particles has expanded significantly in recent years. Whereas 10-15 years ago, the predominant use of colloidal Au was in biological transmission electron microscopy, a wide variety of recent papers describe interesting physical properties [17,18] and possible applications. [19] For example, Mirkin's group has developed colorimetric DNA sensors based on colloidal Au and their SPR. [20] Moreover, organized two-dimensional (2-D) and three-dimensional (3-D) arrays of colloidal Au nanoparticles are now occupying the attention of several groups. [21-24] Due to their extremely large surface area, monometallic and bimetallic noble metal colloids, including gold, have been used as active catalysts in the hydrogenation of alkenes in biphasic or organic media, [25,26] hydrosilylation of olefins in organic solutions, [27] and the oxidation of carbon monoxide in aqueous solution at subambient temperature (below 0 °C and even at –70°C). [28-30] Other potential applications include miniaturized electronic devices, ultrafast optical communication, data storage and non-linear optics. [12]

I. 3. Synthetic Polymeric Hydrogels

Synthetic polymeric hydrogels are defined as three-dimensional swollen networks of hydrophilic homopolymers or copolymers that are covalently or ionically crosslinked.

[31] Polymeric hydrogels, when placed in a compatible aqueous medium, are able to swell and retain the volume of the adsorbed solvent or solution. The resulting polymer exhibits both liquid-like and solid like properties. [31] The liquid-like properties come from the fact that the major constituent (more than 90%) is water. The solid-like properties are due to the network formed by the crosslinking reaction that makes the hydrogel more like elastic solids. [31] Thus a gel can be viewed as a container of solvent made of a three dimensional mesh.

The most characteristic property of a hydrogel is that it swells in the presence of an aqueous media and shrinks in its absence. [32] The capacity of hydrogels to absorb the aqueous media could be enormous and can be as much as 1000 times the weight of the polymer. [31] The nature, predominantly the hydrophilicity/hydrophobicity of polymer chains and the crosslinking density determine the extent of swelling. A gel is typically a large crosslinked macromolecule, which forms network extending from one end to the other and occupying the whole reaction vessel. [33] The term hydrogel is referred to a material currently in swollen state but upon drying, the swollen network of the hydrogel collapses due to the high surface tension of water rendering a xerogel or a dry gel. [32] The overall shape of the hydrogel is preserved during the swelling and shrinking process.

Synthetic hydrogels have been extensively studied for the past five decades and this field still remains very active. Hydrogels can be designed to exhibit controllable responses as to shrink or expand with changes in external environmental conditions. [34] The extent of swelling or de-swelling in response to the changes in the external environment of the hydrogel could be so drastic that the phenomenon is referred to as volume collapse or phase transition. [35]

The classification of hydrogels depends on their physical structure and chemical composition. A common classification includes homopolymeric hydrogels and *co*-polymeric hydrogels that can be either electrically neutral or they can carry the charge to form ionic hydrogels. Interesting group of hydrogels are interpenetrating networks (IPNs). [36]

Homopolymers are referred to as a polymer network with crosslinked or uncrosslinked skeletal structure formed from just one kind of the monomer. Homopolymers, which are crosslinked, find important applications such as slow drug delivery devices and contact lenses. An important category of crosslinked homopolymeric hydrogels are poly(hydroxyalkyl methacrylates). Among them, the poly(2-hydroxyethyl methacrylate), (PHEMA), is the most widely studied and used of all synthetic hydrogel materials. [37,38] There are some uncrosslinked homopolymers, which have been of interest to a number of researchers. [39] Poly(*N*-vinyl-2-pyrrolidinone) (PNVP), poly(acrylamide) (PAM), poly(ethylene glycol) (PEG) and poly(vinyl alcohol) (PVA) are classed as uncrosslinked water-soluble homopolymers.

Co-polymeric hydrogel networks are comprised of two or more different monomer species with at least one hydrophilic component, arranged in a random, block or alternating configuration along the chain of the polymer network. [40] The *co*-polymeric hydrogel networks are generally covalently or ionically crosslinked structures, which are not water soluble. [31] A wide range of important *co*-polymeric hydrogels with vast combinations of compatible monomers, some of which include poly(NVP-*co*-HEMA), poly(HEMA-*co*-MMA) and poly(HEMA-*co*-AA) have been studied. [41]

Interpenetrating Polymer Network, IPN, an important class of hydrogel materials, are defined as two independent crosslinked synthetic and/or natural polymer components contained in a single network form. Park *et al.* [34] have described the IPN formation between a pH sensitive hydrogel and temperature sensitive second polymer. This IPN is pH and temperature sensitive. Since there is no chemical bonding between the two polymeric components, each component may retain its own properties while the proportion of each network can be varied independently thus obtaining the desired combinations of the properties of the two macromolecule components. [42]

"Smart" Hydrogels

Particular kind of polymeric hydrogels are the "smart" or "intelligent" gels. Their "intelligence" comes from the discontinuous volume phase transition which they undergo when stimulated by physical and chemical factors, e.g., changes in temperature, solvent composition, pH, ionic strength, electric or magnetic field, or light. [43] As the result of such conformational transformation the gel can exist in two states, the swollen and collapsed state.

Among stimuli responsive polymeric hydrogels, temperature sensitive gels are the most popular and most extensively studied. Thermoswelling hydrogels contain hydrophilic monomers such as acrylamide, acrylic acid, and methacrylic acid. On the other hand, the main examples of thermoshrinking hydrogels are composed of monomers like *N*-methylacrylamide, *N*,*N*-diethylacrylamide, and *N*-isopropylacrylamide (NIPA), whose hydrophobic substituents make them less hydrophilic. [44] Thermoshrinking gels undergo reversible swelling and de-swelling in response to changes in environmental temperature. [45] Hoffman *et al.* [46] in their studies on hydrophobic thermo-responsive

hydrogels based on *N*-isopropyl acrylamide and methacrylic acid defined a low critical solution temperature (LCST) as the temperature, which induces the polymer to collapse. [47-49] For poly-NIPA gels the volume phase transition was reported 32 – 33 °C. When at a low temperature, this gel is completely transparent in its swollen state. At temperature above the lower critical solution temperature it becomes opaque and collapses. Incorporation of hydrophilic acrylic or sodium acrylate monomers increases the LCST. [50] The phase transition temperature of *N*-methylacrylamide for the homopolymeric gels is 78°C. [51] Poly(*N*-vinylisobutyramide) gel, an isomer of poly-NIPA gel, in which the position of the nitrogen and carbonyl are exchanged, has phase transition temperature of 40 °C. [52]

In some cases the thermal phase transition can be induced by light. To induce such transitions, photosensitive moieties such as dyes [53] or metal nanoparticles [54] are embedded in a thermally reversible polymer matrix and irradiated at their resonance wavelengths. Conversion of the light energy to heat through nonradiative relaxation causes hydrogel heating and, for polymers with a lower critical solution temperature (LCST), results in their volume phase transition (deswelling). The gold particles absorb the incident radiation and then relax by nonradiative processes, thereby heating the surrounding material. [55] By modulation of the incident laser power and/or gold particle doping level, one can then modulate the local temperature in the hydrogel assembly and thereby control formation of glassy materials from colloidal crystals. This absorption process is accompanied by a subsequent local heating of the surrounding hydrogel material, which then undergoes a thermally initiated deswelling event. [56]

N-isopropylacrylamide and chlorophylin *co*-polymer network were synthesized to obtain the light sensitive gel. [53] The chromophore can absorb light and subsequent thermal dissipation of light energy and the local temperature increment is proportional to the chlorophyllin density, thus proportional to the polymer density. The phase transition of this gel is probably generated by local heating of the *N*-isopropylacrylamide polymer chain. [57]

Some gels undergo phase transition as the solvent composition varies. The revolutionary discovery of these stimuli responsive gels made by Tanaka was based on the acrylamide gel that swells in water and gradually shrinks as acetone is added to the solution. [44] Hydrogels based on uncharged *N*-isopropylacrylamide and the ionic ampholyte *N*-acryloyl-*L*-histidine shrink in the presence of sulfate, chloride, perchlorate and nitrate. This transition strongly depends on the pH of the system. [57] Recently, Hirotsu [58] and Amiya [59] reported that the addition of alcohols lowers the transition temperature of NIPA gels. The effect of alcohols on the PNIPA solutions was also observed by Otake *et al* .[44] The transition temperature became lower with increasing number of carbons in the alcohol.

Poly(acrylic acid) and poly(methacrylic acid) [43] hydrogels are among the first investigated ionic gels which swell when the pH of solution increases. According to the concept of Donnan equilibrium, an increase in the ionic strength of the swelling agent increases the ionization of a weak polyelectrolytes system thus leading to high swelling activity. [60] However, once the ionic hydrogel has been fully ionized, further increase in the ionic content of the swelling agent will cause the hydrogel to de-swell due to the screening effect of the counterions. Anionic gels are normally un-ionized at a pH lower

than the gel's pK_a, while cationic gels display the opposite behavior and the pH is dependent on the pK_b of the gel. [61]

Ionic hydrogels, which could be cationic, containing basic functional groups (e.g. primary amines) or anionic, containing acidic functional groups (e.g. carboxylic acid), have been reported to be very sensitive to changes in the environmental pH. [31] The swelling properties of the ionic hydrogels are unique due to the ionization of their functional group. The diameter of gold nanoparticles covered with a layer of aqueous hydrogel was examined as a function of pH. [62] UV-vis spectra showed broad increase in the extinction band intensity with decreasing pH. This phenomenon arises from the swelling-collapsing properties of the hydrogel coating. At high pH, the hydrogel is water-swollen due to charge-charge repulsion, and one observes predominantly absorption due to the gold core. Under acidic conditions, however, the diameter of the hydrogel-coated gold nanoparticles shrinks, and a scattering due to the hydrogel rich phase of the polymer, which densely coats the gold nanoparticle surface can be observed. This swelling and collapsing phenomenon was also readily observed visually as characterized by color changes of the particle solution (hot pink at high pH and milky white at low pH).

Most useful pH-sensitive polymers swell at high pH values and collapse at low pH values; the triggered drug delivery occurs upon an increase in the pH of the environment. Such materials are ideal for oral delivery systems, in which the drug is not released at low pH values in the stomach but rather at high pH values in the upper small intestine. [63]

Since their discovery, hydrogels have been used in many areas. One of the common applications is in agricultural field mainly as water storage granules. Swellable hydrogel delivery systems are also commonly utilized for controlled release of agrochemicals and nutrients of importance in agricultural applications to enhance plant growth with reduced environmental pollution. [64] Hydrogels have been commonly utilized commercially in other important industrial areas such as cosmetics, food industry, photography and instrumentation.

The field of biomedical research has advanced rapidly in the past several years, mainly as a result of attempts to replace body tissues with natural or synthetic biomaterials. [65] Success in the application of biomaterials is strictly confined to their biocompatibility. Controlled delivery of drugs has been one very important application, where hydrogels have been extensively used. [31] Delivery of bioactive agents through sustained release devices has been a major field of research over the last three decades.

A variety of methods have been used to target biologically active molecules to the specific site and extend their therapeutic lifetimes once inside the body. The use of swellable materials for drug delivery applications has followed experimental and theoretical investigations of drug transport in polymeric delivery systems.

I. 4. Gold Nanoparticles in Polymeric Gels

Although very popular due to specific and interesting properties, stimuli responsive polymeric gels and gold nanoparticles, have hardly been studied together. Recently there is a growing interest in new hybrid nanoparticles, where a metallic nanoparticle is coated with a polymeric layer, leading to a so-called core - shell structures. [66] The organic shell determines the chemical properties of such materials and

their interaction with the environment, whereas their physical properties are determined by the size and shape of the metal core and the surrounding organic layer. [67] The widely used procedure to obtain gold nanoparticles embedded in polymeric matrix involves polymerizing the matrix around the nanoparticles [68] and leads to chemically bounded polymer to a metal core. [66,69,70] The first step of this procedure is to synthesize gold nanoparticles followed by the polymerization process.

Synthesis of Gold Nanoparticles

A wide range of techniques for the synthesis of gold nanoparticles focused on controlling the size and shape of the resulting particles has been developed in recent years. Among them physical and chemical methods can be distinguished. Gold nanoparticles can be directly generated from bulk gold using physical methods such as metal-vapor synthesis, [71] laser ablation [72] or thermolysis. [73] UV, [74-a,b] near IR [75] and ultrasonic irradiation [76] were also used. Chemical routes use reduction of gold compounds.

Gold nanoparticles in solution tend to be fairly unstable so special precautions have to be taken to avoid their aggregation. Variety of stabilizers that associate with surface of the particle, providing charge or solubility properties that keep the nanoparticles suspended, and thereby prevents their aggregation, were reported.

Citrate Reduction

The reduction of aqueous solution of tetrachloroauric acid, $HAuCl_4$, by sodium citrate introduced by Turkevich in 1951 [77] is the simplest and by far the most commonly used procedure to synthesize gold nanoparticles. [76,79] It leads to nearly monodispersed, spherical particles of 15-20 nm in diameter. Citrate itself and its oxidation products (e.g.

acetone dicarboxylate) can act as stabilizing agents, if no other stabilizer is used. [80] As the consequence of a weakly bound citrate coating the particles have a negative surface charge and therefore they repel each other. In 1973 Frens reported that the size of colloidal gold nanoparticles could be easily controlled and manipulated by the initial concentrations of chloroaurate ion and citrate. [81]

Although sodium citrate is the most common reducing agent, gold nanoparticles can also be synthesized using other reducing agents such as: tannic acid, white phosphorus, [82] hydrazine, [83] hydrogen, [84] carbon monoxide, [85] hydroxylamine, [86,87] and mild agents like ascorbic acid. [88,89] Reducing solvents such as alcohols, [90] formamide, [91] and ethers [90] can also be used in the synthesis of metallic nanoparticles.

The Brust-Schiffrin Method (Two-Phase Synthesis with Thiols)

More recently, inspired by the Faraday's biphasic method, Brust and Schiffrin developed new technique to synthesize Au nanoparticles. [15,22] This technique had a considerable impact on the overall field of colloidal gold nanoparticles and it opened an entirely new route to understanding the stability, reactivity and self-assembly of metallic particles in nonpolar media. To prepare gold particles with diameter between 1.5 and 5.2 nm, an aqueous solution of chloroaurate was transferred to toluene using tetraoctylammonium bromide as the phase-transfer reagent and reduced by $NaBH_4$ in the presence of dodecanethiol. This procedure led to the formation of stable gold nanoparticles protected by self-assembled monolayers of long chain thiol ligands that strongly bind gold due to the soft character of both Au and S. Due to high affinity of the thiol to the Au surface, gold nanoparticles can be dried to a powder without coalescence and repeatedly isolated and redissolved in common organic solvents without irreversible

aggregation or decomposition. Such particles can be easily handled and functionalized just as stable organic and molecular compounds.

Soon the method proposed by Brust was extended to a single phase system, [22] which opened the way to the synthesis of gold nanoparticles stabilized by a variety of functional thiol ligands. [92] Subsequently, many publications appeared describing the use of the Brust- Schiffrin procedure for the synthesis of other stable nanogold particles that contained functional thiols. [93-95]

Stabilization of Gold Nanoparticles

An important aspect of successful synthesis of colloidal gold nanoparticles is the stabilization that prevents them from coagulation between particles. This stabilization can occur in many different ways, such as electrostatic repulsion, steric hindrance, by ligand molecules or by embedding in nanocapsules like micelles. Chemical modification of gold surfaces by using alkanethiols, polymers, dendrimers, and other molecules as stabilizers can be achieved either by the synthesis of colloidal gold with an organic monolayer in a one-step procedure or by surface modification of already available colloidal gold.

The most important stabilizing molecules for gold nanoparticles of any size are thiols. A wide variety of thiol molecules such as straight-chain alkanethiols, [93,98] glutathione, [99] p-mercaptophenol, [100] aromatic alkane thiol, [101] phenyl alkanethiols, [102] and γ-mercaptopropyl-trimethoxysilane [103] have been used to protect gold particles. The interactions of alkanethiols with the gold nanoparticles surface cause the thiol molecules self assemble in a well ordered, densely packed manner on the nanoparticle surface to form self-assembled monolayers (SAMs). Thiols protected gold nanoparticles

can be further functionalized through a place exchange reaction with chemically reactive groups [96,104] such as proteins, and other biomolecules. The place-exchange reaction was extensively studied by Murray *et al.* [93,95,96,98,102,104] Recently, several groups have demonstrated the synthesis and modification of gold nanoparticles with a single functional group attached to the surface. [93,98,105] The significance of such nanoparticles lies in that they can be essentially treated and used as molecules to react with other nanobuilding blocks or chemicals. As a result, nanomaterials may be assembled using traditional chemical reactions, with all the nanobuilding blocks covalently bonded together.

The alkanethiolate molecules protecting the gold nanoparticles have the potential to develop novel technological applications such as chemical sensing, catalysis, colorimetric assays for DNA detection, biosensors, etc. [97,106]

Other sulfur-containing ligands, such as xanthates [107] and disulfides, [108-110] di- [111] and trithiols [112] and resorcinarene tetrathiols [113] have been used to stabilize gold nanoparticles.

Polymers in Stabilization of Gold Nanoparticles

Besides thiols some polymers can be used to stabilize gold nanoparticles. The most common polymers used to prevent coagulation of gold nanoparticles are poly(vinyl-pyrrolidone), PVP, [114,115] and poly-(ethylene glycol). [82,116] They both can be used to prepare gold nanoparticles incorporated into ordered polymer matrices. For instance, nanogold particles in PVP were prepared by hydrazine reduction of incorporated tetrachloroauric acid, $HAuCl_4$, ($HAuCl_4$-loaded block copolymer). [114,115] These phenomena were also obtained with (styrene-*block*-ethylene oxide). [117,118] Polystyrene-

block-poly(4-vinylpyridine) (PS-PVP) diblock copolymers micelles were used to synthesize nanometer-sized gold particles. [119] Nanoparticles of improved stability against long-term aggregation were prepared using poly(styrene)-*b*-poly(2-vinylpyridine) (PS-*b*-P2VP) star-block copolymer micelles. [120] Functionalized polymers have also been used as stabilizers. Poly(ethylene glycol)-based polymers were used to fabricate a gold nanoparticles based sensor that reversibly binds lectin for recognition and bioassay. [121]

Gold nanoparticles of average size between 1 and 50 nm have been stabilized by many water-soluble polymers. The advantage of such systems over the aqueous sols is that the resulting polymer-coated gold particles could be stored in the dry state and redispersed in water to yield sterically stabilized suspensions. [70] Conjugation with Au nanoparticles requires that the polymer should bear an amine or thiol group at one terminus. [122] Gold nanoparticles were stabilized by the nitrogen lone electron pair on the backbone of polymethylphosphazene, $[Me(Ph)- PN]_n$. [123] Thiolated polymer ligands are more efficient than alkanethiols in preparing small sized gold nanoparticles and stabilizing the particles in solutions as well as in increasing their thermoresistance. Importantly, the properties and potentials of monolayer protected Au clusters, MPCs, may be extended when using polymer ligands with different architectures to stabilize gold nanoparticles. [66]

Two different approaches are used to achieve nanoparticle-polymer composites. The first technique consists of the *in situ* preparation of the nanoparticles in the matrix. This is effected either by the reduction of metal salts dissolved in the polymer matrix [124] or by the evaporation of metals on the heated polymer surface. [125] The second approach

involves polymerizing the matrix around the nanoparticles [68] and leads to chemically bounded polymer to a metal core. [66,69,70,122,125-127] The synthesis of the gold nanoparticles with chemically bound polymer grafts can be carried out in two ways "grafting-to" and "grafting-from". In a "grafting-to" method a covalently attached polymer monolayer is formed by a contact of the metal surface with dilute solution of polymer by coupling reactions, chemical bonding, electrostatic interactions, or spin coating. Polymers end-capped with a thiol [66] or sulfur-containing group [122] and polymers with a disulfide between two chains have been used [70] instead of small alkanethiol ligands to prepare directly the polymer MPCs of gold nanoparticles.

In 1998 Murray *et al*. [60] reported for the first time gold clusters with bonded polymeric monolayers. In their work, they described a monolayer-protected Au cluster (MPC) based on a monolayer of thiolated polymer, α-methoxy-ω-mercapto-poly(ethylene glycol) (PEG-SH), synthesized in modified Brust reaction. [92] This polymer was selected for its potential to yield improved core stabilization, to induce aqueous solubility and provide isolation of dry, nonaggregated nanoparticles that can be redissolved without change. Clusters protected by alkanethiolate- and modified alkanethiolate-monolayers are water insoluble, which limits their biological sensing applications. Alkanethiolate ligand was selected because dissolution of $LiClO_4$ electrolyte in solvent-free PEG-S-MPC provides new polymer electrolyte media, a semisolid with an ionically conductive nanophase around a metallic core. [129]

Lowe *et al.* [130] used four water-soluble *co*-polymers: anionic poly(sodium 2-acrylamido-2-methyl propane sulfonate) (PAMPS), cationic poly((*ar*-vinylbenzyl)trimethylammonium chloride) (PVBTAC), neutral poly(*N*,*N*-dimethyl-

acrylamide) (PDMA), and zwiterionic (betaine) poly(3-[2-*N*-methylacrylamido)-ethyl dimethyl ammonio propane sulfonate-*block*-*N*,*N*-dimethylacrylamide) (PMAEDAPS-*b*-PDMA) to "graft-to" the surface of gold nanoparticles.

Mangeney *et al.* [70] reported on gold colloids, which are covalently derivatized with hydrophilic polymer brushes bearing terminal disulfide groups and being compatible with biological applications. Simple direct mixing of the gold colloids with polymer solutions resulted in "grafting onto" the metal surface. They used polymers based on the monomer: *N*-[tris(hydroxymethyl)methyl]acrylamide and *N*-(isopropryl)acrylamide; the first monomer gives polymers that are nonionic, very hydrophilic, biocompatible, and inert to biological fouling. Moreover, the high number of primary hydroxyl groups enables facile post-functionalization. Second monomer produces a thermoresponsive homopolymer in aqueous solution, exhibiting a conformational collapse above a lower critical solution temperature (LCST).

Other polymer layers "grafted-to" the surface of gold nanoparticles include poly[mercaptomethylstyrene-*co*-(*N*-vinyl-2-pyrrolidone)] [131] or thiol end-capped polystyrene. [132] Size-controlled synthesis of gold nanoparticles was conducted by using the inorganic polymer, poly(methylphenylphosphazene), in which the lone pairs of electrons on nitrogen acted as interaction points to stabilize the formed gold nanoparticle. [123] The resulting polymeric monolayer was further derivatized and used for the specific recognition of analytes. However, the methodologies described above are only useful for producing polymer layers with a relatively low graft density. The attaching functionalized polymers onto the surface of nanoparticles with typical diameters of 2-5 nm would not result in a compact core-shell system for steric reasons.

In "grafting-from" strategy monomers are polymerized directly on the end functionalized three dimensional self assembled monolayers, 3D SAM's, gold nanoparticles surfaces, carrying polymerization initiating species. Jordan *et al.* [126] used 11-hydroxyundecane-1-thiol (HO-$(CH_2)_{11}$-SH, HUT)-functionalized gold nanoparticles as the starting material for the polymerization of 2-substitted-2-oxazolines to prepare a nanocomposite where the gold core was coated with an amphiphilic shell with a well-defined hydrophilic/lipophilic balance.

Mandal [127] and Ohno [128] used self-assembled monolayers (SAM's) of bromofunctionalized thiolates on gold nanoparticles to initiate polymerization of methyl methacrylate monomer. Since the Au-S bond is not stable at high temperature, the polymer chains grown from the terminal bromine on a SAM are not stable to high temperatures (110-150 °C). To solve this problem, they have used copper(I) bromide/1,4,8,11-tetramethyl-1,4,8,11-tetraazacyclotetradecane (Me_4Cyclam) as a catalyst system to grow the polymer layer at room temperature. In this method, gold nanoparticles are first prepared in the presence of 11-mercapto-1-undecanol, MUD. The MUD is one of the most common thiols used in such kind of synthesis. A self-assembled monolayers consisting of MUD then forms around individual gold nanoparticles, thereby stabilizing the suspension. The MUD functionalized gold nanoparticles are then esterified with 2-bromoisobutyryl bromide to prepare a Br-terminated gold surface. Finally, Br-terminated gold nanoparticles are used as macroinitiators for the polymerization of methyl methacrylate from the gold nanoparticle surfaces. The properties of the core-shell nano- or microparticles prepared by "grafting from" method can be tuned by changing the composition of the particle or by attaching copolymers with

different composition and functionality. Shell thickness and surface uniformity can also be controlled by this polymerization technique. [132]

Different way to synthesize nanocomposite materials consisting of colloidal gold nanoparticles embedded in thermoresponsive poly(N-isopropylacrylamide) hydrogel was proposed by Langer *et al.* [133-a,b] First they prepared crosslinked poly(NIPA) containing side chain terminated with thiol groups and then generated the gold nanoparticles *in situ* of hydrogel templates. The thiol groups may form complexes with Au(III) ions. These ions were reduced upon the addition of a reductant, such as $NaBH_4$ and materials with metallic gold particles tightly attached to crosslinker formed.

Willner and *co*-workers [134] have successfully used the phenomenon of reversible volume phase transition to introduce gold nanoparticles into the gel by a "breathing" mechanism. It consisted of breathing-out in an aprotic solvent (e.g. acetone) and breathing-in in an aqueous solution containing nanoparticles. This mechanism was used for the fabrication of nanoparticle/hydrogel composites with interesting solvent-switchable electrical and photoelectrochemical properties on macroscopic Au electrodes.

Polymerization Procedures

The most common polymerization method for synthesis of polymeric gels is free radical polymerization. It consists of chain reactions in which every polymer chain grows by addition of a monomer to the terminal free radical reactive site called “active center”. The addition of a monomer to this site induces the transfer on active center to a newly created chain end. The mechanism of the free radical polymerization can be divided into three distinct stages, initiation stage when free radical active center is formed, propagation stage based on successive addition of a large number of monomer

molecules to radical center (new radical forms that is larger by one monomer unit) and a termination stage when the growth of the polymer chain is terminated irreversibly. The advantages of the free radical polymerization are applicability for a wide range of polymerizable groups and tolerance to many solvents, small amounts of impurities and many functional groups present in the monomers. It also has some limitations inherent to its mechanism. In particular, it is difficult to control molar masses and polydispersities as well as to introduce defined end-groups, or to prepare special macromolecular architectures such as block copolymers. In order to overcome these limitations, new strategies in free radical polymerization have emerged recently, often referred to as "controlled" or "living" free radical polymerization.

Controlled/living free-radical polymerization is a promising alternate to living anionic polymerization, as a radical process is more tolerant to functional groups and impurities, and can be carried out under relatively simple experimental conditions. Therefore, this method has attracted great attention in the past decade, and many efforts have been made to improve the level of the polymerization control, such as stable free radical polymerization (SFRP) [135] and atom transfer radical polymerization (ATRP) [136] and reversible addition–fragmentation chain transfer (RAFT) process. [137] Among them, RAFT polymerization is developed as a versatile "living" radical technique. [138]

The methods listed here are widely used in synthesis of nanogold-polymer composites. It was shown that the "grafting-to" strategy is an especially useful for preparation of polymer stabilized gold clusters, if combined with a living polymerization technique. This is because the polymer ligands can be well-defined prior to being employed to prepare gold nanoparticles. Particularly, this strategy is promising when a

polymer from a RAFT reaction bearing dithioester end groups is directly used as a passivant. The dithioester end groups are reduced to thiols when adding a reducant to the mixed solution of tetrachloroauric acid, $HAuCl_4$, and the RAFT polymer, and the gold cores are passivated with the resulting thiols. Just recently Lowe *et al.* [122] reported the synthesis of gold nanoparticles stabilized by anionic, cationic, neutral, and zwitterionic *co*-polymers.

Reversible addition fragmentation chain transfer (RAFT) polymerization [139] has - along with other equally important living free radical techniques [140] - revolutionized free radical polymerization, as it allows for the generation of complex macromolecular architectures such as comb, star, and block *co*-polymers with narrow polydispersities. The RAFT polymerization is finding applications for generating novel structures and materials in bioengineering and nanotechnology applications. Some applications include the manufacture of biocompatible nanocontainers for drug delivery applications. [141]

If living polymerization techniques such as living radical, [142] living ionic polymerization techniques, [126] or ring-opening metathesis polymerization, [143] are applied, better uniformity and controlled thickness of the "brush-type" polymer shells on the surface of various solids are possible to obtain. Jordan *et al.* [126] used the surface-initiated living cationic polymerization to prepare a nanocomposite where the gold core was coated with an amphiphilic shell with a well-defined hydrophilic/lipophilic balance. Mandal *et al.* [127] and Ohno *et al* .[128] introduced surface-initiated atom transfer radical polymerization (ATRP) of methyl methacrylate from the surface of nanosize gold. In the same way Nuss [144] synthesized gold nanoaprticles coated with poly(*n*-butyl acrylate). Tenhu *et al.* [145] reported a controlled radical polymerization (reversible addition-

fragmentation chain transfer polymerization, RAFT) of NIPA from the surface of gold nanoparticles, and showed that the optical properties of gold could be varied by the thickness of thermoresponsive polymer brush. Kim *et al.* [146] applied surface initiated atom transfer radical polymerization, SI-ATRP, of NIPA from microparticles and flat surfaces for the application to cell culture. They also used SI-ATRP to synthesize cross-linked Au nanoparticles-poly-NIPA core/shell hybrid structures as well as the brush-type hybrids and studied the effect of the cross-linking on the thermoresponsiveness of hybrids.

I. 5. Physical Properties of Synthetic Hydrogels Modified with Gold Nanoparticles

The materials composed of polymeric hydrogels and colloidal gold nanoparticles show specific properties that are the combination of individual characteristic of nanogold particles and gels. The two, most important features are surface plasmon resonance resulting from the presence of gold nanoparticles and volume phase transition due to presence of stimuli responsive matrix in which these gold particles are embedded.

Surface Plasmon Resonance

Gold nanoparticles in aqueous sols or polymeric gels have a characteristic red color, which arises from their nanometer size and reflects a phenomenon called surface plasmon resonance, SPR. [17] The SPR is observed as strong absorption band in the visible region around 520 nm for 12 nm particles and it is due to collective oscillation of the electron gas at the surface of nanoparticles (6s electrons of the conduction band for gold nanoparticles) that is induced by electromagnetic field of the incoming light. The nature of the SPR and the physical explanation of the optical properties of gold

nanoparticles were first described by Gustav Mie in 1908. [147] The main assumption of Mie's theory (sometimes referred to as Lorenz-Mie theory since Lorenz probably was first to contribute to this theory) is that the particle and its surrounding medium are each homogeneous and describable by their bulk optical dielectric functions. According to this theory, the total cross section composed of the surface plasmon absorption and scattering is given as a summation over all electric and magnetic oscillations. The resonances denoted as surface plasmons were described quantitatively by solving Maxwell's equations for spherical particles with the appropriate boundary conditions. [12] For a sample of dilute (noninteracting) containing N nanoparticles per unit volume and path length d, the extinction cross section per particle, Q_{ext}, is related to the conventional absorbance through the proportionality [12]:

$$A = \log_{10}\frac{I_0}{I_d} = \frac{NQ_{ext}d}{2.303} \qquad (1.5.1)$$

where d is the optical path length and I_0 and I_d refer to the initial and final light intensities. For particles much smaller than the wavelength of the incident light in the medium (~10%), Q_{ext} is expressed as:

$$Q_{ext} = \frac{24p^2R^3e_m^{3/2}}{l}\frac{e_2(w)}{(e_1(w)+2e_m)^2+e_2(w)^2} \qquad (1.5.2)$$

where R is the radius of gold particle, λ is the wavelength of light, e_m is the dielectric constant of the medium the nanoparticles are embedded into, and e_1 and e_2 are real and imaginary components of e, the frequency (ω) dependent dielectric constant of the particle (assumed equal to that of bulk metal). For metals, the dielectric constant is a complex number related to index of refraction n and absorption coefficient k as

$$e = e_1(w) + ie_2(w) = (n + ik)^2 \qquad (1.5.3)$$

and the magnitude e_1 and e_2 are strong functions of the frequency of the applied electric field (wavelength of the incident light).

The origin of the strong absorption, which results in the bright colors of nanoparticles, is found in the denominator of Equation 1.5.2. The electric field of the interacting light wave induces an oscillating dipole in the particle. The surface charge build up in the particle acts as a restoring force. The extinction has a resonance, and thus an absorption maximum, at the frequency where the denominator of Equation 1.5.2 takes its minimum. If e_2 is small (which is not the case for gold), resonance is obtained when $e_1 = -2\, e_m$. The minimization of the denominator is often referred to as the plasmon resonance condition.

The optical properties, in particular the position of the plasmon resonance peak, are strongly influenced by the surrounding medium. Introduction of a thin surface layer results in a new set of scattering coefficients, which can be determined by solving the boundary condition equations of the additional layer. Additional complications can be seen when interactions between neighboring particles are considered. When particles aggregate, mutual dipoles are induced due to the electrodynamic interactions, usually resulting in a red shift of the plasmon features. [148,149] An extensive theoretical treatment of the electro-dynamical properties of particle aggregates can be found in reference. [150]

Very small nanoparticles (less than 1-2 nm) do not display SPR phenomenon, as their electrons exist in discrete energy levels and are regarded as undergoing primarily one-electron excitation with a limited amount of electron correlation. The damping of the surface plasmon mode follows a $(\text{radius})^{-1}$ dependence due essentially to surface

scattering of the conduction electrons [12]; this decrease of intensity of the surface plasmon bands as particle size decreases is accompanied by broadening of the plasmon bandwidth. On the other hand, bulk metals have a continuous absorbance in the UV/vis/IR region (which effectively collapses into a single plasmon absorbance in the case of a nanoparticle). [151]

As reported in [152], the SPR of the assemblies of metal nanoparticles can be significantly tuned by varying the interparticle distance between adjacent nanoparticles. In this case, a red-shift of the SPR peak is usually observed when the particles approach each other. For example, the surface plasmon resonance absorption (SPR) band of individual gold nanoparticles with core diameter around 15 nm appears at approximately 510 nm. When these gold nanoparticles are linked by DNA, the SPR band red-shifts and gives a blue or purple color to the nanoparticle solution. [153]

UV-vis spectroscopy allows determining the interactions between gold nanoparticles and polymers in terms of changes in SPR signal. Sun *et al*. [154] observed no significant interactions between nanoparticles and polylysine, PLL, backbone that otherwise would alter the surface electron density of the gold nanoparticle, resulting in damp and broadening of the surface plasmon absorption band, as well as a change of the absorption of the organic moieties bounded to the particle surface.

Tenhu's group [145] analyzed the optical properties of poly(NIPA) monolayer protected gold clusters depending on a solvent. They found that the surface plasmon absorption band at around 520 nm is enhanced due to the aggregation or a close contact between nanoparticles. Moreover, the shift in the absorbance can be correlated with the size of the gold nanoparticles and the dielectric constant of the surrounding medium. No

particular differences in the absorption maximum of poly(NIPA) monolayer protected gold particles in different solvents were found: λ_{max} was 515, 517, 518, and 522 nm in DMF, THF, methanol, and acetone, respectively. The only exception was the aqueous dispersion, λ_{max} = 535 nm. According to the dynamic light scattering, DLS, measurements the MPC-poly-NIPA particles were aggregated in THF, acetone, and water, whereas no aggregation was observed in DMF and methanol. The red shift of the λ_{max} in water was explained by the association of the MPC-poly-NIPA particles. The lower λ_{max} values for the aggregated samples in THF and acetone may result from the lower dielectric constants than that of water.

Suzuki [155] studied the effect of temperature on the absorption spectra of the hybrid particles built of gold nanoparticles and NIPA-*co*-glycidyl methacrylate. At 20 °C an absorption peak was measured at 522 nm. The position of the peak measured at 40 °C was red-shifted and observed at 533 nm. The intensity increased in the visible region due to the Rayleigh scattering of the shrunken particles. These thermal transitions of hybrid molecules were completely reversible, indicating that the gold nanoparticles did not attach to each other in the shrunken state of the hybrid particle.

Volume Phase Transition

Similarly to unmodified gels, polymeric hydrogel with incorporated colloidal gold nanoparticles show a low critical solution temperature (LCST) transition. It means that at certain temperature the polymer undergoes the coil-to-globule phase transition. For poly(NIPA) this temperature, called also cloud point, was reported as approximately 32 °C [13,138] and it depends on the type and amount of crosslinker used. Langer *et al*. [133-b] described Au-NIPA gels containing high content of *N*,*N*-cystamine bisacrylamide, CBA

crosslinker that do not undergo phase transition and remain optically transparent even at 48 °C. Volume phase transition temperature and water content in gel matrix can also be modulated by introducing hydrophilic monomer such as acrylic acid, AA. An increase of AA content in the *co*-polymer network can reduce or even eliminate its temperature sensitivity. [156] Limited swelling properties was observed when Au(III) ions were introduced into NIPA-CBA polymer for *in-situ* reduction. [133-a] It was explained in the following way: immobilization of charged ions within a hydrogel results in an afflux of water to balance the osmotic pressure build-up, which causes the hydrogel to swell. This is known as the Donnan effect of polyectrolyte gels. [157] The degree of osmotic swelling is therefore dependent on the amount of immobilized charges, which is proportional to the surface area of Au nanoparticles. Below their low critical solution temperature, LCST, stimuli responsive polymers are soluble in aqueous solution, but upon raising their temperature above the LCST, such polymer becomes insoluble and aggregates in solution. The low critical solution temperature, LCST, transition of stimuli responsive polymers is reversible because upon lowering the temperature below the LCST, the polymers redissolve in solution. For NIPA this transition was found to be discontinuous. [158] The microscopic view of the volume phase transition for NIPA gels with incorporated gold nanoparticles is shown in Figure 1.1.

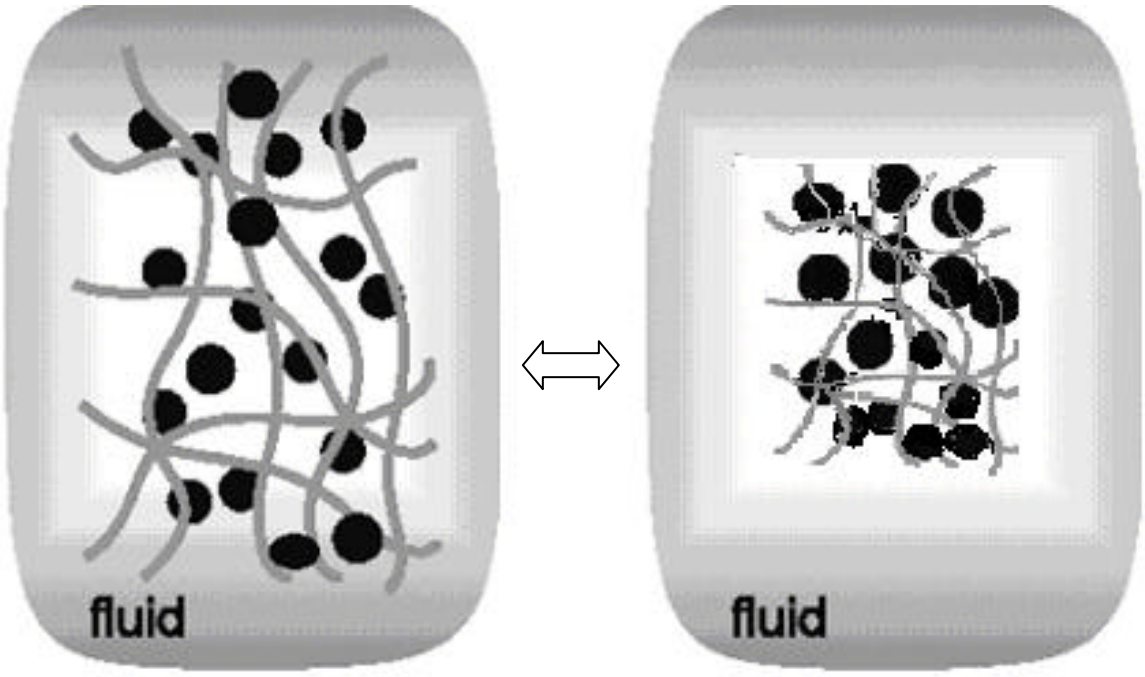

Figure 1.1. The microscopic representation of volume phase transition. On the left – gel before the collapse and on the right – gel after collapse. [74b]

Phase transition of polymeric gels is a result of a competitive balance between attractive forces that act to shrink the polymer network and repulsive forces that act to swell the network. [159] The attractive forces are mainly van der Waals, hydrophobic interaction, ion-ion interaction, and hydrogen bonding. The repulsive forces include the electrostatic interaction between the polymer charges of the same kind and the osmotic pressure by counter ions. Poly-NIPA hydrogel is temperature responsive due to hydrophobic interactions between a polymeric network and water. At a molecular level, the LCST transition is accompanied by a conformational change of the polymer chain from a disordered, random coil to a more ordered, collapsed globule.

Polymeric gels showing opposite behavior to NIPA were also studied. Interpenetrating networks of poly(acrylic acid) and poly(acrylamide) when swollen by water were in a swollen state at high temperature and in collapsed state at low temperature. This transition was governed by hydrogen bonding. [160]

Temperature-sensitive polymer gels have been investigated for applications in drug delivery systems, [161] and actuators, [162] where quick responsive gels are desired. [163] Understanding of the kinetics of such response is then important issue. The pioneering theory of gel swelling or shrinking was developed by Tanaka and Fillmore (TF). [164] According to TF theory, the time, τ, of swelling of spherical gels is given by following equation:

$$\tau \approx R^2/D \qquad (1.5.4)$$

where R is the radius of gel sphere and D is the cooperative diffusion coefficient, respectively. The D value that describes diffusion of polymer molecules in a solvent is defined as $D = E/f$, where E is the longitudinal bulk modulus of the network, and f is the coefficient of friction between the network and the solvent in gel. [165] As one can see the process of gel swelling is diffusion controlled and the rate strongly depends on the size of the gel. For typical polymer gels, D is in the order of 10^{-7}-10^{-6} cm^2/s, depending on the polymer concentration and cross-link density. It is not easy to increase the value of D by a factor of 10^2 or more. Therefore, a reduction of a gel size has been the only way to achieve quick response. The smaller the gel particle, the quicker the gel swells or shrinks. Due to their small dimensions, microgels and core-shell nanocomposites are very promising systems. Temperature-sensitive aqueous microgels were first synthesized in 1986 by Philip Chibante. [166] The size of microgels ranges from single nm to several

μm. Recently explored nanoshell systems offer the dimensions up to several hundreds nm. Due to the small size the volume phase transition can be completed in seconds what makes them very promising materials for a temperature triggered drug or chemical release matrix. Recently, considerable amount of work has been performed in microgel systems [167] and several theories of gel swelling/shrinking have been proposed. [168] However, the essential feature of equation 1.5.4 remains unchanged. For example with the shear modulus introduced to original TF theory by Li and Tanaka, [169] this theory became applicable to cylindrical gels. The nature of shear modulus is to keep the system in shape, for example minimize the nonisotropic deformation of a gel. When the diameter of a spherical gel is the same as the diameter of a cylinder and the thickness of the disk, this model predicts that the effective diffusion coefficients of long cylinder and large disk gel are 1.5 and 3 times smaller than that of a spherical gel. The relaxation times for these long cylinder and large disk gels are approximately 2.0 and 5.7 times longer than that of a sphere. This modified model had successfully predicted the swelling of a long cylinder and large disk gels.

In addition, the TF theory does not account for shrinking kinetics across the temperature of phase separation. Hirose and Shibayama [170] were studying kinetics of the volume phase transition in poly(*N*-isopropylacrylamide-*co*-acrylic acid) gels. The shrinking/swelling behavior across the volume phase transition temperature has been investigated for cylindrical gels made of poly(*N*-isopropylacrylamide-*co*-acrylic acid) and poly(*N*-isopropylacrylamide). In the case of NIPA homopolymer gel, the shrinking process was strongly slowed down by the phase separation, while the swelling process was well reproduced by the Tanaka – Fillmore theory. It was found that in the case of

neutral NIPA gels, quasistatic heating results in a steep decrease in swelling ratio at the volume transition temperature, above which the gel size does not change with temperature. [171] On the basis of these results of gel shrinking, Hirose and Shibayama proposed a shrinking mechanism for NIPA gels. The NIPA neutral gels can be assumed to consist of lightly cross-linked and heavily cross-linked regions. The presence of these kinds of regions is now well known as spatial inhomogeneities. [172] If a gel is heated slowly, the cross-link-rich regions can adjust their position and/or orientation to fit a new equilibrium and finally reach an equilibrium shrunken state.

When the polymer chains are attached by one end to a solid substrate or an interface with a sufficient density, referred to as a polymer brush, they are crowded and forced to stretch away from the solid surface to avoid overlapping. Therefore, as suggested by theoretical predictions, [173] the strong interchain interactions are present in the brush and cause a broadening of the transition of polymer chains, distinct from the behavior of flexible chains free in solution where the polymer chains adopt a random coil conformation. Tenhu *et al.* [174] were studying thermally induced phase transition of poly(NIPA) brush bearing either a phenylpropyl end group or a carboxyl end group attached to gold nanoparticles. They found for the first time that these brush shells show two-phase transition. The part of a polymer chain that is closer to the gold undergos the first transition at lower temperature, while the segments in the outer zone show the transition at higher temperature.

I. 6. Applications of Smart Gels Modified with Gold Naoparticles

Since the stimuli responsive properties of hydrogels and optical properties of gold nanoparticles do not change upon combining them together, the possible applications of

such relatively new composite materials should cover the areas where the components were used separately. In recent years nanocomposite materials consisting of colloidal metal nanoparticles embedded in synthetic polymer hydrogels have attracted attention due to their potential applications. Given their biocompatible nature and unique optical properties, gold nanoparticles are particularly attractive as components in thermally responsive biomaterials. [175] They appear as attractive alternatives to non-aqueous systems with the advantage of being compatible with biological molecules, cells and tissues. [176] These hybrid particles can be used as new materials for sensors, biosensors or drug delivery systems. [177] Molecularly imprinted crosslinked poly(NIPA) gel with incorporated gold nanoparticle was used as a material for SPR sensor chip responsive to changes in dopamine or adrenaline concentration. The sensing mechanism was based upon the selective binding of a given analyte accompanied by swelling that causes a blue shift in the plasmon absorption band of the immobilized gold nanoparticles. This blue shift was a result of changes in proximity of the gold nanoparticles immobilized in the imprinted polymer. [178,79]

Sershen and Halas [180] developed a new class of nanoparticle shells designed to strongly absorb near-infrared light. They incorporated gold-gold sulfide nanoshells, into poly(NIPA-*co*-AA) hydrogels to produce a photothermally modulated drug delivery systems. Light at wavelengths between 800 and 1200 nm is transmitted through tissue with relatively little attenuation, absorbed by the nanoparticles, and converted to heat. The release of methylene blue and proteins of varying molecular weight from such hydrogels was investigated. It was found that the nanoshell-composite hydrogels could release proteins in multiple bursts as a response to repeated near-IR irradiation. When

the temperature of the copolymer exceeds the low critical solution temperature, LCST, the hydrogel collapses, causing a burst release of any soluble material held within the hydrogel matrix. Significantly enhanced drug release from composite hydrogels has been achieved in response to irradiation by light at 1064 nm.

Kim and Lee [62] described hybrid nanoparticles consisted of a gold core coated with a biocompatible hydrogel polymer shell that served as unique drug-delivery vehicles that have the ability to respond to ambient changes in pH and/or temperature.

Of particular interest is the possible electrical switching of nanometer-scale immobilized hydrogel films, because electrical switching can be accomplished much faster than in pH- or temperature-switched materials, and because it may be possible to create three-terminal devices in which the magnitude of fluid transport is controlled by a (third) control voltage.

Interest in nanometer-scale hydrogels is driven by the ultimate goal of coupling them to control of electrokinetic transport in nanocapillary array membranes [181] and by the possibility of achieving rapid switching, compared to macroscopic films. [182] A gold nanoparticle/hydrogel composites with solvent switchable electronic properties was synthesized by introducing gold nanoparticles in crosslinked polyacrylamide gels in the presence of $ZnCl_2$ and *N*,*N'*-methylenebisacrylamide. The switching properties of the composite were demonstrated by the difference in resistivity between the swollen and shrunken gold nanoparticle/polymer composite. This effect is attributed to a shorter interparticle spacing in the shrunken polymer, decreasing the resistance of the polymer layer and enhancing the electric communication between the redox-label and the electrode. [139] It was shown that the incorporation of Au nanoparticles in poly(NIPA) by

a thermal breathing-in process, reduced the electron transfer resistance in the solid composite material.

Such thermosensitive gold nanoparticles can be potentially incorporated into "smart" liquid cell windows that block the solar heat by turning transparent windows opaque at high temperature. Thus, thermosensitive Au nanoparticles may have potential use for stimuli-responsive applications. [183]

Chilkoti *et al.* [69] used the change in optical properties of colloidal gold upon aggregation to develop an experimentally convenient colorimetric method to study the interfacial phase transition of an elastinlike polypeptide (ELP). This thermally responsive, genetically encoded biopolymer was covalently attached to mercaptoundecanoic acid functionalized gold nanoparticles. The thermally triggered hydrophilic-to-hydrophobic phase transition of the adsorbed ELP resulted in a formation of large aggregates due to interparticle hydrophobic interactions and caused a color change from red to violet.

Due to its thermoresponsiveness, a poly(NIPA)-based hydrogel and its hybrids have been studied for applications to switchable molecular filters, packing materials for separation, and actuators [184,185] whereas the catalytic properties of gold can be used in catalysis.

I. 7. Characterization Methods

Many techniques that were previously applied in experimental studies of nanogold particles and polymeric hydrogel individually can be used for characterization of these new composite materials. We will describe them shortly starting with those that are the scope of our research.

Electrochemical Methods

A fundamental knowledge of molecular mobility and electrostatic interactions is related to diffusion of ions and molecules in a given system. [186] In this research we were interested in transport of small molecules in gels modified with gold nanoparticles. The diffusion coefficient values can be conveniently used as a measure of molecular transport. The main experimental approach is to use electrochemical techniques such as voltammetry and chronoamperometry on microelectrodes. Microelectrode is defined as the electrode having its active (conducting) area in shape of a disk with a radius of a few micrometers. Electrodes with the active surface as small as 10 nm were reported. [187] They usually consist of conducting nanowire imbedded into a tube made of an inert material, such as glass or Teflon. The electrode material may be a conducting inert metal, such as platinum or gold, pyrolytic graphite or glassy carbon, a semiconductor, such as tin or indium oxide, or a metal coated with a film of mercury. [188] The main advantage of microelectrodes over the regular size electrodes is that the current flow is very low and even in solutions of very low conductivity such as organic liquids, the ohmic drop is very small. The other feature related to microelectrodes is that steady state current can be obtained at microelectrode and it makes diffusion coefficient measurements using microelectrode very convenient. [189]

Cyclic Voltammetry and Steady State Voltammetry

When cyclic voltammetry is used at microelectrode, the steady state current independent of time can be achieved. For any reduction process of the kind $O + ne \rightarrow R$ in solution, when the applied potential is sufficiently negative, the reaction can be activated regardless of its kinetics. The concentration of oxidized reagent at the surface of electrode will be quickly reduced to zero. The diffusion equation when disk microelectrode is used can be written in following way:

$$\frac{\partial C_O(r,z,t)}{\partial t} = D\left[\frac{\partial^2 C_O(r,z,t)}{\partial r^2} + \frac{1}{r}\cdot\frac{\partial C_O(r,z,t)}{\partial r} + \frac{\partial^2 C_O(r,z,t)}{\partial z^2}\right] \qquad (1.7.1)$$

where r describes radial position normal to the axis of symmetry at $r = 0$, and z describes linear displacement normal to the plane of the electrode at $z = 0$. The D value is the diffusion coefficient of oxidized species, O, that in the solution has concentration C_O^* and diffuses in time t. To solve this equation the following boundary conditions are needed:

$$C_O(r,z,0) = C_O^* \qquad (1.7.2a)$$

$$\lim_{r\to\infty} C_O(r,z,t) = C_O^* \qquad (1.7.2b)$$

$$\lim_{z\to\infty} C_O(r,z,t) = C_O^* \qquad (1.7.2c)$$

These conditions show that at the beginning of experiment, when $t = 0$, the initial concentration of reagent O is C_O^*. The other conditions express that the areas distant from the electrode are unperturbated by the experiment. The next boundary condition comes from the recognition that can be no flux of O into or out of the mantle, since O does not react there:

$$\left.\frac{\partial C_O(r,z,t)}{\partial z}\right|_{z=0} = 0 \qquad (r > r_0) \qquad (1.7.3)$$

The conditions defined to this point apply for any situation in which the solution is uniform before the experiments begins and in which the electrolyte extends spatially beyond the limit of any diffusion layer. The final condition defines the experimental perturbation and it is as follow:

$$C_O(r,0,t) = 0 \qquad (r \le r_0,\ t > 0) \qquad (1.7.4)$$

The solution to these equations were proposed by Aoki and Osteryoung [190] in terms of a dimensionless parameter, $t = 4D_Ot/r_0^2$, that represents the squared ratio of the diffusion length to the radius of the disk. For any experimental system, τ becomes an index of time, t, and the current-time curve is

$$i = \frac{4nFAD_OC_O^*}{pr_0} f(t) \qquad (1.7.5)$$

At long time, when $t > 1$, the function $f(t)$ can be expressed as:

$$f(t) = 1 + 0.71835t^{-1/2} + 0.05626t^{-3/2} - 0.00646t^{-5/2}... \qquad (1.7.6)$$

When the τ becomes very large, the steady state current is established and the Equation 1.7.5 reduces to the following formula:

$$i_{ss} = 4nFD_OC_O^*r_0 \qquad (1.7.7)$$

This equation shows that diffusion coefficient can be determined from the steady state current in a straightforward way.

Chronoamperometry

The advantage of chronoamperometry is that it can be used to determine diffusion coefficient of probe molecules when their concentration is not known. In chronoamperometric measurements current is sampled in a function of time when two potentials are applied. For any general reaction $O + ne \rightarrow R$, potential E_1 is chosen in the region where faradaic process does not occur. Potential E_2 is negative enough for the reaction to occur. The dependence of current vs. time is pretty complex and it covers three time regimes. The current-time curve is given by Equation 1.7.6. Shoup and Szabo [191] provided a single empirical relationship covering the entire range of τ with an accuracy better than 0.6% at all points.

$$\frac{I(t)}{I_{ss}} = 0.7854 + 0.8862t^{-1/2} + 0.2146e^{-0.7823t^{-1/2}} \qquad (1.7.8)$$

For the short time region, ($t < \frac{r^2}{D} \cdot 10^{-4}$, for < 1% error), the diffusion layer remains thin compared to r_0, the radial diffusion does not manifest itself appreciable, and the diffusion has a semi-infinite linear character. Therefore, the corresponding current is Cottrell current. The normalized time dependent current, $I(t)/I_{ss}$, within the 1% of the deviation of Equation 1.7.8 is given by [192]:

$$\frac{I(t))}{I_{ss}} = 0.7854 + \left(\frac{p^{1/2}}{4}\right) r_d (Dt)^{-1/2} \qquad (1.7.9)$$

When the experiment enters the intermediate time regime, the diffusion layer is getting thicker and its thickness is close to r_0 and radial diffusion become important. The current is larger than that of pure linear diffusion. The current density on the electrode is not

uniform anymore. The current density on the edge is larger than the central area because the edge is more accessible geometrically to the diffusing electroactive molecules and ions.

For long times, ($t > \frac{r^2}{D} \cdot 10^2$, for < 1% error), the diffusion field expands and its thickness is much larger than r_0. The current approaches to the steady state condition. The normalized time dependent current, $I(t)/I_{ss}$, within the 1% of the deviation of Equation 1.7.6 is given by:

$$\frac{I(t)}{I_{ss}} = 1 + \frac{2}{p^{3/2}} a(Dt)^{-1/2} \qquad (1.7.10)$$

where $I(t)$ is the current at time t, I_{ss} is the steady state current, a is the radius of the electrode. A plot of $I(t)/I_{ss}$ vs. $t^{-1/2}$ yields a straight line, whose slope can be used to determine the D without knowing the concentration of electroactive probes.

The other electrochemical techniques commonly used for transport studies in polymeric substances include conductivity measurements, [193] scanning electrochemical microscopy, [194] and transient generation-collection methods. [186] These methods provide very fast, relatively inexpensive, and accurate sources of information on transport properties of polymeric systems.

Other Methods

The optical properties of stimuli responsive polymeric gels with incorporated gold nanoparticles were analyzed by UV spectroscopy since gold nanoparticles show strong absorption of visible light. The hybrid materials exhibit enhanced optical limiting in comparison to individual nanoparticles, presumably due to the interparticle electromagnetic interactions between particles in close proximity that can be also easily

detected by UV-vis spectroscopy. Direct imaging of gold particles imbedded into hydrogels was possible by various reliable, high resolution microscopies. Transmission electron microscopy, TEM, is the one that is most commonly used. To see the poly-NIPA layer, the samples were stained with phosphotungstic acid. [146] The morphology and elemental composition of the composite polymeric gels were characterized by field emission scanning electron microscopy (FE-SEM), and energy-dispersive X-ray scattering (EDX), respectively.

The average particle size of gold nanoparticles and morphological changes that occurred in response to variations in temperature and pH were evaluated using dynamic light scattering (DLS).

Techniques that bring information of the polymer include IR spectroscopy. The amount of poly-NIPA coating on the gold core surface was determined by a thermogravimetric analysis (TGA). [195] The molar mass and the polydispersity of each poly-NIPA sample were determined by size exclusion chromatography (SEC), [195] gel permeation chromatography. [145] In situations when determination of the molar masses by size exclusion chromatography is not possible due to the partial adsorption of the polymers on the column material, the ^{1}H NMR translational self-diffusion measurements can be applied instead. Self-diffusion coefficients in water allow estimating the magnitude of the average molar masses. It is possible to evaluate a hydrodynamic radius for the polymers considered as random coils in a good solvent, and to convert the corresponding characteristic radii into polymer lengths or conversely to an average molar mass from the appropriate scaling law. [70] Photon correlation spectroscopy was used to determine hydrogel particle size and polydispersity. [196]

The volume phase transition can be studied by such techniques as fluorescence spectroscopy, dynamic light scattering (DLS), [197] differential scanning calorimetry (DSC) [198] and fluorescence spectroscopy. [199]

II. STATEMENT OF OBJECTIVES

In today's world, new materials are fundamental for development and advancement of new technologies. Two classes of materials that have recently drawn a great deal of attention are polymeric cross-linked polymeric gels and colloidal gold nanoparticles. If the specific characteristics of the gels, such as their response to external stimuli and the unique properties of gold nanoparticles such as surface plasmon resonance can be combined in a novel material, it would open new possibilities in many areas of biotechnology such as drug delivery systems and biosensors, and other sensing applications.

The objectives of this work include development of the methodology for the synthesis of temperature-responsive poly(*N*-isopropylacrylamide), NIPA, polymeric gels modified with colloidal gold nanoparticles and their characterization. We will investigate the effect of gold nanoparticles on the temperature of the volume phase transition of the NIPA polymeric gels as well as effect of polymeric matrix on optical properties of nanogold particles. We will study transport properties of these new materials in terms of the diffusion of small molecular probes in polymeric matrixes. We will investigate the separation properties of these polymeric materials; we will analyze the influence of the volume phase transition of the distribution of molecular probes in collapsed gels and expelled solutions. The knowledge of mass transport properties of the gold-modified polymeric gels and their potential separation properties is of great importance in their potential applications as drug delivery systems, sensors or electrolytes for batteries. To the best of our knowledge, there are no reports on these properties of polymeric gels modified with gold colloidal particles.

We will also determine the effect of the ionic strength on the volume phase transition temperature and mass transport in the gels. We will compare results obtained for gold modified materials with these for pure polymeric gels to evaluate the effects of gold on the properties of the gels.

Our main experimental approaches will include variety of electroanalytical techniques such as voltammetry and chronoamperometry with regular size- and microelectrodes and spectroscopic and optical methods.

We expect the results of this work to contribute to the better understanding of the properties of temperature responsive polymeric gels including their modification with metal nanoparticles and to open possibilities of their new applications in sensors and drug delivery systems.

III. EXPERIMENTAL

III. 1. Reagents

Tetrachloroauric acid ($HAuCl_4 \cdot 3H_2O$), sodium citrate, *N*-Isopropylacrylamide (NIPA), *N*,*N'*-methylenebis-acrylamide (BIS), *N*,*N*,*N'*,*N'*-tetramethylethylenediamine (TMED), ammonium persulfate ($(NH_4)_2S_2O_8$) and lithium perchlorate ($LiClO_4$) were purchased from Aldrich. 1,1'-Ferrocenedimethanol ($Fc(MeOH)_2$) and sodium borohydride ($NaBH_4$) were purchased from Fluka. All chemicals were of 99.0 - 99.9% grade and they were used as received. Gels and solutions were prepared using high purity water (18 MΩ cm, Milli-Q, Millipore system).

III. 2. Apparatus

All electrochemical experiments were performed using a Perkin-Elmer, PARC potentiostat (model 283) and controlled via a PC computer. Cyclic voltammetry and staircase voltammetry measurements were carried out in a jacketed glass cell with a three-electrode system consisting of a Pt pseudoreference electrode, a Pt wire counter electrode, and a Pt disk (0.5 cm^2) or a Pt microdisk (d = 11 μm) (Project Ltd., Warsaw, Poland) working electrodes. A refrigerated circulator (Isotemp model 1016P, Fisher Scientific) controlled the temperature of the cell. For chronoamperometry measurements a sample was placed in a Faraday cage to eliminate noise. Before each experiment, the working electrode was polished with aluminum oxide powder of various sizes (down to 0.05 μm) on a wet pad, rinsed with water, and then air-dried. The surface of a microelectrode was inspected optically with a Nikon model Epiphot 200 microscope.

The UV-vis spectra were recorded using a Hitachi U-2010 spectrophotometer with polystyrene cuvetts (light path b = 1 cm).

Transmission electron microscopy (TEM) images were obtained using a JEOL electron microscope. A small drop of a sample (gold suspension or ground polymer reswollen in water) was placed on a copper-coated Formvar grid and excess solution was wicked away by a filter paper. The grid was subsequently dried in air, covered with carbon and imaged on a transmission electron microscope. The accelerating voltage was 80 kV.

IV. SYNTHESIS OF NIPA GELS MODIFIED WITH GOLD NANOPARTICLES

IV. 1. Synthesis of Gold Nanoparticles

Colloidal gold nanoparticles with average diameter of 2.7 nm, 13 nm and 18 nm, were synthesized in aqueous solutions by chemical reduction of $HAuCl_4 \cdot 3H_2O$ with Na_3-citrate. Na_3-citrate also provided stabilizing layers around the colloidal gold particles. Water was chosen as the solvent due to simplicity of use and well-known swelling process of the NIPA polymer. Gold colloids were prepared according to the protocols already presented in the literature. [78,79] All glassware was thoroughly cleaned in aqua regia (3 HCl:1 HNO_3, v/v), rinsed in distilled water and air-dried prior use. To prepare the solution of 2.7 nm-diameter particles, called "seeds", 5 mL of 1% aqueous $HAuCl_4 \cdot 3H_2O$ was added to 500 mL of vigorously stirred H_2O. After 1 minute 5 mL of 1% aqueous Na_3-citrate was added followed one minute later by addition of 5 mL of 0.075% $NaBH_4$ in 1% Na_3-citrate. The mixture was stirred for additional 5 minutes and stored at 4 °C until needed. The number of gold atoms (N) in each cluster can be calculated from Equation 4.1.1, [200]

$$N = \frac{r\left(4pr^3/3\right)}{M_{Au}/N_A} \qquad (4.1.1)$$

where r is the density of gold (19.3 g/cm^3), r is the radius of gold particle in cm, M_{Au} is the atomic weight of gold (196.97 amu) and N_A is Avogadro's number ($6.02 \cdot 10^{23}$) and it was found to be $6.8 \cdot 10^2$ Au atoms/nanocrystal. On the basis of the particle size determined from the transmission electron micrographs (d = 2.7 nm determined from TEM images) and the initial gold concentration in $[AuCl_4]^-$ complex ($[AuCl_4]^-$ = 25.4

mM), the nanocrystal density in the prepared suspension was estimated to be $3.5 \cdot 10^{-7}$ mol nanocrystals/L. Calculations were done with assumption that all gold in $[AuCl_4]^-$ complex ion is reduced to Au^0. The pH of such prepared colloid was measured 5.07.

13 nm Au particles were prepared in a 1-L round-bottom flask equipped with condenser. 500 mL of 1 mM $HAuCl_4 \cdot 3H_2O$ was brought to 100 ^oC under refluxing conditions. While stirring vigorously, 50 mL of 38.8 mM sodium citrate was quickly added, resulting in color changes of the originally yellow solution to transparent, to dark blue/gray, and finally, to burgundy red. Boiling was continued for 10 min. Then the heating mantle was removed and the mixture was stirred continuously for additional 15 min. Transmission electron microscopy (TEM) indicated a particle size of 13 nm. The initial gold concentration in $[AuCl_4]^-$ complex ion was 1 mM and the nanocrystal density was estimated to be $1.0 \cdot 10^{-8}$ mol nanocrystals/L with $6.8 \cdot 10^4$ Au atoms/nanocrystal calculated from Equation 4.1.1. The pH of this colloid solution was measured 5.58 (literature reports ~5 [201]) and its ionic strength was reported I = 15.8 mM. [201]

Similar procedure was applied to synthesize 18 nm Au particles. 500 ml of 0.01% was brought to boil with vigorous stirring in a 1-L round-bottom flask equipped with a condenser. 7.5 mL of 1% Na_3-citrate was added resulting in a blue solution which eventually turned red-violet. Boiling continued for an additional 10 min, the heating source was removed and the colloid was stirred for another 15 min. The initial gold concentration in $[AuCl_4]^-$ was 0.254 mM and the nanocrystal density was estimated $2.1 \cdot 10^{-9}$ mol nanocrystals/L with $1.8 \cdot 10^5$ Au atoms/nanocrystal calculated from Equation 4.1.1. TEM data indicated an average diameter of 18 nm. The pH of this colloidal suspension was 4.37.

The volume ratio of gold to water was $2.5 \cdot 10^{-6}$ for 2.7 and 18 nm colloids and $9.3 \cdot 10^{-6}$ for 13 nm colloidal solution. The volume fraction was calculated from the initial concentration and volume of the gold chloride used to prepare the colloidal solution.

The gold nanoparticles used in this work, with diameters between 2.7 and 18 nm, are much larger than these called "gold clusters" such as thiolate-stabilized monolayer protected clusters reported as containing from 11 to 145 Au atoms per cluster. [202]

IV. 2. NIPA Gel - Preparation

The NIPA polymeric gel was synthesized by a conventional free radical polymerization method according to Petrovic and Zhang with some modifications. [203] 8.7 g of NIPA monomer and 0.1554 g of *N,N'* - methylenebisacrylamide (BIS) (cross-linker) were dissolved in an organic reaction kettle containing 350 mL of deionized water. The mol fraction of each monomer was 0.99:0.01 for NIPA and BIS, respectively. The pregel solution was placed in a water bath at temperature 15 ^{o}C and it was deoxygenated with argon for 30 min. Then 49.8 mg of ammonium persulfate (initiator) was added to the solution followed by addition of 560 µL of *N,N,N',N'* - tetramethylethylenediamine (TEMED) (accelerator) from syringe. The gel formed quickly (less than 1 hour) and was allowed to sit overnight before purification process.

IV. 3. Purification of NIPA Gels

The purification of the gels was a necessary step to eliminate the presence of reactive monomers or initiator that could react with the electroactive probe, change its concentration and complicate our interpretation of the transport properties of these materials. Gel was purified by heating it to approximately 80 °C that is above the

temperature of the volume phase transition. The gel shrunk and it expelled solution carrying unreacted reagents and impurities. This solution was poured out. Then several hundred milliliters of deionized water were added to collapsed gel and allowed to reswell at room temperature for few hours. The purification process that can be compared to the squeezing and refilling of a sponge was repeated 5 times. Once washing was completed the gel was dried in an oven at 80 °C for couple of days. The hard, dark violet polymeric material was ground to a fine powder and as that used for the further analysis.

IV. 4. Incorporation of Gold Nanoparticles into Polymer Matrix

To introduce gold colloid into the NIPA gel several different methods were tested. The simplest one consisted of an addition of solution of colloidal gold into previously synthesized and ground NIPA polymer powder. The resulting gel was nonuniform and as that, did not have any further value. The other methods were based on an addition of the ground polymer either to the solution of $HAuCl_4$ before heating or to the boiling solution of $HAuCl_4$ just before adding the citrate. In each case the resulting gel was nonuniform. The last method consisted of introducing the gold colloid into a gel by mixing it with the components of a polymerization mixture. The NIPA monomer and *N*,*N*'-methylenebisacrylamide (BIS) (cross-linker) were dissolved in a reaction kettle containing a solution of colloidal gold before the polymerization was initiated by ammonium persulfate. 13 nm gold colloids were diluted adequately to have the same initial concentration of $[AuCl_4]^-$ as in colloid of 2.7 and 18 nm. This method yields uniform, well-defined polymeric network with incorporated gold nanoparticles. The formed NIPA gels with incorporated gold nanoparticles were purified by the method described

previously and schematic synthesis of NIPA-Au polymer crosslinked with *N,N'*-methylenebisacrylamide is shown in Figure 4.1.

Upon polymerization the color of gels containing 2.6 and 13 nm gold nanoparticles changed from red to purple. For 18 nm particles this change was much less profound. It can mean that the distance between particles decreased since the volume fraction of dispersed Au particles increased. Also the colloidal solutions are sensitive to organic substances that cause the particles to conglomerate resulting in bluish tint. [204]

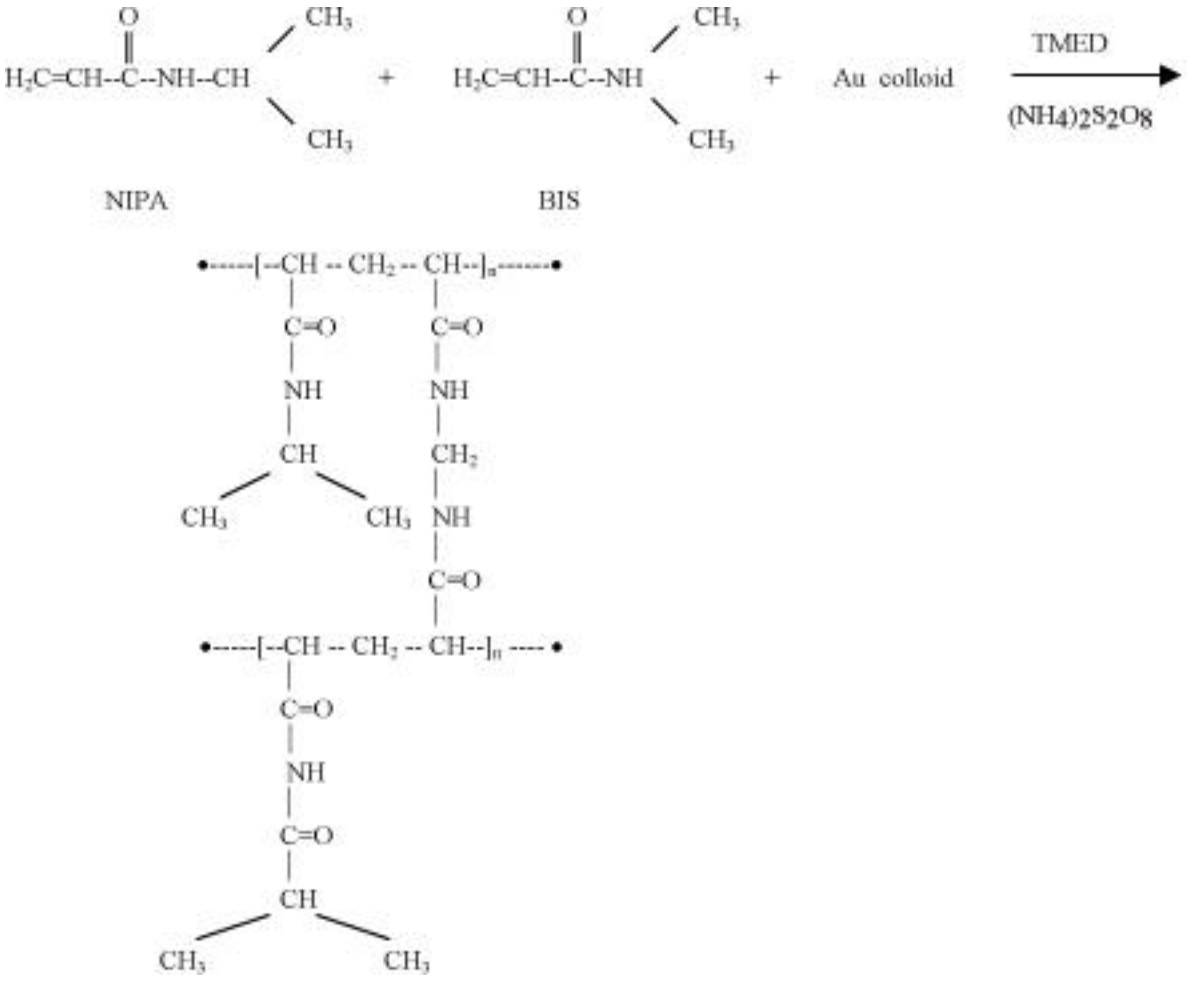

Figure 4.1. Schematic representation of synthesis of NIPA-Au gel.

V. CHARACTERIZATION OF NIPA GELS MODIFIED WITH GOLD NANOPARTICLES

V. 1. Temperature of Volume Phase Transition

Hydrogels containing NIPA exhibit a temperature-induced reversible volume-phase transition from a swollen to a collapsed state. The temperature of this transition is called lower critical solution temperature (LCST) or cloud point, and for NIPA gels was reported as 32 ^{o}C. [47] Below 25 °C, water is a relatively good solvent for NIPA polymer and the suspension of the gold nanoparticles appears as a transparent solution. In the transition regime, water becomes a poor solvent as polymer-water H-bonds are broken and NIPA undergoes conformation changes and exposes much of its hydrophobic surface, including both intrachain "coil-to-globule" transitions and interchain self-association. Intrachain collapse causes the individual polymer to become hydrophobic, while interchain self-association within a single particle drives the surface of the gel particle to switch from hydrophilic to hydrophobic. [183] The temperature of this transition was determined for neat and gold modified NIPA gels. A small sample of a swollen gel (approximately 5 mL) in the test tube was placed in a Fisher Scientific circulator cell and the visual appearance of the sample was monitored. The temperature was raised and cloud point that is the temperature of the phase transition was determined as the one, at which turbidity first became apparently visual. Measurements were performed for freshly prepared neat polymer and gels containing 2.7, 13 and 18 nm gold particles. The temperature at which the NIPA gels become turbid was 31.8 ± 0.2 °C, whereas the complete volume phase transition was observed at 34.8 ± 0.2 °C. Effect of polymer concentration was determined for samples containing 2 – 6 wt % of neat

polymer and polymer modified with gold particles of 2.7, 13 and 18 nm size. An average temperature of the volume phase transition was 32.2 ± 0.4 °C. This temperature is the same within experimental error as that for the neat NIPA gel and it did not change with various concentrations of polymer. It was not influenced by the size of gold nanoparticles. The change of the volume phase transition temperature of NIPA gels is expected when a degree of crosslinkage changes, or a type of a crosslinking agent is changed. [205,206] Clearly, gold nanoparticles do not interact very strongly with poly-NIPA segments, and do not participate in a crosslinkage of the polymeric structure. As the result of the volume phase transition approximately 93% of solution mass was expelled from each sample.

V. 2. UV-vis and TEM Characterization

UV-vis spectroscopy and transmission electron microscopy (TEM) were used to determine shape, size and size distribution of gold nanoparticles in colloids and in polymeric gels.

UV-vis Spectroscopy

As described in section I. 5 the surface plasmon resonance, SPR, absorption band becomes obvious only when the gold nanoparticle core diameter is larger than 2 nm and the SPR absorption band can be identified from both, the sols and gels in which such particles are embedded. [154,207,208] UV-vis experiments result in the values of maximum absorbance wavelengths that are good indicators of the size of gold nanoparticles. It was shown that as the diameter of gold colloidal particles increases, the absorption peak shifts to longer wavelengths. [209] In our experiment UV-vis spectroscopy was used to confirm

the size of gold nanoparticles in an aqueous colloidal systems and NIPA polymeric gels. Figure 5.1 shows the absorption spectra for 2.7, 13 and 18 nm Au nanoparticles in sols recorded at room temperature. Pure water was used as the background systems. The gold concentration in NIPA gels was fixed to correspond to 0.25 mM of initial concentration of gold in $[AuCl_4^-]$ complex.

Figure 5.1 shows that as the diameter of the particles increases, particle plasmon resonance shifts toward the red end of the spectrum and the peak slightly broadens. The peak width at the half maximum (PWHM) is defined as twice the difference between wavelength of maximum absorbance, λ_{max}, and the wavelength of half maximal absorbance to the red of λ_{max} and it reflects the peak broadening. [210] The largest value of PWHM, 99 nm, for 2.7 nm particles compared to 86 and 92 nm for 13 and 18 nm particles, respectively, is the result of wider size distribution among spherical particles. Peak broadening can also be the consequence of the presence of elliptical particles. The plasmon band is affected by the dispersed metal particle size, the relative permittivity of the surrounding matrix and the volume fraction of metal phase. [211]

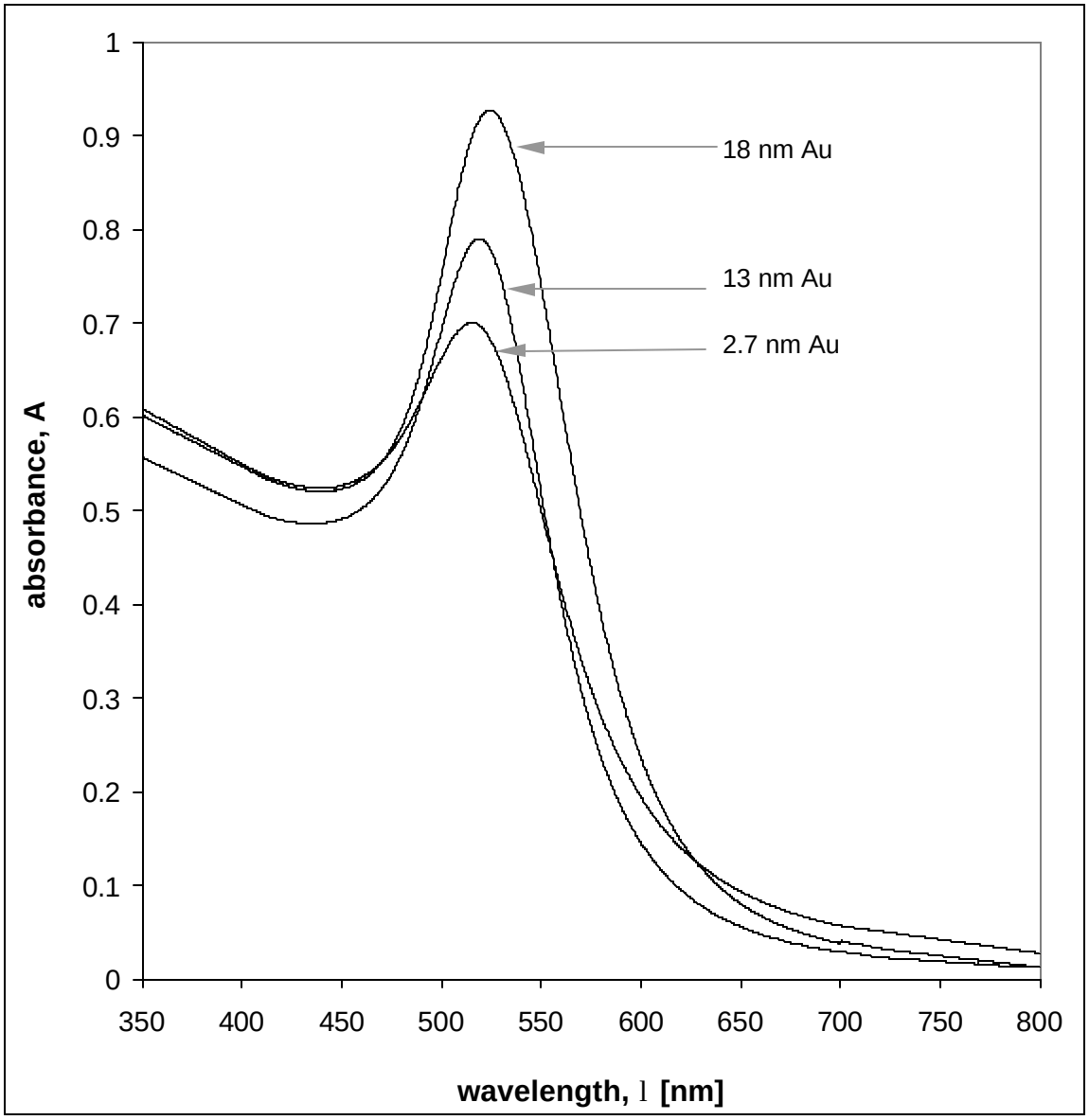

Figure 5.1. UV-vis spectra of 2.7, 13 and 18 nm colloidal gold particle suspensions in an aqueous solution.

UV-vis spectra of colloidal gold nanoparticles with diameter of 2.7, 13 and 18 nm incorporated into polymeric matrix are presented in Figure 5.2. The wavelength of maximum absorbance for gold in the NIPA gel is shifted toward longer wavelengths and the plasmon band decreases in intensity comparing to the neat colloid. The decrease in intensity arises because the refractive index of the polymer is different from that of water and gold nanoparticles, which leads to an increase in UV scattering. [62] The red shift can be attributed to the change of dielectric constant of the surrounding medium [145] but it also indicates that there probably is a dipole-dipole interaction between particles in close proximity. [149] For 13 nm Au there is plasmon band seen in the spectrum as a shoulder at λ=600 nm and it is most likely due a colloidal aggregation of particles in gel. [212]

The wavelengths of maximum absorbance for 2.7, 13 and 18 nm gold particles in colloids and gels are presented in Table 5.1 and for the sols these results are in good agreement with the literature. [78,79] For gold nanoparticles in gels Tenhu *et al.* [174] reported the red shift of the SPR by 20 nm comparing to gold sols, which is more than the one observed in our experiments.

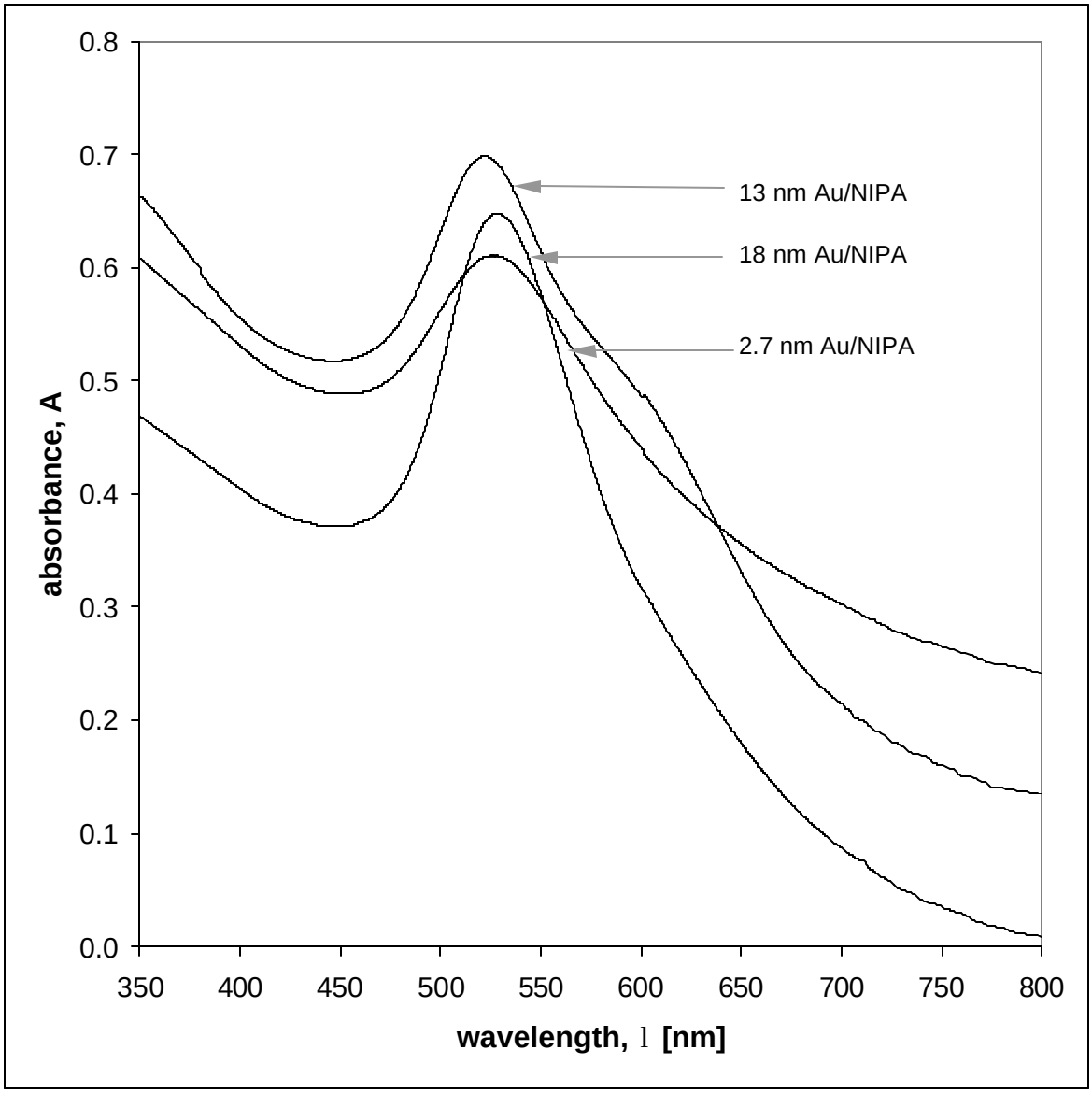

Figure 5.2. UV-vis spectra of colloidal gold nanoparticles incorporated into NIPA (spectra collected before drying).

Table 5.1

Experimental values of the wavelengths corresponding to maximum absorbance in sols and NIPA gels modified with gold nanoparticles.

diameter of Au particles [nm]	λ_{max}	
	colloidal suspensions	**NIPA-gels**
2.7	515 nm	521 nm
13	519 nm	523 nm
18	525 nm	528 nm

Changing the Au colloid to water ratio, we prepared series of solutions in which concentration of gold was varied. The UV-vis spectrum for each diluted solution was recorded. Then these solutions were used in preparation of NIPA gels and the gels were analyzed by UV-vis spectroscopy. The linear response of the absorbance as a function of Au concentration was obtained in analyzed concentration range. For 2.7 nm and 13 nm particles in gel versus neat colloidal suspension, molar extinction coefficient decreased by approximately 40% and 60%, respectively. The absorbance was found to increase linearly when the concentration of polymer in the sample varied between 2 and 6 % wt. The sample of appropriate calibration curves for 13 nm Au are shown in Figure 5.3.

Stability of neat colloidal suspensions and NIPA gels modified with gold nanoparticles was monitored over a period of fourteen weeks. This study showed that the colloids do not agglomerate over time without the exposure to external stimuli such as light. If exposed to light, flocculation occurred but the wavelength of plasmon band measured for gold suspension did not change. Intensity of peak decreased by less than 10%.

Polymeric gels modified with gold were exposed to light, and their behavior was monitored as well. Their wavelength of maximum absorbance and intensity did not change during the period of study, indicating that the new material is stable over time.

The solutions expelled from the gels modified with gold nanoparticles during the washing step were analyzed by UV-vis spectroscopy. The recorded spectra have not shown any signs of gold absorbance. This indicates that gold nanoparticles are retained in the gel and they are not rinsed out during the purification step, and consequently during the volume phase transition process.

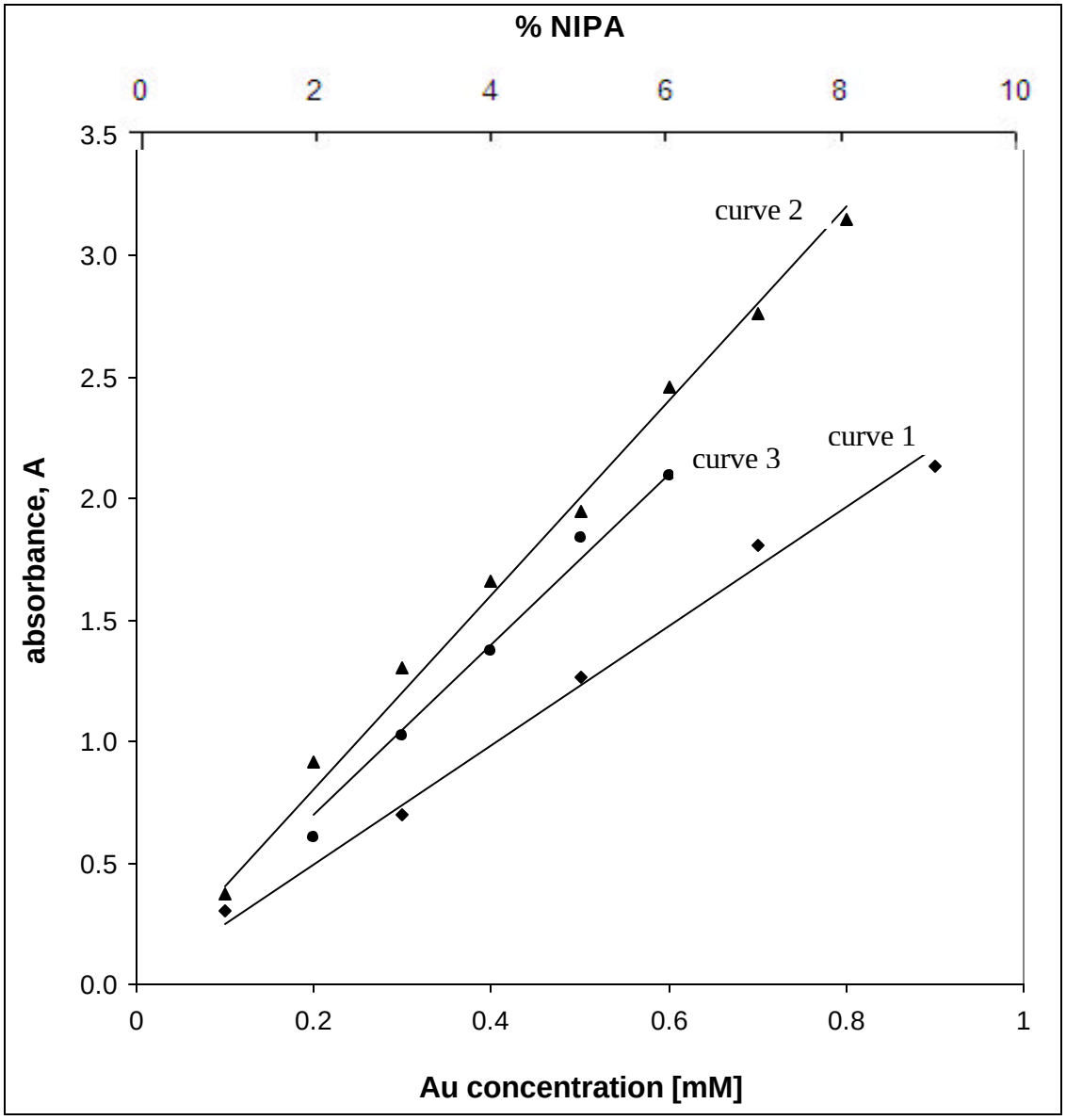

Figure 5.3. Dependence of the UV-vis absorbance on the concentration of 13 nm Au colloidal particles in sol (■) and NIPA gel (▲) media (curve 1 and 2 – absorbance vs. concentration of Au). Dependence of UV-vis absorbance on the concentration of NIPA polymer (●) (curve 3 – absorbance vs. % NIPA)

TEM Analysis

The average diameter of the colloidal gold nanoparticles in solution and in polymeric matrix was determined by transmission electron microscopy. Figures 5.4 (A-C) present TEM images of spherical and monodispersed gold particles in colloidal solution. The corresponding size distributions are shown as histograms. A fairly narrow peak distribution for larger particles and slight broadening for 2.7 nm particles was observed and it is in good agreement with the values of peak width at the half maximum reported in chapter V. 2. The TEM-derived particle diameter is 2.7 ± 0.5 nm (723 particles counted), 13.0 ± 1.7 nm (602 particles counted) and 18.0 ± 2.7 nm (666 particles counted). Less than 30% of 18 nm particles are elliptical with maximum axes ratio 1:1.5.

Image of 13 nm Au particles in the NIPA gel and their size distribution is shown in Figure 5.5. The average diameter was found to be 14.0 ± 1.5 nm based on 115 particles. The images were taken at five different spots of each analyzed grid.

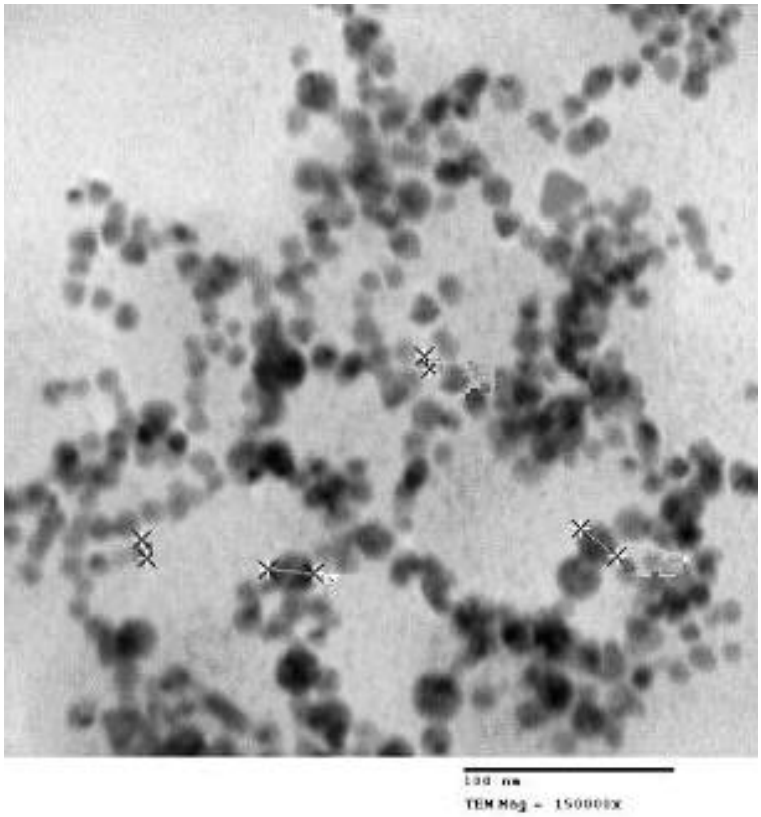

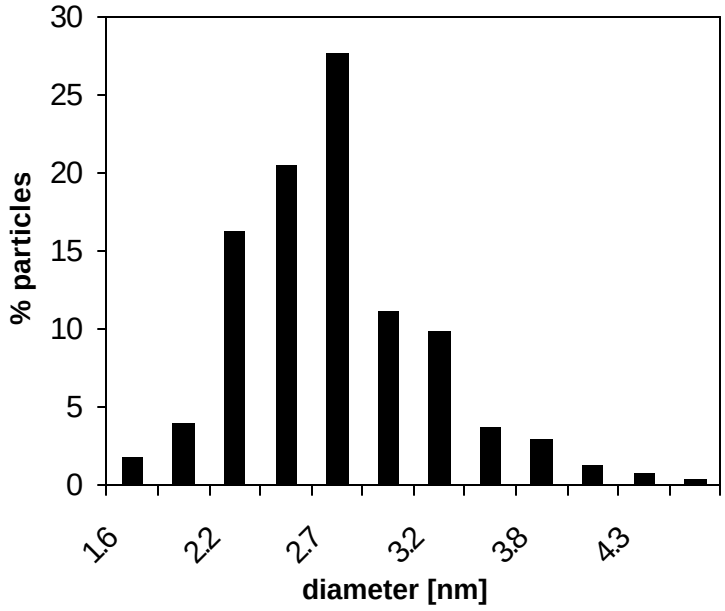

Figure 5.4-A. TEM image and size distribution of 2.7 nm Au particles in colloidal solution.

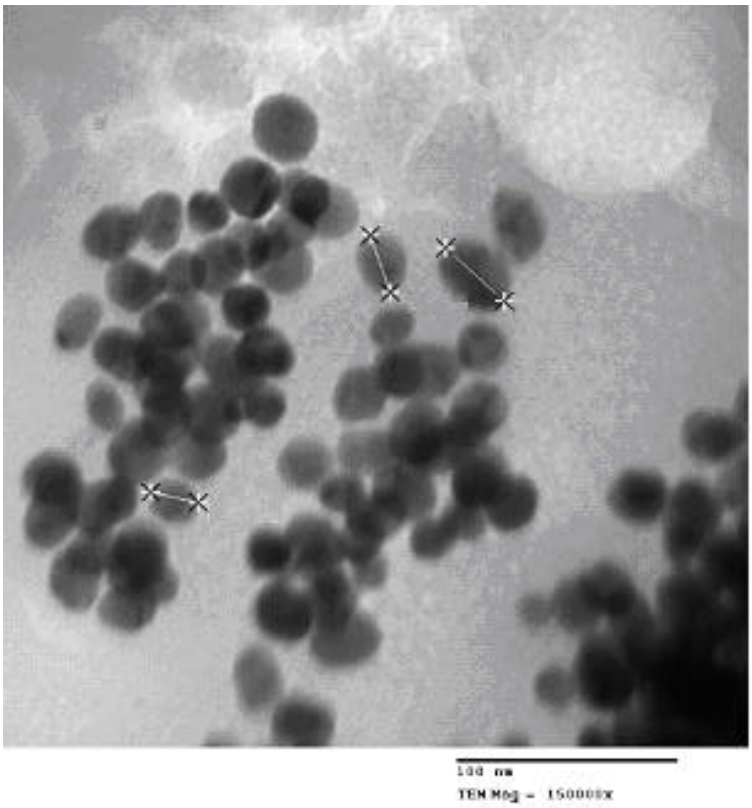

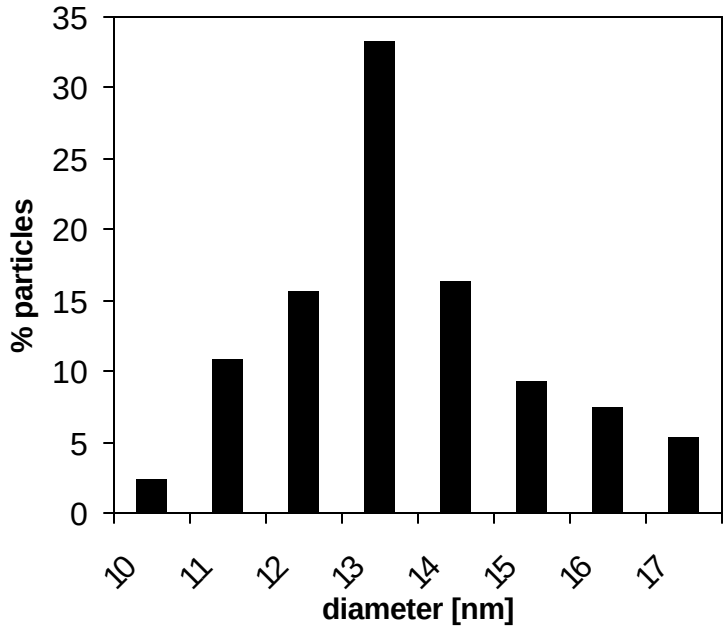

Figure 5.4-B. TEM image and size distribution of 13 nm Au particles in colloidal solution

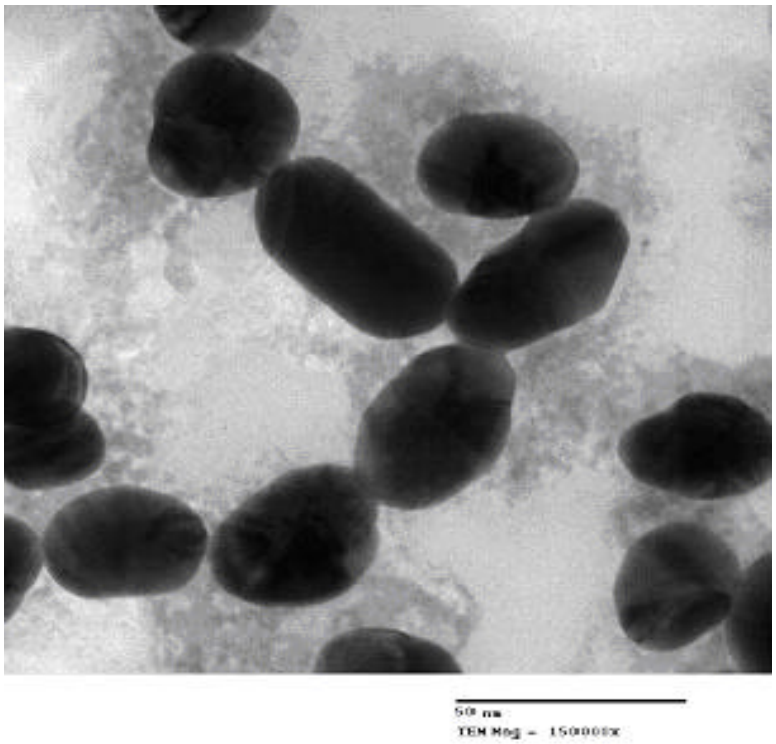

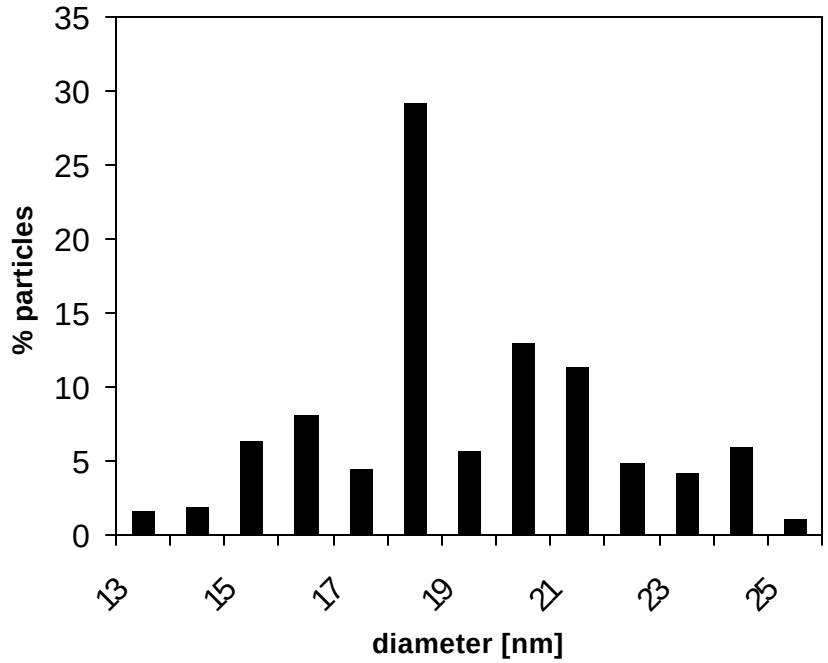

Figure 5.4-C. TEM image and size distribution of 18 nm Au particles in colloidal solution

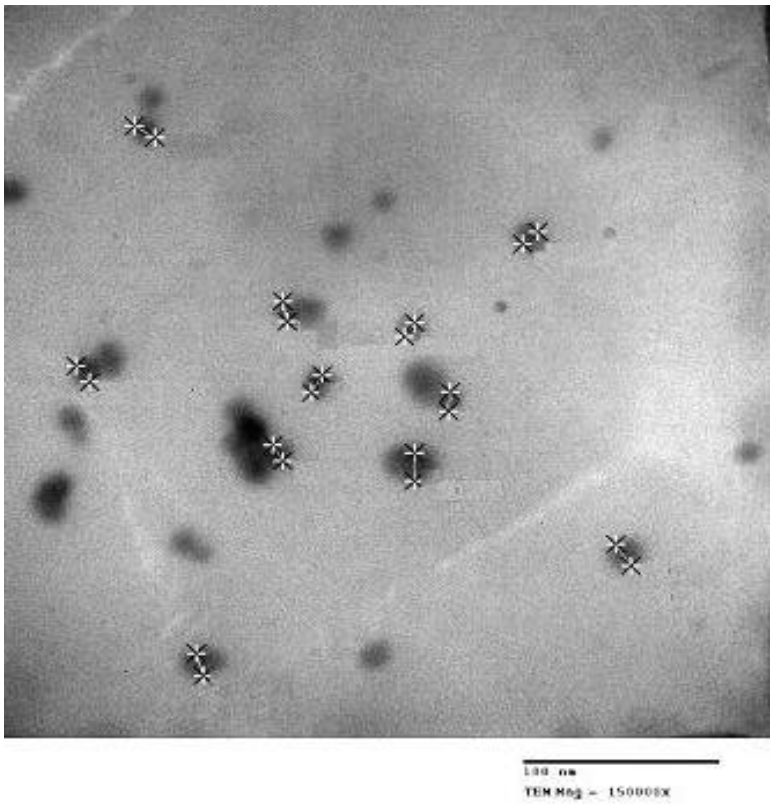

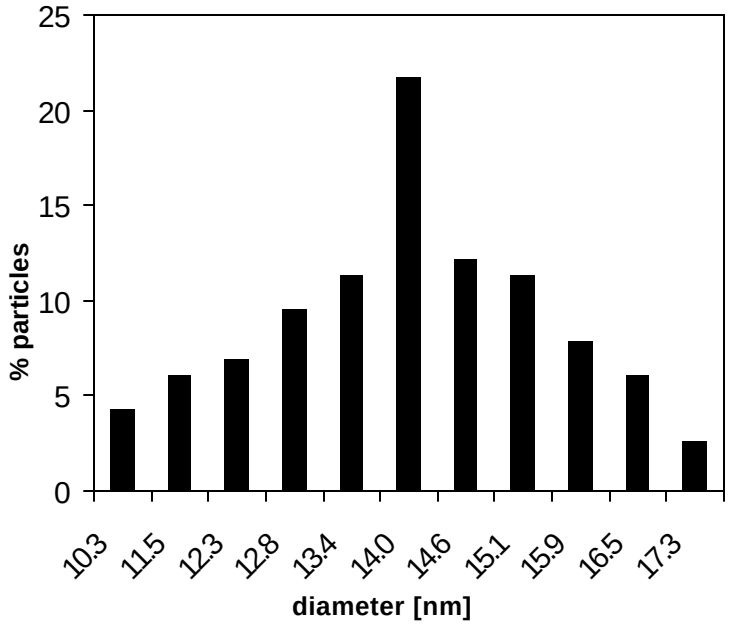

Figure 5.5. TEM image and size distribution of 13 nm Au particles in NIPA gel

V.3. Potential Window

To determine the potential window for neat NIPA gels and NIPA gels modified with gold nanoparticles, cyclic voltammetry at Pt disk electrode was applied. The reference electrode was Pt-wire. The current-potential signals were measured at 25 °C in the presence of 5 mM $LiClO_4$ used as the supporting electrolyte. Colloidal suspensions were degassed with argon. The potential windows were compared with the ones in oxygenated solutions and sample voltammograms are shown in Figure 5.6. The small peak observed at approximately –0.3 V is from the reduction of oxygen. Figure 5.7 shows cyclic voltammograms in 4% NIPA gels with gold particles of different sizes. Potential window of unmodified gel is also presented. As one can see, there is no significant influence of the presence of gold nanoparticles on the potential window.

Figure 5.8 presents the effect of polymeric matrix and the concentration of NIPA in the gel network on potential window. The cyclic voltammograms were recorded in samples of NIPA gels modified with 13 nm Au of various concentrations of NIPA and compared with that in 13 nm colloidal gold sol. Oxygenated colloid of 13 nm particles was used as the background. The currents are lower in NIPA gels; however, the difference is not very significant.

All samples of colloidal gold nanoparticles in aqueous sol and in NIPA gel, as well as neat gel are electrochemically inactive in potential range between +1.0 V and –0.1 V. It means that neither gold nor NIPA matrix should interfere with our further experiments with electroactive probe.

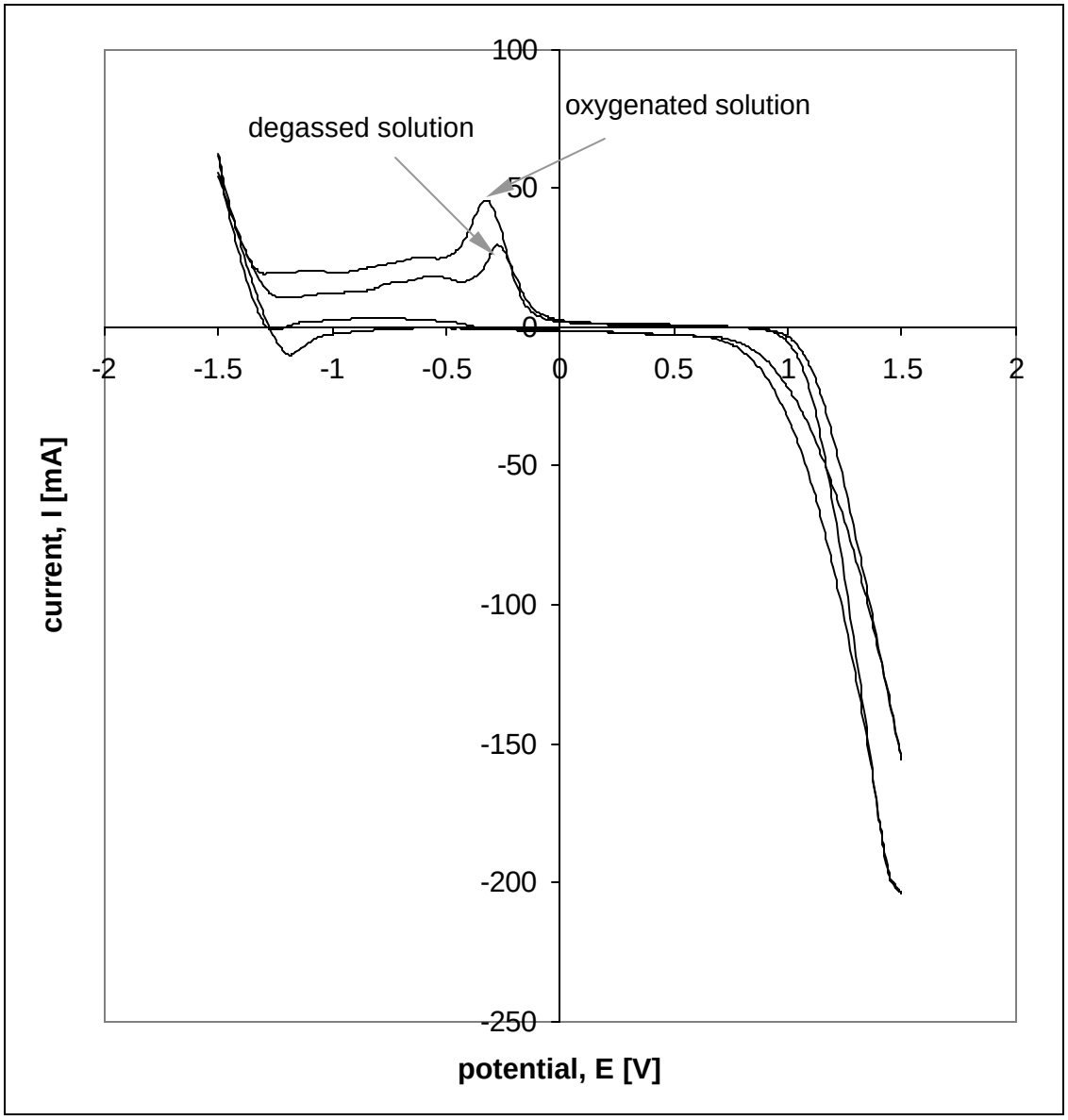

Figure 5.6. Effect of oxygen on potential window of 18 nm gold colloid in 5 mM $LiClO_4$. (Working electrode – Pt disk, reference electrode – Pt wire, T = 25 °C).

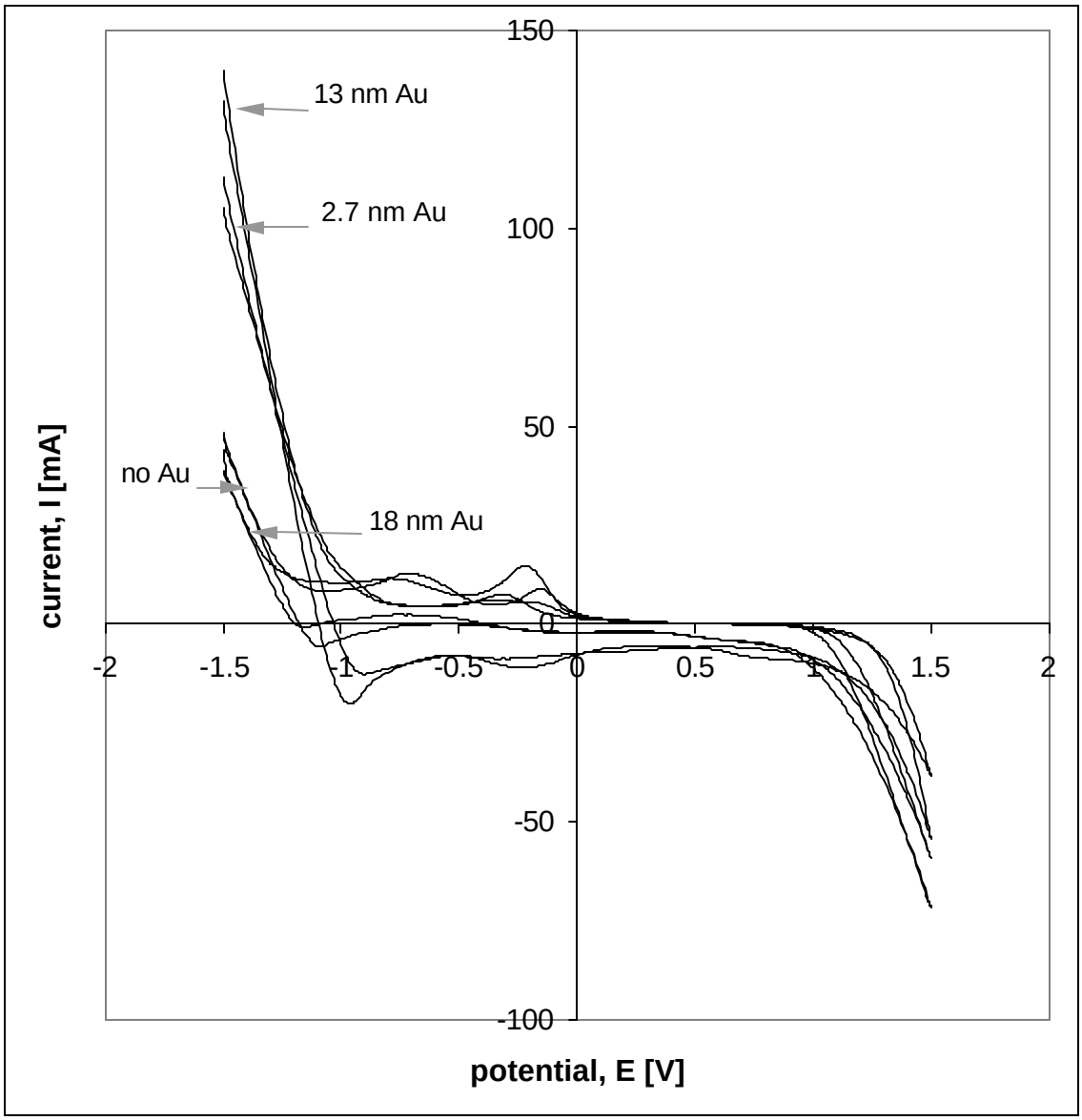

Figure 5.7. Effect of Au particles size in 4% NIPA gel on potential window. (Working electrode – Pt disk, reference electrode – Pt wire, T = 25 °C).

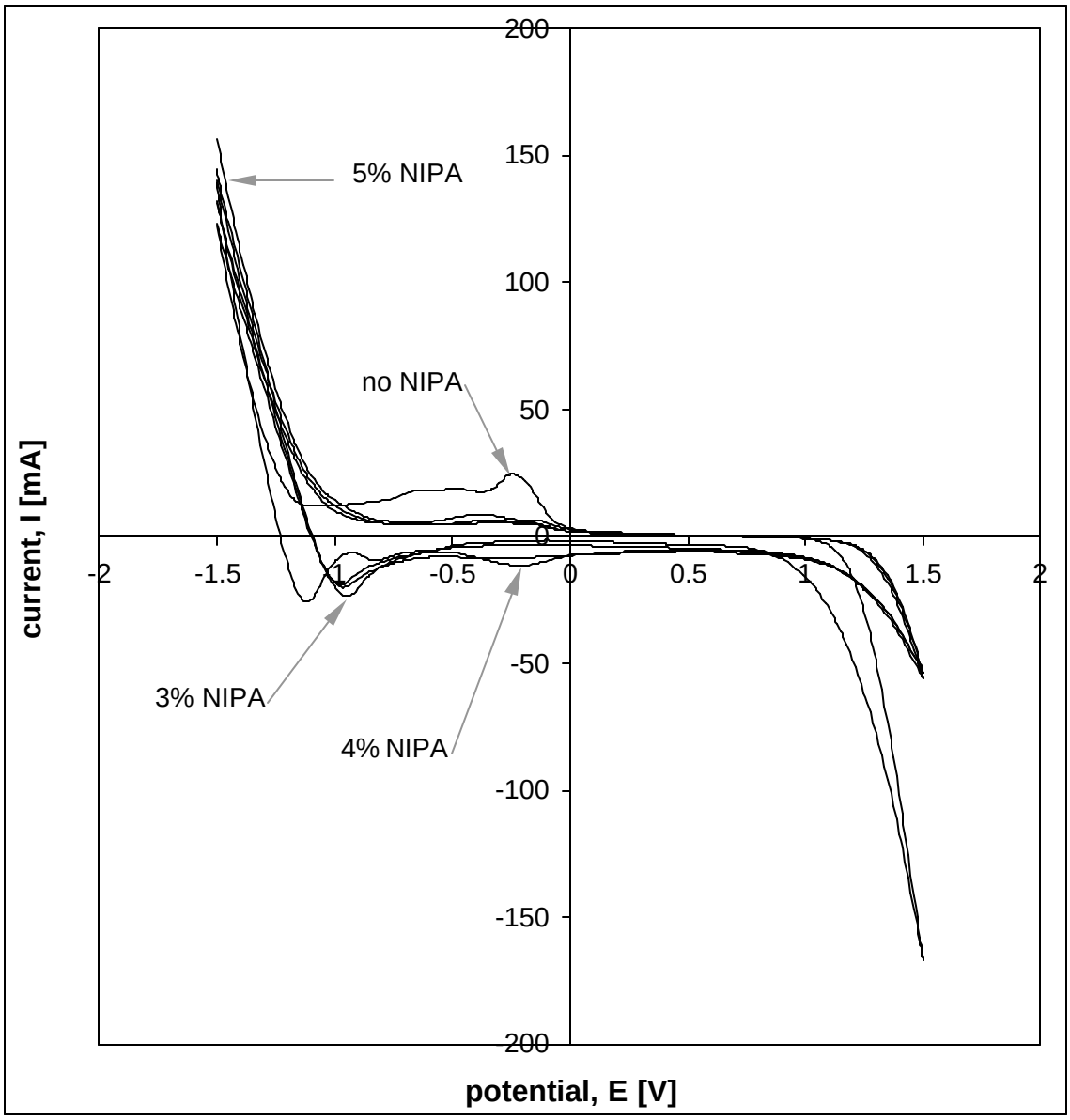

Figure 5.8. Effect of NIPA matrix modified with 13 nm gold particles on potential window. (Working electrode - Pt disk, reference electrode – Pt wire, T = 25 °C); background – oxygenated 13 nm Au colloid.

VI. TRANSPORT STUDIES

VI. 1. Preliminary Voltammetric Measurements

Diffusion of $Fc(MeOH)_2$ in Aqueous Suspension of Gold Nanoparticles

1,1'-Ferrocenedimethanol, $Fc(MeOH)_2$, was used as the electroactive probe in all experiments. $Fc(MeOH)_2$ is neutral probe that in aqueous solution can be reversibly oxidized at Pt electrode according to the Reaction 1:

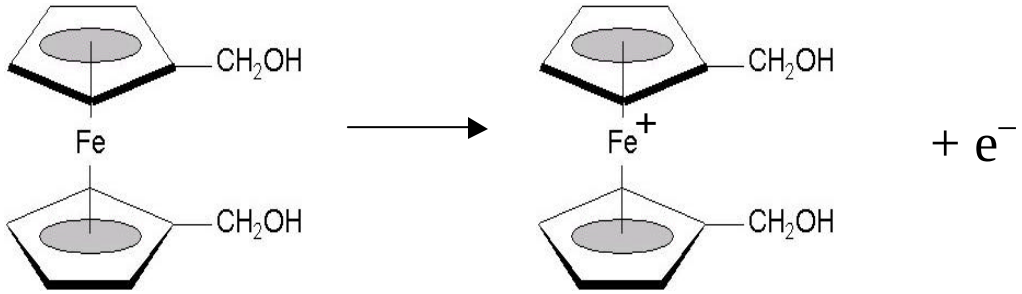

Reaction 1. Oxidation of 1,1'-ferrocenedimethanol, $Fc(MeOH)_2$.

At first the effect of gold nanoparticles on oxidation of $Fc(MeOH)_2$ was analyzed. Series of several dilutions of electroactive probe with gold sols was prepared. Representative voltammograms for oxidation of 2 mM $Fc(MeOH)_2$ in solutions of colloidal gold nanoparticles compared to anodic response in pure water are presented in Figure 6.1.

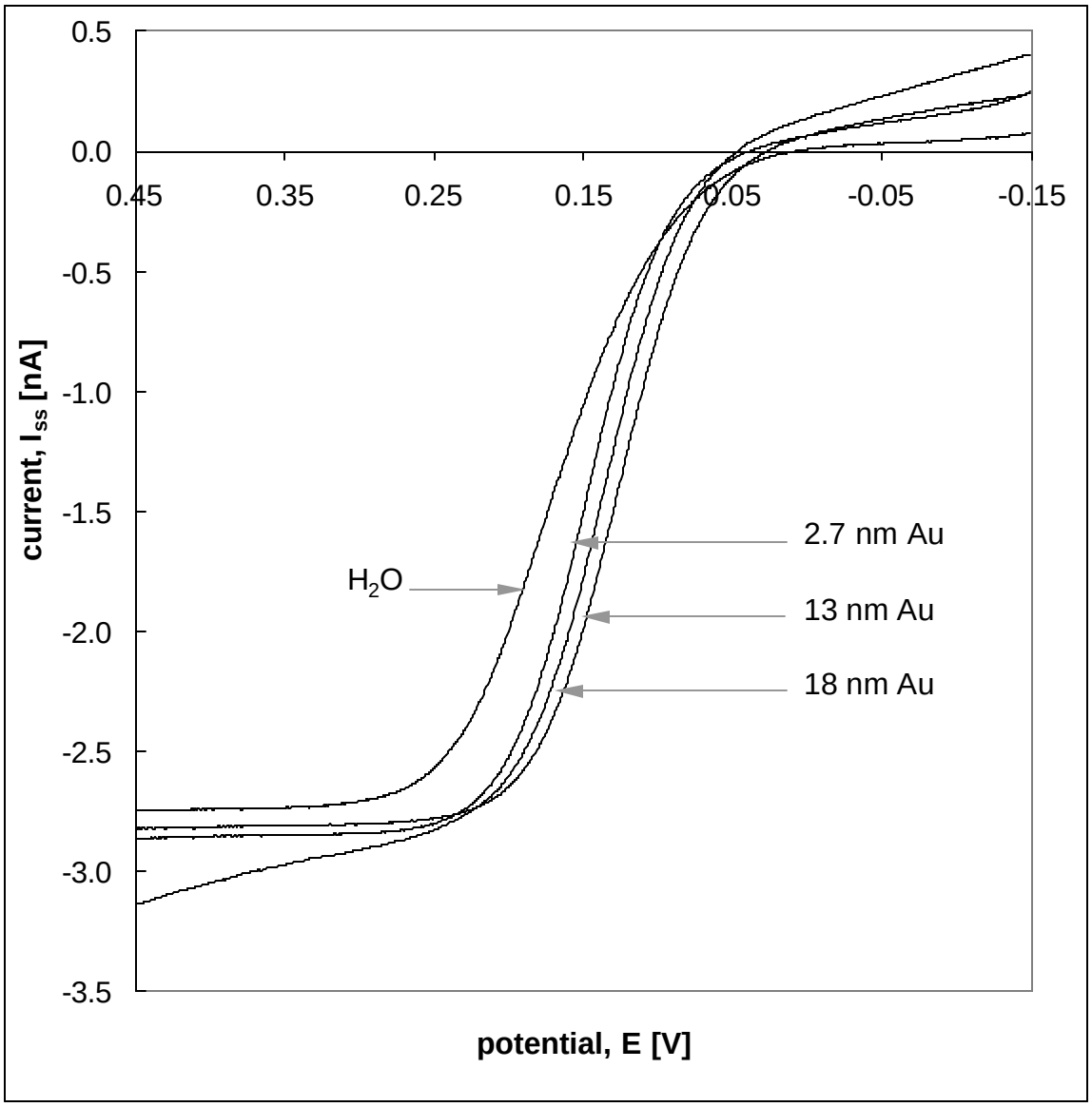

Figure 6.1. Steady-state voltammograms for 2 mM $Fc(MeOH)_2$ in aqueous solution and Au-colloid aqueous suspensions.

As one can see, the presence of gold nanoparticles in a solution of $Fc(MeOH)_2$ does not affect the shape of the recorded voltammograms. The reproducibility was good with relative standard deviation up to 3%. There is a small shift of the oxidation potential, but this is due to the fact that a quasi-reference electrode (Pt wire) was used for this experiment, and the potential of this quasi reference electrode depends strongly on the composition of the solution.

The concentrations of $Fc(MeOH)_2$ in all samples, stock and dilutions, and corresponding diffusion coefficients are shown in Table 6.1. The same experiments were performed using pure water for dilutions of $Fc(MeOH)_2$; see appropriate concentrations in Table 6.1. As one can see, diffusion of an electroactive probe, $Fc(MeOH)_2$, in presence of gold is faster than in pure water. Also, the diffusion coefficients only slightly decrease when the dilutions increase. This decrease is smaller with dilutions in water than in gold colloid. All voltammograms were well defined with relative standard deviation of 5%.

Table 6.1

Diffusion coefficients of $Fc(MeOH)_2$ in aqueous solutions and gold colloid systems

[$Fc(MeOH)_2$]	**$D \times 10^6$, [cm^2/s]**			
	water	**2.7 nm Au**	**13 nm Au**	**18 nm Au**
2.0 mM	6.36	6.33	6.55	6.52
1.5 mM	6.38	6.31	6.47	6.63
1.2 mM	6.39	6.27	6.33	6.55

VI. 2. Transport Studies in Swollen NIPA gels

Preparation of Gel Samples for Electrochemical Measurements

The procedure for introduction of electroactive probe into the gel applies the fact that even after dehydration, the dry polymer can be swelled by a solvent or a solution to reconstitute the gel. [203] This process is reversible and can be repeated several times. Since the polymer with incorporated Au particles can be swelled by a solution of a known and well-controlled composition, this is a very convenient method to introduce any required probes into a gel. $Fc(MeOH)_2$ was used as electroactive probe. Known volumes of 2mM $Fc(MeOH)_2$ solution with supporting electrolyte, $LiClO_4$ (0 – 100 mM), were added to a weighed amount of dry NIPA–Au polymer. The NIPA polymer concentrations were in the range between 2% and 6% (w/v). After sitting overnight at 4° C, a gel was formed with a well-defined polymer-to-solvent ratio and the known concentrations of an electroactive probe. The volume of the swollen gel was equal to the initial volume of the solution used. During the swelling process the gels retained the shape of the container used. There were no signs of gas bubbles inside the gel, and the surface level was flat. The same steps were applied to the blank samples of the NIPA gel and gels with gold particles incorporated into the polymeric matrix (i.e., the gel swollen by an aqueous solution of supporting electrolyte). This allowed us to obtain background signals, and to determine quantitatively the volume of the expelled solution. [213]

Diffusion of $Fc(MeOH)_2$ in Swollen Gels

All experiments were performed in monoliths of poly-NIPA gels with all electrodes immersed in neat and gold modified gels. To determine transport properties of

thermoresponsive NIPA-Au new polymeric materials, one-electron oxidation of $Fc(MeOH)_2$ in such a matrix was studied. Voltammograms for oxidation of 2 mM $Fc(MeOH)_2$ on Pt microelectrode in 2 – 6 % wt. NIPA gels containing 0, 2.7, 13 and 18 nm gold nanoparticles were recorded. The representative voltammograms are presented in Figure 6.2.

In all samples obtained voltammograms were well defined and reproducible, with the relative standard deviation less than 5%. This means that either the presence of polymeric matrix or nanogold particles will not compromise the ability to measure the steady state voltammetric response and make determination of diffusion coefficients of electroactive probe possible. Diffusion coefficients of 2 mM $Fc(MeOH)_2$ in 2 – 6 % wt. NIPA gels containing gold nanoparticles were calculated from the values of steady state currents according to Equation 1.7.7 and the results are presented in Table 6.2.

We found that for analyzed gel samples the diffusion coefficients of $Fc(MeOH)_2$ were approximately 10 – 30% lower than in aqueous solution ($D = 6.35 \cdot 10^{-6}$ cm^2/s) and they decrease when the % concentration of polymer in NIPA gel increase. Also in some instances diffusion of $Fc(MeOH)_2$ was faster in presence of gold. This observation can be explained in two ways. One is geometrical influence of gold nanoparticles. As it was already mentioned, our polymer is the cross-linked system. Gold does not participate in this linkage but it can additionally separate the polymer segments. It would increase free to diffuse volume of entire system. Other explanation that should be considered, accounts for the fact that gold nanoparticles carry the charge that can shield the charge density on polymer chains decreasing hydration effect (See page 90).

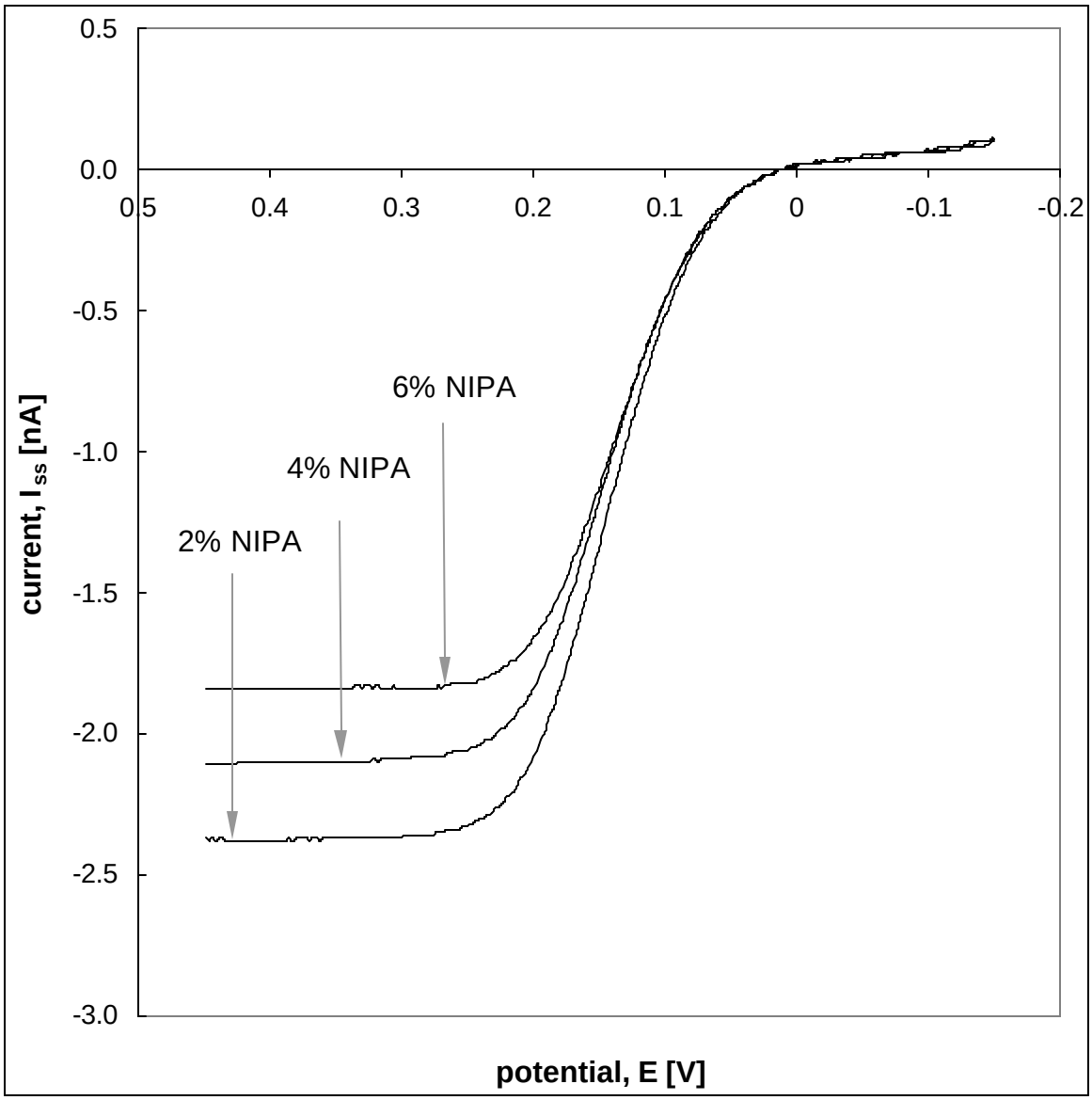

Figure 6.2. Steady state voltammograms for 2 mM $Fc(MeOH)_2$ in NIPA-18 nm Au gel.

Table 6.2

Diffusion coefficients of 2 mM $Fc(MeOH)_2$ in NIPA-Au gels

sample	$D \times 10^6$ [cm^2/s]			
	no Au	**2.7 nm Au**	**13 nm Au**	**18 nm Au**
$Fc(MeOH)_2$+2% NIPA	5.48	5.76	5.57	5.71
$Fc(MeOH)_2$+3% NIPA	5.26	5.51	5.01	5.30
$Fc(MeOH)_2$+4% NIPA	4.85	5.21	4.98	5.01
$Fc(MeOH)_2$+5% NIPA	4.59	5.12	4.6	4.73
$Fc(MeOH)_2$+6% NIPA	4.39	4.56	4.42	4.52

VI. 3. Decrease of Diffusion Coefficients in Swollen Gels

To explain the decrease in the values of diffusion coefficients of $Fc(Me(OH)_2$, *D*, in gels compared to water, different reasons were taken under consideration.

Chronoamperometry

Although the same concentration of $Fc(MeOH)_2$ was used to prepare solutions and gels, the final concentration of the probe in gels can change due to the volume changes during gel preparation. $Fc(MeOH)_2$ could also immobilize on the polymer chains due to hydrophobic interactions. In result, the concentration of mobile molecules of the electroactive probe can decrease causing decrease in values of diffusion coefficients. To make sure that the concentration of $Fc(MeOH)_2$ does not change during swelling process, concentration independent determination of diffusion coefficient of electroactive probe was carried out by chronoamperometry on Pt microelectrode. [205] The normalized current, I_t/I_{ss} was plotted as a function of $t^{-1/2}$ and presented in Figure 6.3. An average intercept of the I_t/I_{ss} vs. $t^{-1/2}$ plots was 0.8734, which is in poor agreement with 0.7854 predicted by Equation 1.7.9. The average values of diffusion coefficients of $Fc(MeOH)_2$ in water and in gels calculated from short time region Equation 1.7.9 are compared with those from steady state voltammetric experiments and they are presented in Figure 6.4. Diffusion coefficients of $Fc(MeOH)_2$ obtained by these two methods are identical within experimental error however the reproducibility of transient current in chronoamperometry was much worse and the relative standard deviation of *D* was up to 30%.

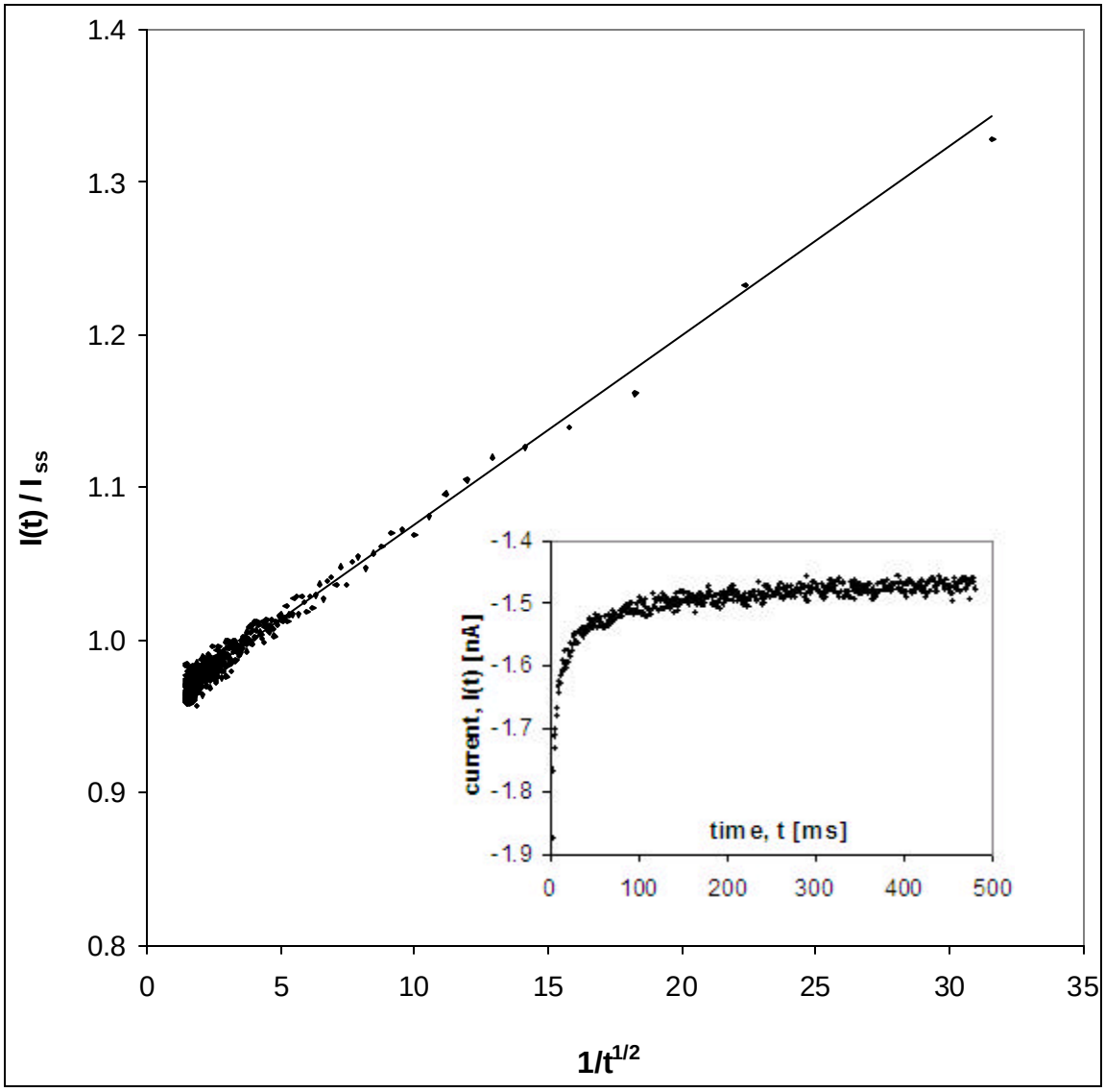

Figure 6.3. Normalized current vs. 1/sqrt(t) for the oxidation of 2.0 mM $Fc(MeOH)_2$ in 4% NIPA gel modified with 18 nm gold particles.

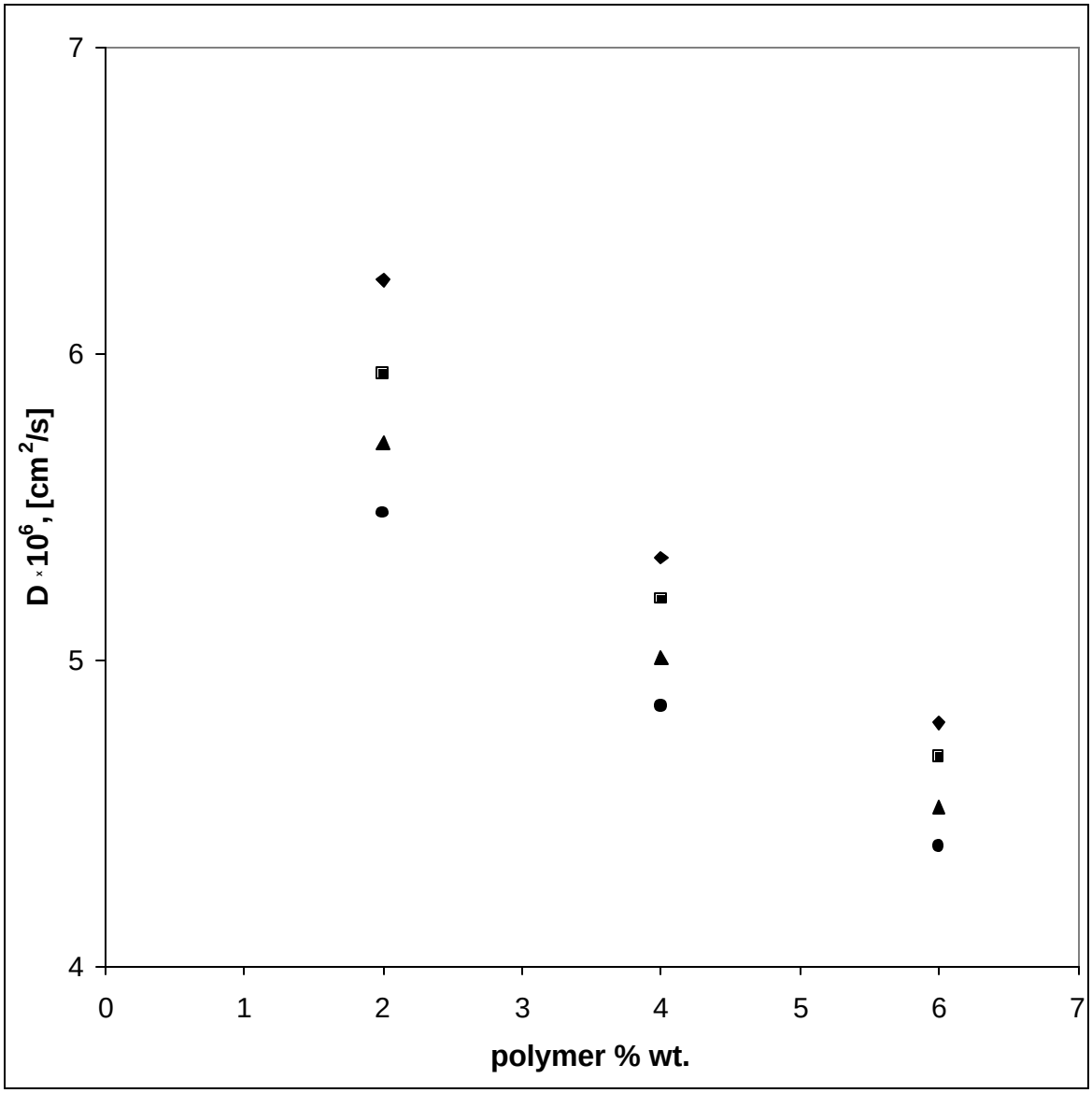

Figure 6.4. The diffusion coefficients of 2 mM $Fc(MeOH)_2$ determined from the steady-state voltammetry and chronoamperometry in 2, 4 and 6% neat NIPA (● - SSV, ■ - chronoamperometry) and NIPA-18 nm Au (▲ - SSV, ♦ - chronoamperometry).

Diffusion coefficients were calculated from the linear plots of normalized current in the function of $1/t^{1/2}$, as:

$$D = \frac{p\ r_d^{\ 2}}{16 \cdot (slope)^2} \qquad (6.2.1)$$

For the experiments performed in the long time regime (up to 20 s) the diffusion coefficients were calculated from the following equation

$$D = \frac{4 r_d^{\ 2}}{p^{\ 3} (slope)^2} \qquad (6.2.2)$$

and they showed the same poor reproducibility.

Diffusion coefficients found using these two techniques differ by less than 10% and we can assume that the concentration of $Fc(MeOH)_2$ did not change significantly during the gel preparation and swelling process. That also means that all $Fc(MeOH)_2$ introduced into polymeric matrix is mobile and electrochemically available. The reason for decrease of D values in gels vs. water must be different.

Macroscopic and Microscopic Viscosity

The decrease in the values of diffusion coefficient can be caused by different viscosities of the two media, water and polymer. According to Stokes-Einstein equation, for ideal solution,

$$D = kT/6\pi\eta r \qquad (6.2.3)$$

the diffusivity of the probe molecules, D, is proportional to the temperature, T, and reversibly proportional to the viscosity, h; r is the hydrodynamic radius and k is the Bolztmann constant. We studied the temperature dependence of diffusivity of

$Fc(MeOH)_2$ in NIPA gels, NIPA-Au gels and in aqueous solution in the presence of 5 mM supporting electrolyte, $LiClO_4$ between 5 and 30 °C. The highest temperature in this range is still below the temperature of the volume phase transition and these gels are in swollen state. The results are presented in Figures 6.5. Stokes-Einstein equation predicts that diffusion coefficient of $Fc(MeOH)_2$ should increase linearly with temperature. But because the viscosity of water and in consequence, aqueous solution is not directly proportional to the temperature, the diffusion coefficient does not increase linearly with temperature. Also, Stokes-Einstein equation does not apply to diffusion in polymeric gels. [193,194] Zhang [206] measured the macroscopic viscosity of 2 mM $Fc(MeOH)_2$ in 2.4% NIPA gel to be $1.5 \cdot 10^5$ cP. It is much larger than that of aqueous solution ($9.4 \cdot 10^{-1}$ cP) but the decrease of diffusion coefficient is relatively small. This is attributed to the comparatively open structure of gels compared to the solid materials.

The values of diffusion coefficients of $Fc(MeOH)_2$ in these samples are presented in Table 6.3 and they were analyzed in terms of Arrhenius-like equation,

$$D = Ae^{-E_a / RT} \qquad (6.2.4)$$

where E_a is the activation energy of the diffusion of the electroactive probe in the aqueous solution or in a gel, A is the frequency factor, R is the gas constant and T is the temperature. The activation energy of diffusion, E_a, for $Fc(MeOH)_2$ reflects the local microscopic viscosity of the solvent in which that species diffuses. [214]

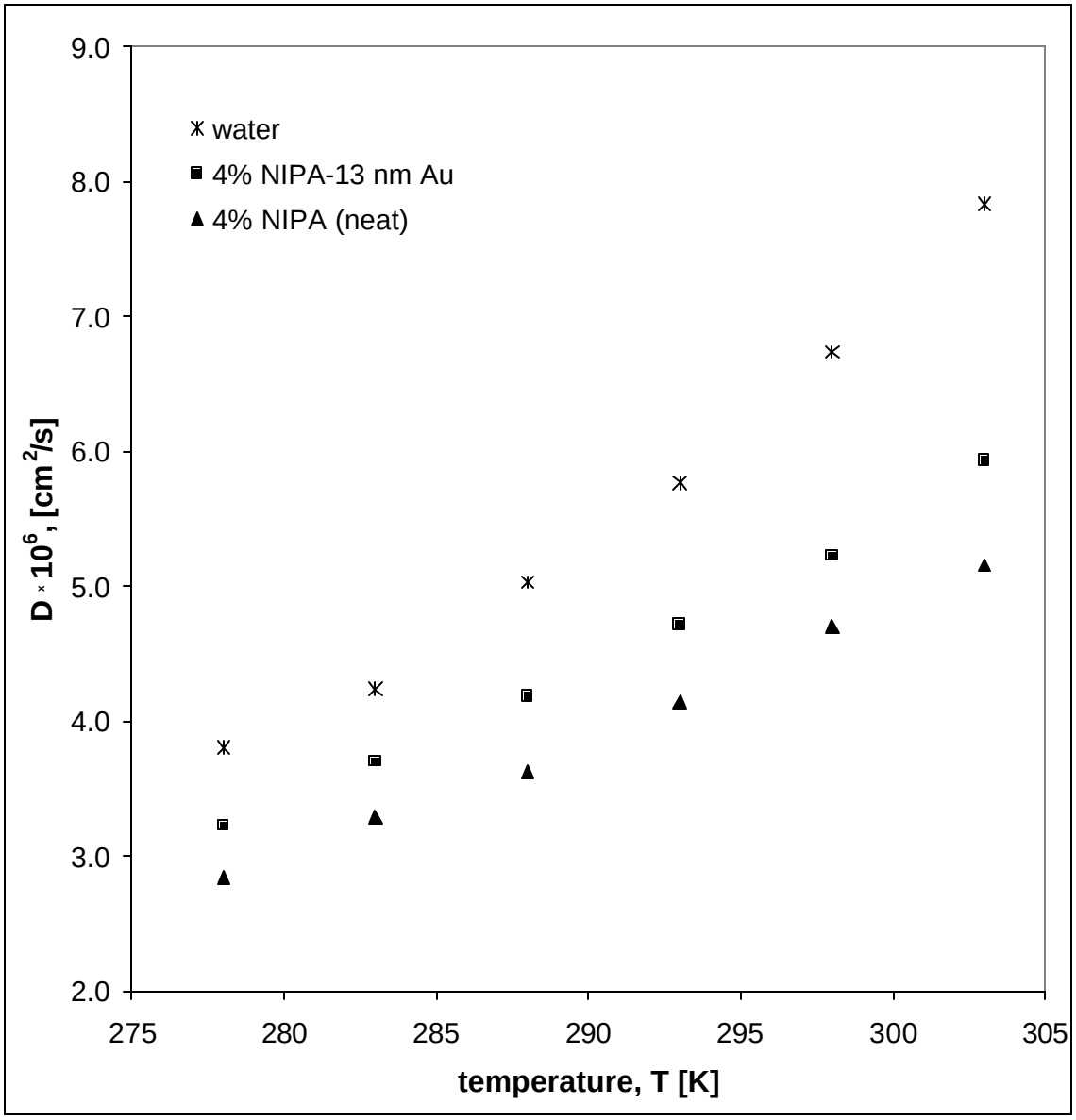

Figure 6.5. Diffusion coefficients of $Fc(MeOH)_2$ in water and in 4% neat and 13 nm gold modified NIPA gels as a function of temperature.

Table 6.3

Temperature dependence of the diffusion coefficient of 2 mM $Fc(MeOH)_2$ in aqueous solution and in 4% neat and 18 nm gold modified NIPA gels ($[LiClO_4]$ = 5 mM)

T [K]	$D \times 10^6$, [cm^2/s]		
	water	**4% NIPA**	**4% NIPA-13 nm Au**
278	3.81	2.84	3.23
283	4.24	3.29	3.70
288	5.03	3.83	4.19
293	5.77	4.44	4.71
298	6.74	5.19	5.23

Figure 6.6 shows the diffusion of $Fc(MeOH)_2$ in neat and gold modified gels analyzed in the form of *lnD* vs. *1/T*. Table 6.4 shows values of E_a and *A* calculated from these plots. E_a for the diffusion of $Fc(MeOH)_2$ in aqueous solution was 18.7 kJ/mol and in NIPA gels it varied from 20.5 to 22.2 kJ/mol. The similar values of activation energy of diffusion of $Fc(MeOH)_2$ in aqueous solution and in the gels suggests that the microscopic viscosity of solvent trapped in NIPA gel network is similar to that in aqueous solution even though the macroscopically observed viscosity of gels is significantly larger than that of aqueous solution. That is due to relatively open structure of gel systems. These values are also in good agreement with the E_a value of 19 ± 1.5 kJ/mol reported by Jacob [214] for diffusion of *N,N,N',N'*-tetramethylethylenediamine (TMED) in an aqueous solution. The slower diffusion of $Fc(MeOH)_2$ in gels may be connected to change of the frequency factor *A* in an aqueous solution and in gels. The average value of frequency factors *A* for the diffusion of $Fc(MeOH)_2$ in various concentrations of gels are in the range $2.5 \times 10^{-2} - 3.8 \times 10^{-2}$, compared to 1.1×10^{-2} for aqueous solution. However, the physical meaning of *A* is not clear yet.

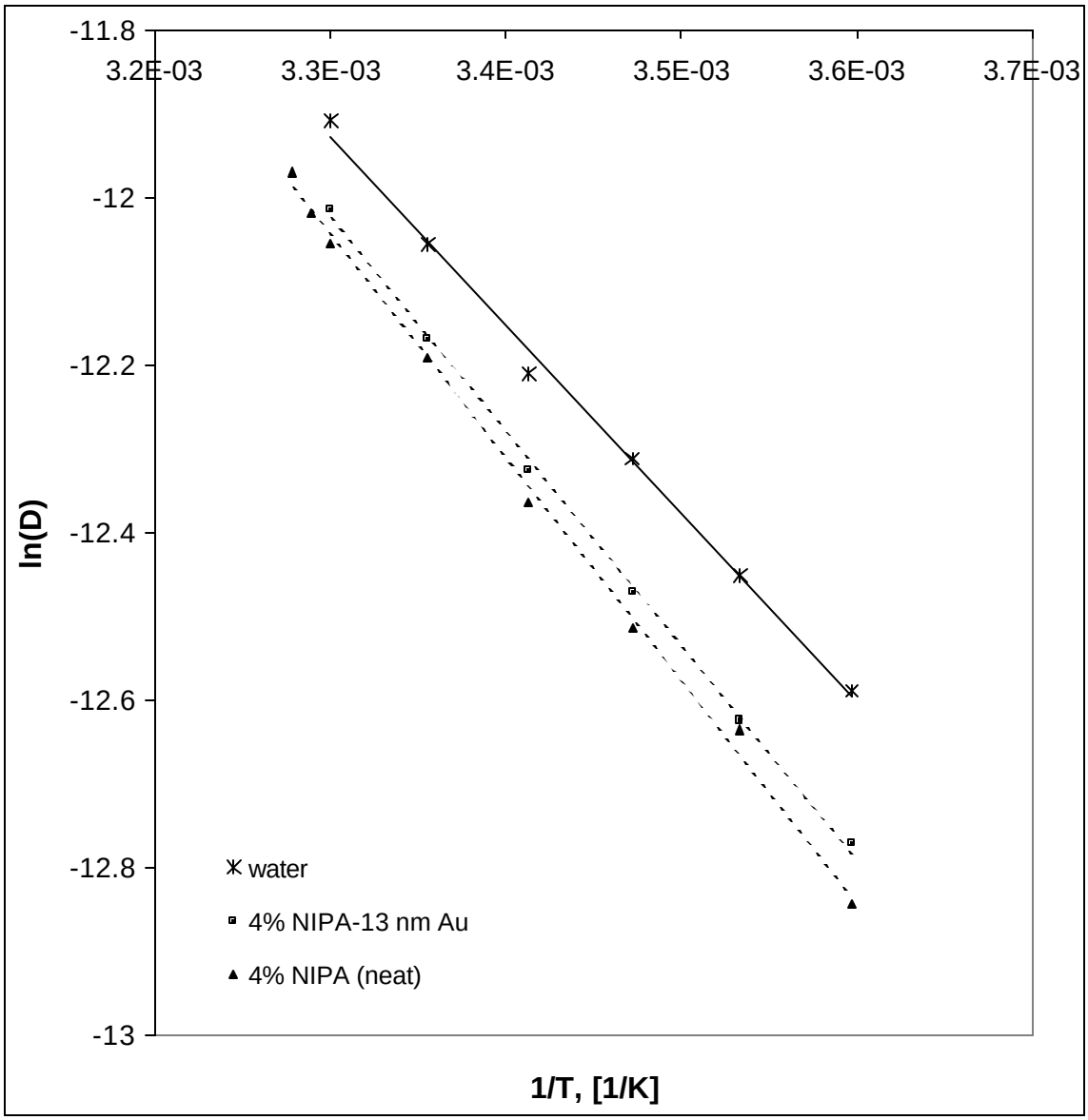

Figure 6.6. Arrhenius plots for the temperature dependence of the diffusion coefficients of 2 mM $Fc(MeOH)_2$ in aqueous solution and in 4% neat and gold modified gels ($[LiClO_4]$ = 5 mM).

Table 6.4

Activation energy of diffusion of $Fc(MeOH)_2$ in aqueous solution and in NIPA gels

sample	**E_a [kJ/mol]**	**A**
aqueous solution	18.7	0.011
4% NIPA	21.2	0.027
4% NIPA-Au	22.1	0.038

Obstruction and Hydration Effect

The explanation of the decrease in diffusion coefficients of $Fc(MeOH)_2$ in swollen, neat and gold modified, gels compared to aqueous solution is based on model proposed by Wang [215] and recently modified by Zhang. [205] According to this model two factors have crucial impact on diffusion of the probe in gels. These facors are "obstruction" and "hydration" effects. "Obstruction" effect is related to the fact that colloidal suspension, polymer macromolecules, or micellar assemblies act as confinement and detour the diffusion of the molecules. As the result, the effective diffusion length increases and diffusion coefficient is reduced as compared to ideal solution. "Hydration' effect is observed when water molecules bound to the surface of colloidal object or polymer molecules. They form a temporally immobilized structured water layer which can increase the volume of hydrated polymer, and it enlarges the "obstruction" effect.

Wang used "obstruction" effect to describe the decrease of self-diffusion of water in the protein aqueous solution. If the shape of ovalbumin molecules is approximated by ellipsoid with principal semi-axes *a*, *b*, and *c*, respectively, and only an "obstruction" effect is considered, the effective diffusion coefficient of water molecules in the solution of protein, *D*, can be expressed in following way:

$$D = D^0 \cdot (1 - \bar{\alpha}\varphi) \qquad (6.2.5)$$

In this equation D^0 and D are diffusion coefficients of water in an ideal solution and in protein solution, respectively, j is the total volume fraction occupied by the hydrated protein molecules and it is defined as $j = 1 - wg$, where w is the weight fraction of water and g is the specific gravity of the solution. $\bar{\alpha}$ is a geometry related coefficient, which is defined as:

$$\bar{a} = \frac{1}{3}\left(a_a + a_b + a_c\right) \qquad (6.2.6)$$

For a round shaped macromolecule, where the three axes are identical, the $\bar{\alpha}$ value is 1. If two axes of the macromolecules are identical and they are much larger than the third one, the $\bar{\alpha}$ value is $+\infty$. For prolate ellipsoids, with two of their principle axes identical, $a = rb = rc$, where $r = a/b$ is the axial ration and $r > 1$, Wang derived the following equations to calculate α_a and α_b:

$$a_a = \frac{1}{\frac{r^2}{r^2-1} - \frac{r}{2\left(r^2-1\right)^{1/3}} \ln \frac{r+\sqrt{r^2-1}}{r-\sqrt{r^2-1}}} \qquad (6.2.7a)$$

$$a_b = \frac{1}{\frac{r^2-2}{r^2-1} - \frac{r}{2\left(r^2-1\right)^{2/3}} \ln \frac{r+\sqrt{r^2-1}}{r-\sqrt{r^2-1}}} \qquad (6.2.7b)$$

To simplify these calculations the shape of molecule can be considered as cylinder. In such case one axis of prolate ellipsoid is significantly longer than the other two axes and according to Wang's calculations, $\bar{\alpha}$ becomes 1.667. Therefore, with proteins treated as cylinder object, the normalized effective diffusion coefficient of water molecules in the protein solution can be expressed as:

$$\frac{D}{D^0} = \left(-1.667\, j + 1\right) \qquad (6.2.8)$$

This equation is limited only to very dilute systems because when the polymer fraction in the gel goes high, for example $\varphi > 1/1.667$, Equation 6.2.8 would lead to the absurd result

that the diffusion coefficient of a species in a gel has a negative value. As already mentioned, Equations 6.2.5 and 6.2.8 were originally used to describe the self-diffusion of water in protein aqueous solutions. Zhang extended this model on diffusion of electroactive probes in cross-linked polymeric gels. He said that diffusion of $Fc(MeOH)_2$ in NIPA gels should obey the same rules as those for solvent molecules. We used "obstruction" effect to describe the decrease of diffusion coefficients of the electroactive probe in gold modified NIPA gels.

Second important factor that can slow down the diffusion of the probe in gels is "hydration" effect. Water in gels can be present in three states. Among them the "bound" water is attached tightly to polymer, "non-bound" water is free to diffuse, and "intermediate" state water molecules interact weakly with the polymer chain. [216] The NIPA polymeric chains in this hydrogel contain carbonyl and amino functional groups that interact with water molecules through the hydrogen bond. Since the "bound state" water and "intermediate" state water increase the volume of polymer and can be treated as a part of the polymer in the hydrogel, Zhang introduced an H coefficient, related to the degree of hydration of polymers. With this modification Equation 6.2.5 can be written as:

$$\frac{D'}{D^0} = \left(-1.667Hj + 1\right) \qquad (6.2.9)$$

If the "obstruction effect" described by Wang is valid in NIPA polymeric gels modified with gold nanoparticles, the diffusion coefficient of electroactive probe molecules in the gel should satisfy Equation 6.2.8. With assumption that the gel consists of long rods swollen by solvent, the value of geometry related coefficient, $\bar{\alpha}$, is 1.667 and Equation 6.2.8 depends only on j. The total volume fraction occupied by the

polymeric units, j, can be obtained experimentally by measuring weight fraction of water in the gels and the density of gels which implies how much space in the gel is occupied by polymers. In our experiment, since the polymer concentration in gels was very small ($\leq$ 6.0%), the density of a gel was almost the same as aqueous solution. If only "obstruction" effect is considered the polymer chains in hydrogel are not hydrated and the value j may be treated as the weight concentration of polymer in the gels. In all our experiments j didn't exceed 6.0% (w/v) and it should have negligible effect on the diffusion coefficients of the probe in gels.

Table 6.5 shows the diffusion coefficients of $Fc(MeOH)_2$ in neat and gold modified NIPA gels, D', for different values of j, where j is defined as a weight concentration of the polymer in the gels. The results from Table 6.5 are demonstrated in Figure 6.7, and they can be fitted to the linear dependent equations also presented in the graph. Theoretical plot of Equation 6.2.9 is shown for comparison. As one can see in Figure 6.7, diffusion coefficient of $Fc(MeOH)_2$ in gels is inversely proportional to the polymer concentration in the gel and it is the result of "obstruction" effect. However, the concentration dependence of the diffusion coefficient of $Fc(MeOH)_2$ in NIPA hydrogel system does not follow completely the "obstruction" effect model. If the weight concentration of the polymer in the gel is regarded as j, the slope of the plot in the Figure 6.7 should be –1.667 as predicted by Equation 6.2.9 (see the theoretical plot). For all gel samples the experimental values are between 4.4 for neat NIPA gel and they decrease to

Table 6.5

Diffusion coefficients of 2 mM $Fc(MeOH)_2$ in neat NIPA gel (top table) and in NIPA gels modified with 2.7, 13 and 18 nm gold particles (bottom table)

% of polymer	j	**D x 10^6 (cm^2/s)**	**D/D^0**
0	0	6.35	1
2	0.02	6.13	0.965
3	0.03	5.67	0.893
4	0.04	5.32	0.838
5	0.05	5.06	0.797
6	0.06	4.77	0.751

% of polymer	j	**NIPA – 2.7 nm Au**		**NIPA – 13 nm Au**		**NIPA – 18 nm Au**	
		D x 10^6 (cm^2/s)	**D/D^0**	**D x 10^6 (cm^2/s)**	**D/D^0**	**D x 10^6 (cm^2/s)**	**D/D^0**
0	0	6.35	1	6.35	1	6.35	1
2	0.02	5.76	0.907	6.13	0.965	6.28	0.990
3	0.03	5.51	0.868	5.53	0.871	5.83	0.918
4	0.04	5.21	0.820	5.48	0.863	5.51	0.867
5	0.05	5.12	0.806	5.06	0.797	5.20	0.819
6	0.06	4.56	0.718	4.93	0.777	4.98	0.784

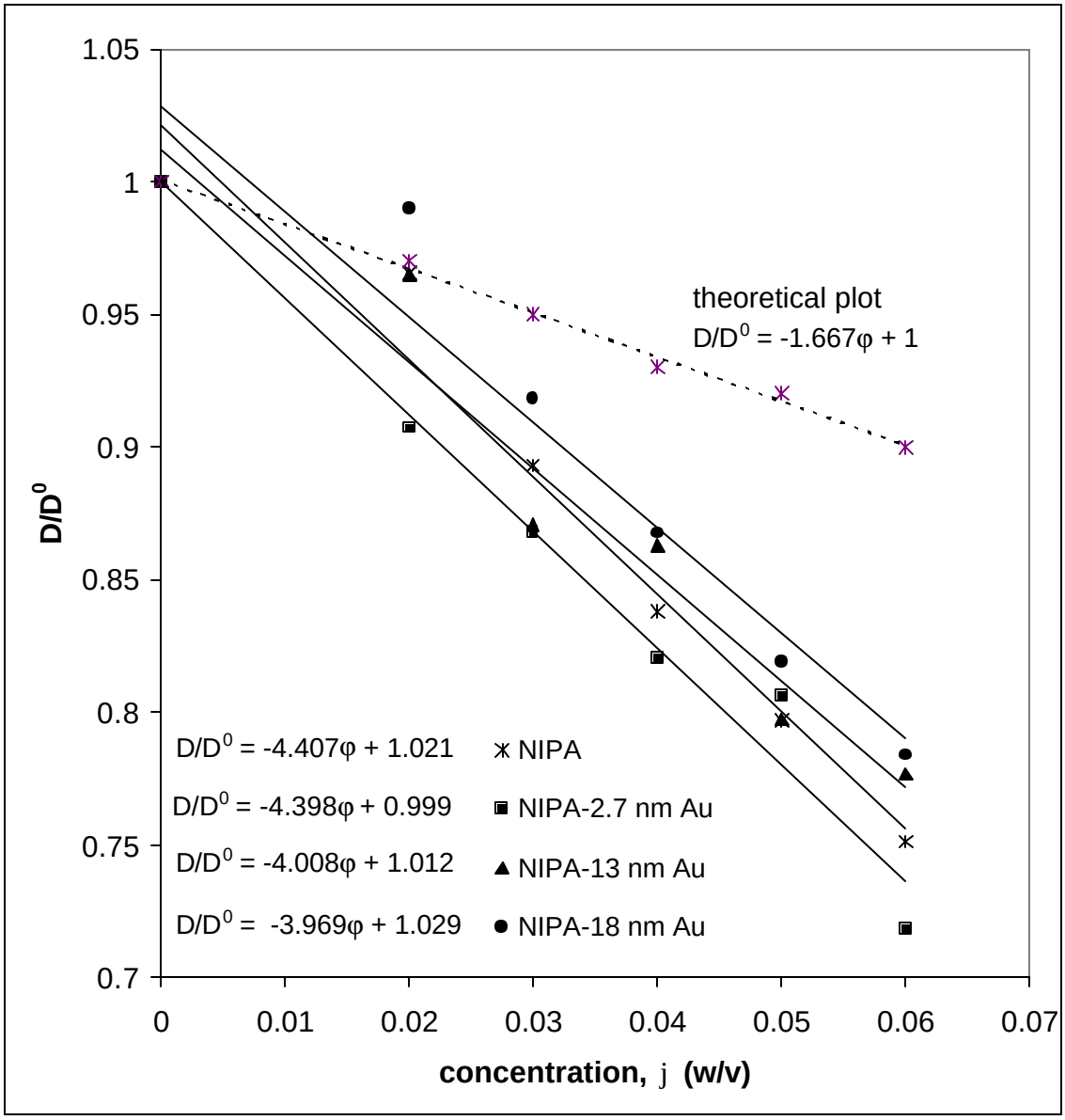

Figure 6.7. Normalized diffusion coefficient (D/D^0) of 2 mM $Fc(MeOH)_2$ vs. concentration of NIPA polymer is neat gels and gels modified with 2.7, 13 and 18 nm gold particles.

4.0 for the NIPA gels modified with gold nanoparticles. This is between 2.6 – 2.4 times larger than the value predicted by Wang.

If the geometry related coefficient, $\bar{\alpha}$ is correct, it seems that the volume fraction of the polymer in the hydrogel is expanded 2.5 times compared to polymeric volume fraction in unhydrated state. Similar disagreement was previously discovered by Duval *et al.* [217] in a colloidal system of synthetic clay dispersed in water. They found that the volume fraction of solid colloid measured from a self-diffusion of water experiment was six times larger than the actual solid volume fraction in the system (0.12 vs. 0.02). The experimental value was "unrealistically high" according to the authors, because it would be related to a 3 nm thick water layer on the surface of the clay platelets. Although the reason for this difference is still not clear, several authors [217-219] connected it to the "hydration effect", which comes from the water molecules firmly attached to the polymer that form a temporarily immobilized water film around the polymer chain due to hydration or another hydrodynamic effect.

In our experiments the average value of hydration coefficient, *H*, determined from the slopes of the plots in Figure 6.7 for NIPA gels modified with gold nanoparticles is 2.4. For neat NIPA hydrogel *H* is 2.6. The slightly larger value of hydration coefficient for NIPA-Au gels means that in the presence of Au particles the hydration effect is reduced.

The hydration coefficient *H* is related to the properties of polymers and the interactions between the polymers and solvents. These interactions are hydrogen bonding, specific absorption, and hydrodynamic effects. *H* is independent of the concentration of electroactive probes, if the probe concentration is low, and there is no

interaction between the polymer and probes. If we know the diffusion coefficient of the molecule in an aqueous solution, the hydration *H* value of a polymer in its hydrogel, and weight concentration of polymer in that gel, the diffusion coefficient of that molecule in the gel can be predicted by Equation 6.2.9. For a given polymeric gel system, *H* value can be determined by plotting D/D^0 vs. concentrations of polymer in gel.

VI. 4. Effect of $LiClO_4$ on Diffusion of $Fc(MeOH)_2$ in NIPA Gels

Effect of Supporting Electrolyte on Temperature of the Volume Phase Transition

In Chapter V.1 we have shown that the presence of gold nanoparticles does not affect the temperature of the volume phase transition. Following the same procedure we examined effect of supporting electrolyte, $LiClO_4$, on the temperature of the collapse of 4% neat NIPA gel and gel containing 2.7, 13 and 18 nm gold nanoparticles. Only one concentration of $LiClO_4$, 100 mM, was analyzed. The temperature at which turbidity first became apparently visual for neat and Au-modified polymers swollen in 100 mM $LiClO_4$ was 32.8 ± 0.2 °C, whereas the complete volume phase transition was observed at 33.8 ± 0.4 °C. For polymers prepared in pure water, these temperatures were higher, 32.2 ± 0.4 °C and 35.0 ± 0.5 °C, respectively; in all cases we did not observe any influence from the presence of gold nanoparticles. This small increase in temperature of the volume phase transition for gels that contain 100 mM $LiClO_4$ can be explained in terms of weaker attractive forces that act to shrink the polymer and more hydrophilic character of the system.

Effect of Supporting Electrolyte on Absorbance Spectra of Gold Nanoparticles

To determine effect of electrolyte on surface plasmon band, UV-vis spectroscopy was applied. The absorbance spectra of 2.7, 13 and 18 nm in 4% NIPA gels swollen by 100 mM $LiClO_4$ were recorded at room temperature and compared with gels prepared in water. Aqueous suspensions of colloidal gold containing 100, 50, 25 10 and 0 mM $LiClO_4$ were also analyzed and sample spectra are shown in Figures 6.8 and 6.9. As one can see presence of $LiClO_4$ in the solution used to swell the polymer samples did not affect the wavelength of maximum absorbance. However, the values of absorbance were up to 17% higher for gold nanoparticles in gels without the electrolyte. Different behavior of colloidal gold nanoparticles was observed in aqueous solution of $LiClO_4$. Higher concentration of electrolyte in aqueous colloids caused aggregation of gold nanoparticles. The colloidal suspension changed color from red to blue. The wavelength of maximum absorbance red shifted and eventually two wide peaks appeared. These changes were most observed for 18 and 13 nm Au particles.

Effect of Supporting Electrolyte on Diffusion of $Fc(MeOH)_2$ in Aqueous Solution

Typical steady state voltammograms for the one-electron oxidation of $Fc(MeOH)_2$ in water at 25.0 °C in the presence of $LiClO_4$ ([$LiClO_4$] was 0, 1, 5, 25, 50 and 100 mM) were recorded and selected results are presented in Figure 6.10. Concentration of $Fc(MeOH)_2$ was 2 mM. All recorded voltammograms were well defined and reproducible, with relative standard deviation less than 5% determined for five repetitive experiments. Diffusion coefficients, D, of electroactive probe in the presence of various concentrations of $LiClO_4$ (0 – 100 mM) were determined from the values of steady state limiting current, I_{ss}, according to Equation 1.7.7. Results are presented in Table 6.6.

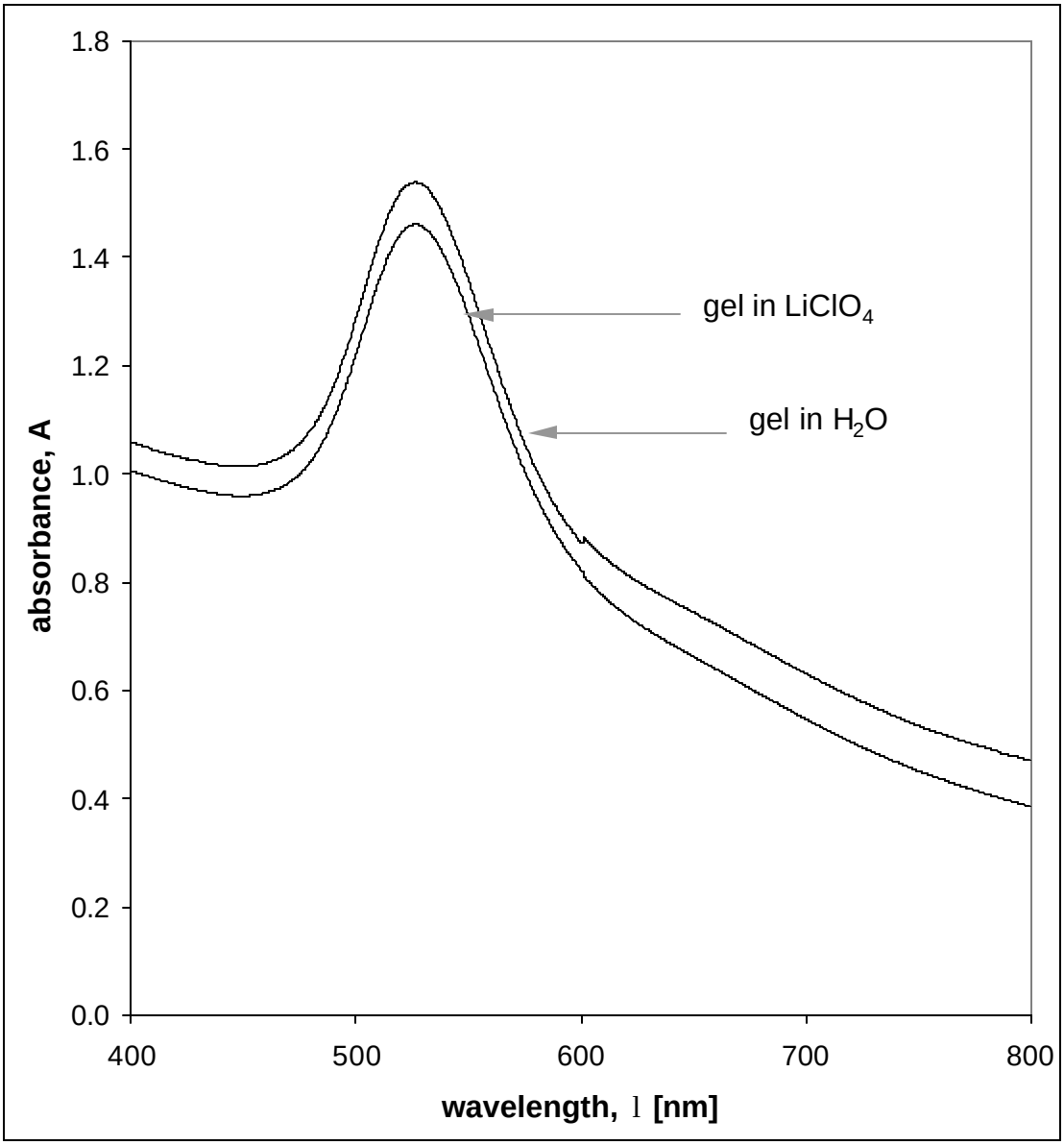

Figure 6.8. UV-vis spectra of 18 nm Au in 4% NIPA gel swollen by water and 100 mM $LiClO_4$.

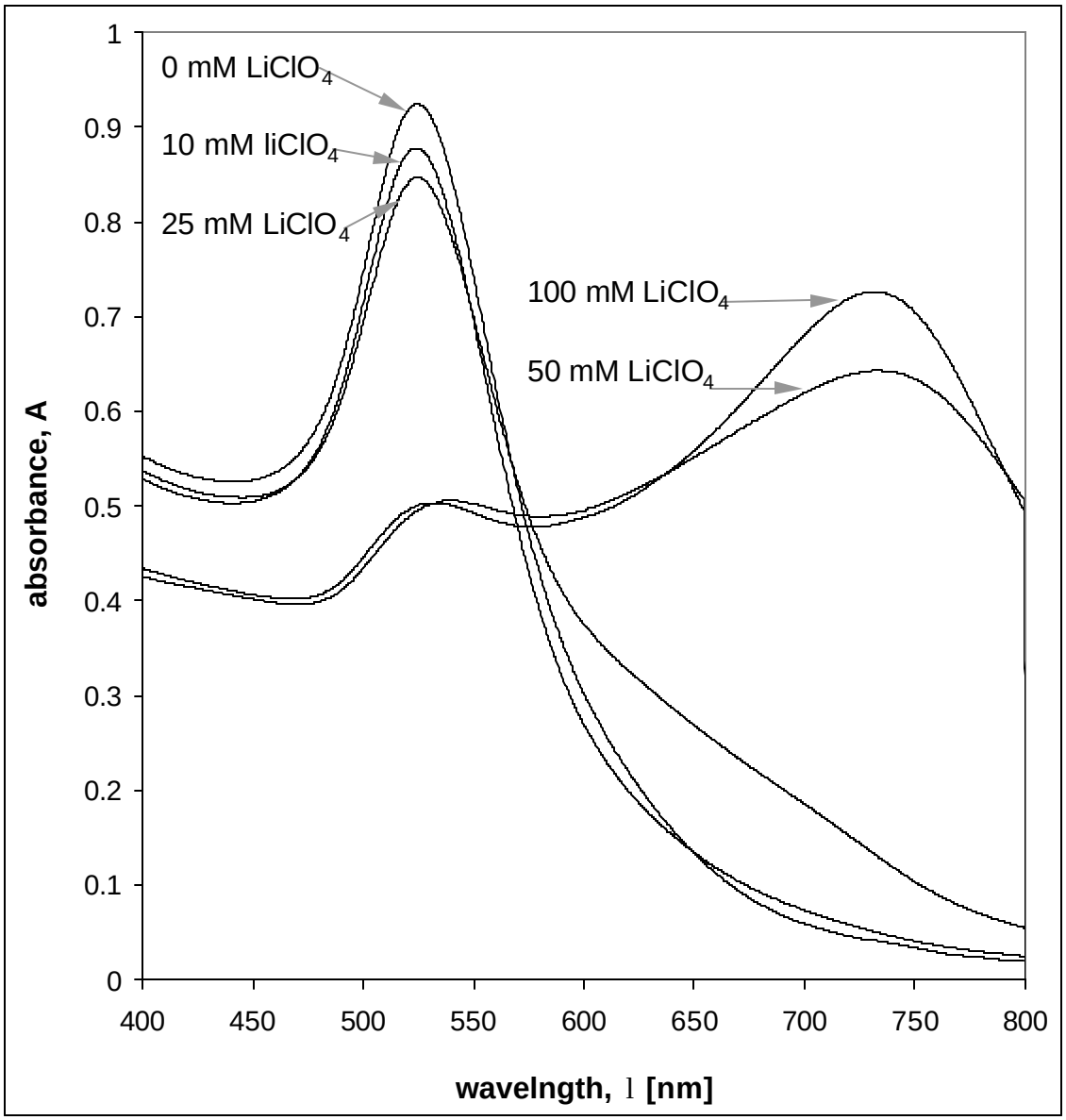

Figure 6.9. UV-vis spectra of 18 nm Au in sol containing 0, 10, 25, 50 and 100 mM $LiClO_4$.

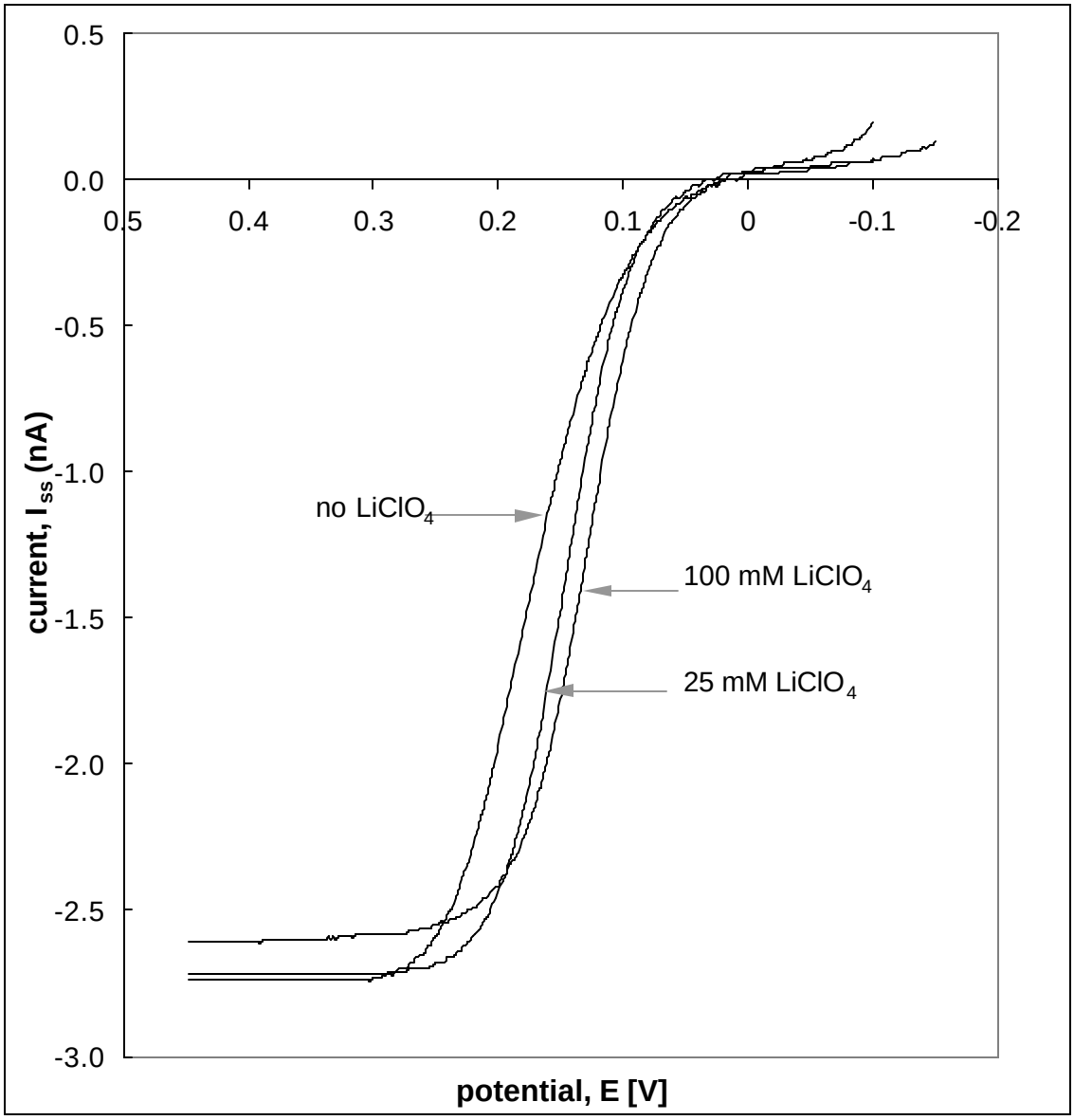

Figure 6.10. Steady state voltammograms for 2 mM $Fc(MeOH)_2$ in 0, 25 and 100 mM $LiClO_4$.

Table 6.6

Diffusion coefficients of 2 mM $Fc(MeOH)_2$ in aqueous solution of $LiClO_4$

($[LiClO_4]$ = 0 – 100 mM)

$[LiClO_4]$ (mM)	**D x 10^6 , (cm^2/s)**
0.0	6.35
1.0	6.31
5.0	6.30
25.0	6.29
50.0	6.13
100.0	6.06

The value of diffusion coefficient of $Fc(MeOH)_2$ in 100 mM $LiClO_4$ was reported in literature as $6.04 \cdot 10^{-6} \pm 3.9 \cdot 10^{-7}$ cm^2/s [206], which is in good agreement with our results. Results presented in Table 6.6 show that diffusion coefficients decreases when the ionic strength of the solution increases. This can be explained by the Stokes-Einstein equation that describes the diffusion coefficient of molecules in an ideal solution.
In the case of an ideal solution (or a very diluted solution), one would expect to find an inversely proportional relationship between the diffusion coefficient and the solution viscosity. The viscosity of 100 mM $LiClO_4$ in 2 mM $Fc(MeOH)_2$ was measured using an Ostwald viscometer with a water flow time of about 100 sec at 25 °C and it was found that η = 0.908 cP. Viscosity of water measured at the same conditions is η = 0.8937 cP. We can see from the Stokes-Einstein equation (Equation 6.2.3) that when viscosity of solution with electrolyte is higher then the diffusion coefficient is smaller and *vice versa*.

Effect of temperature on diffusion of $Fc(MeOH)_2$ in aqueous solution and in the presence of various concentrations of $LiClO_4$ was determined and this relationship is shown in Figure 6.11. The values of diffusion coefficients increase when temperature of the solution increases which agrees well with Stokes-Einstein equation. The non-linear behavior is due to the fact that relationship viscosity-temperature is not linear.

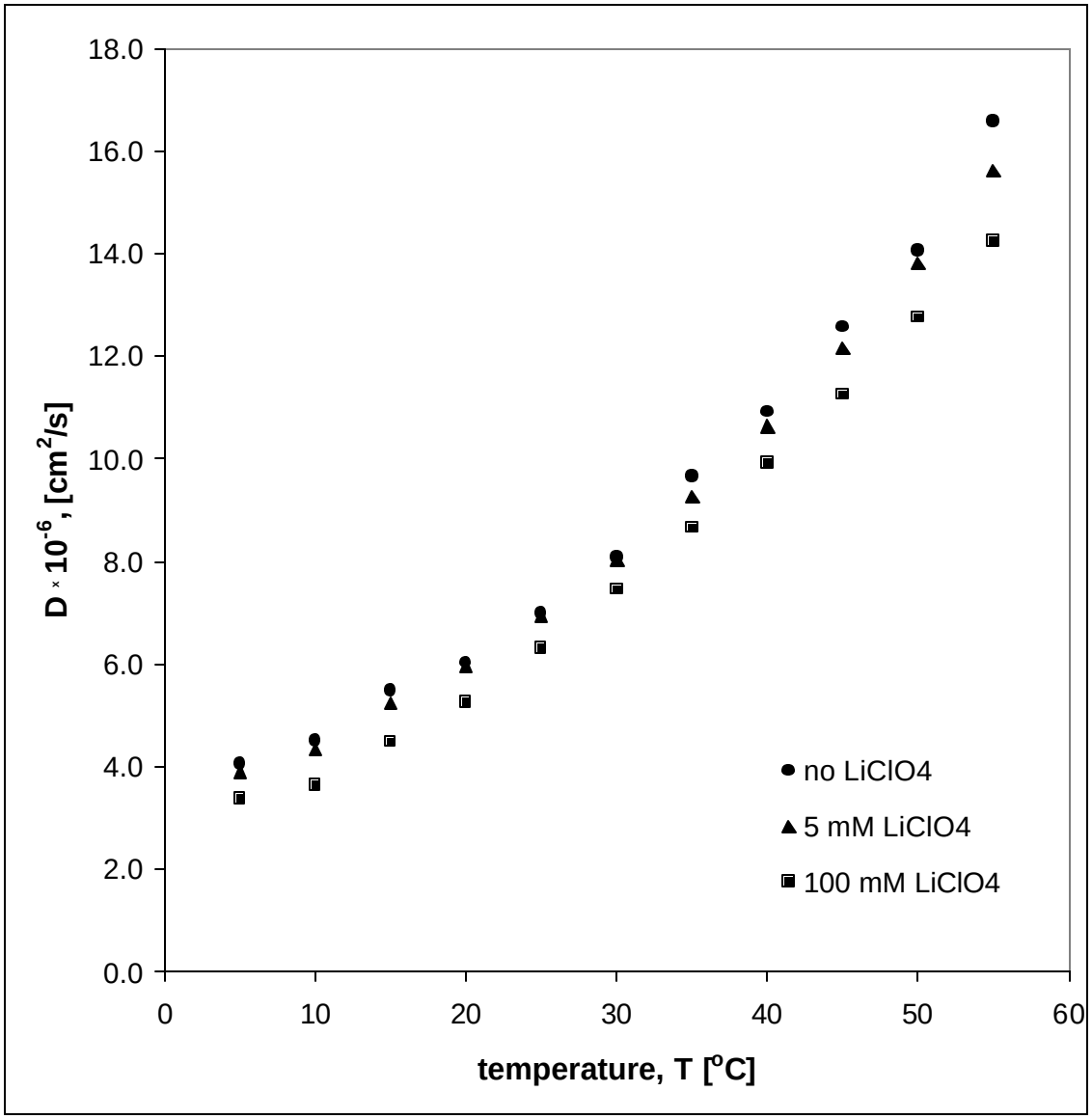

Figure 6.11. Effect of temperature on diffusion of 2 mM $Fc(MeOH)_2$ in presence and absence of electrolyte.

Effect of Supporting Electrolyte on Diffusion of $Fc(MeOH)_2$ in NIPA Gels

The oxidation of $Fc(MeOH)_2$ in neat and gold modified NIPA gels swollen by solution of the electroactive probe in 0 – 100 mM $LiClO_4$, was studied. In all samples the voltammograms were well defined, reproducible and the relative standard deviation of the limiting current was less than 5% (calculated from 5 voltammograms). Figure 6.12 presents the effect of supporting electrolyte, $LiClO_4$, on diffusion of electroactive probe in 2-6 wt.% neat NIPA gels. Effect of electrolyte on diffusion in gels modified with 2.7, 13 and 18 nm gold nanoparticles was also studied. Selected set of results is presented in Figure 6.13. Diffusion coefficients of $Fc(MeOH)_2$ in 2-6 wt.% NIPA and NIPA-Au gels with constant concentration of $LiClO_4$, are approximately 10 % – 15 % smaller than that in an aqueous solution. This decrease can be explained in terms of "obstruction" and "hydration" effects. Diffusion coefficients of $Fc(MeOH)_2$ are higher for gels modified with gold nanoparticles. This can be explained in terms of geometrical influence of nanogold particles that can additionally separate the chains of crosslinked polymer and increase free to diffuse volume. Other explanation is that charged gold nanoparticles shield the charge density on polymer, which decrease the hydration effect. Diffusion of $Fc(MeOH)_2$ in NIPA and NIPA-Au gels decrease when the concentration of electrolyte increases at constant concentration of polymer in gels. As one can see, the trend in the change of diffusion coefficient values of $Fc(MeOH)_2$ in both types of gel, neat and gold modified, was also similar. These similarities indicate that the electrochemical characteristics of the prepared gel are independent of the gold particles size.

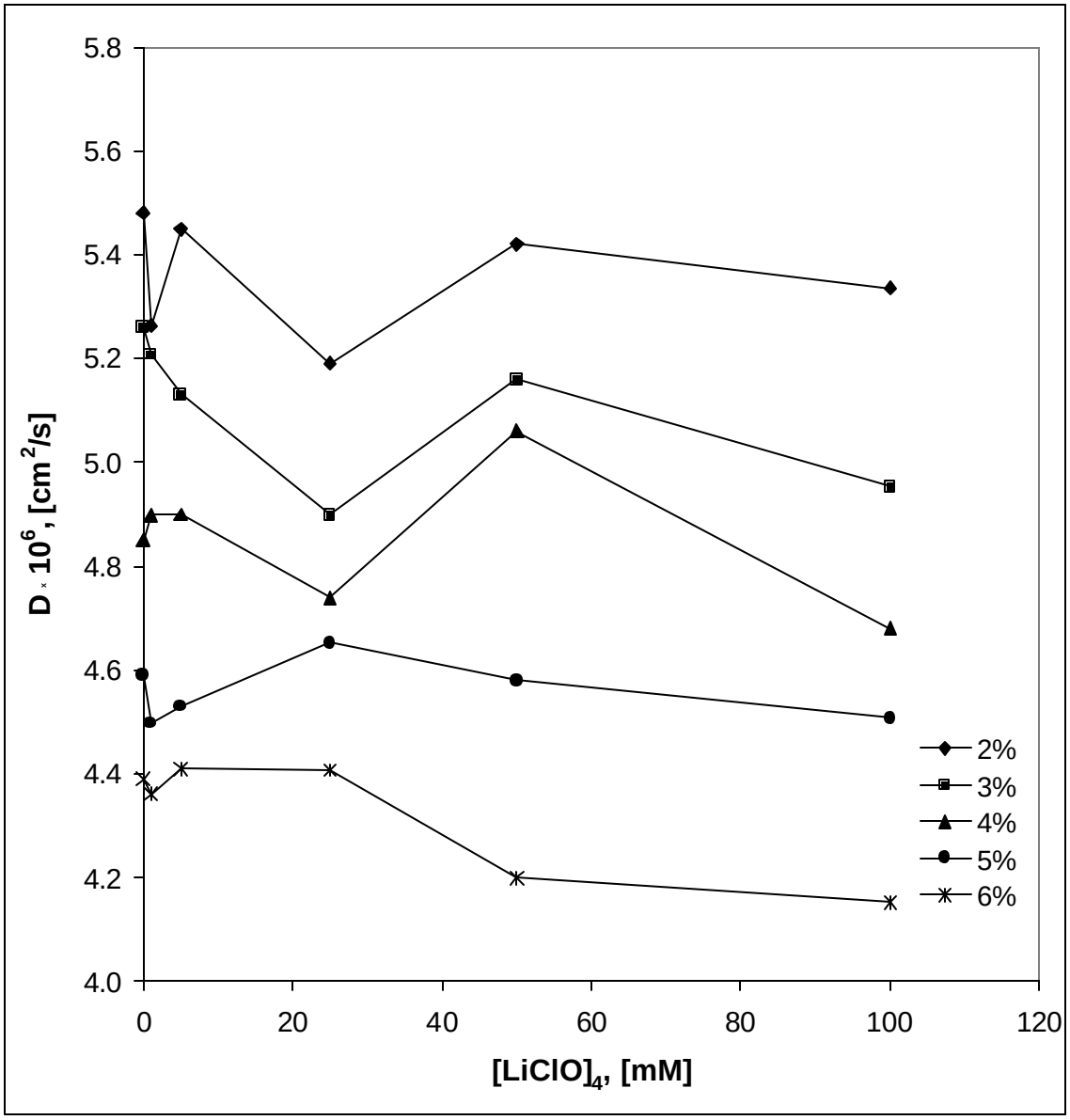

Figure 6.12. Diffusion coefficients of 2 mM $Fc(MeOH)_2$ in neat NIPA gels containing 0 - 100 mM supporting electrolyte, $LiClO_4$.

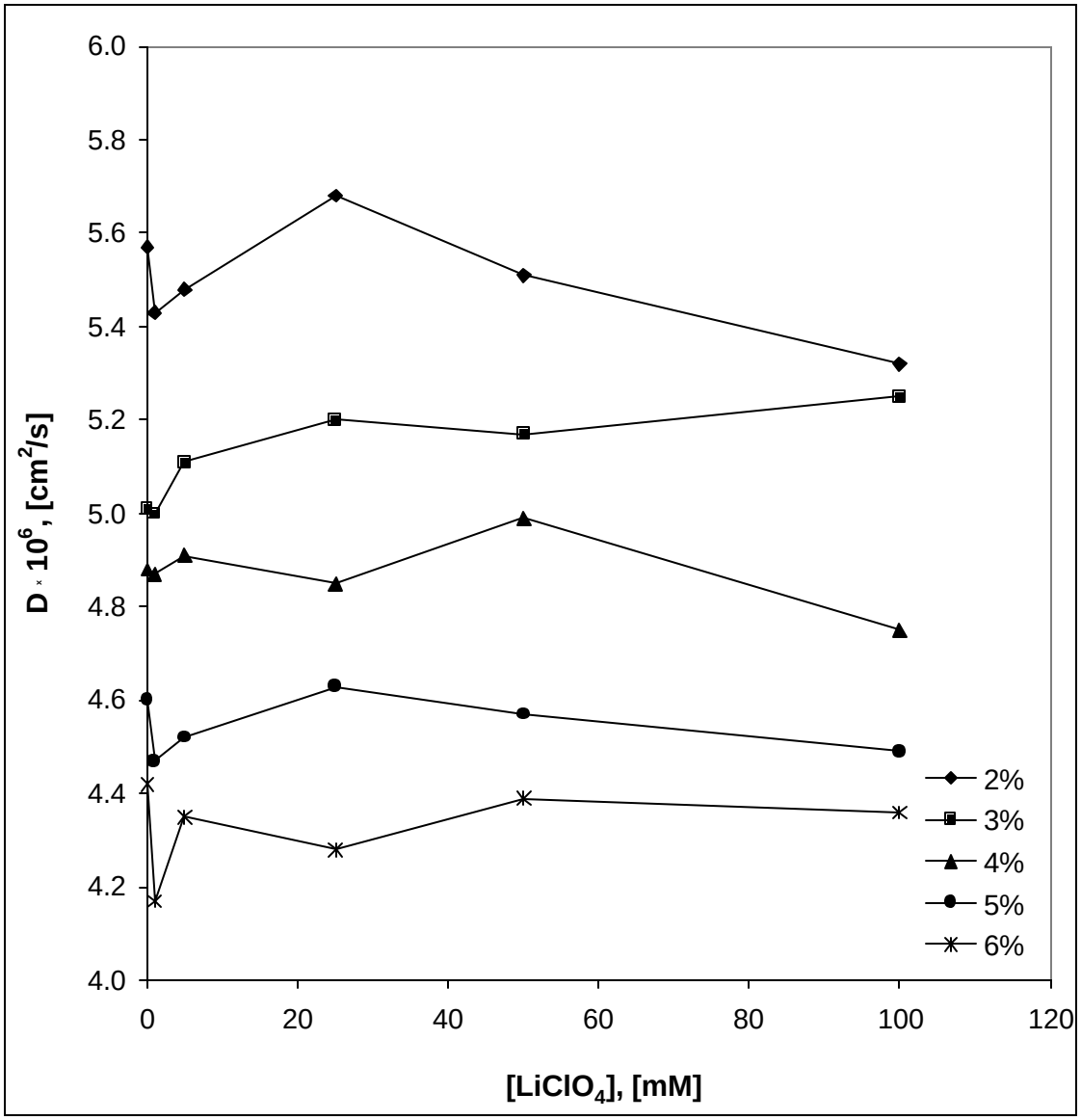

Figure 6.13. Diffusion coefficients of 2 mM $Fc(MeOH)_2$ in NIPA gels modified with 13 nm Au, containing 0 - 100 mM supporting electrolyte, $LiClO_4$.

VI.5. Effect of Volume Phase Transition on Transport in Gels

Effect of Temperature on the Steady-State Current

At temperature above 32 °C the NIPA and NIPA-Au gels undergo volume phase transition. As the result, the solution expelled from the gel and collapsed polymer are present as two phases. Transport of $Fc(MeOH)_2$ in collapsed neat and gold modified polymers was studied using steady state voltammetry. Sample voltammograms for the oxidation of $Fc(MeOH)_2$ in 4% NIPA modified with 13 nm Au particles before and after volume phase transition is shown in Figure 6.14. The initial concentration of electroactive probe in swollen gel was 2 mM. We found that the oxidation current of the electroactive probe in shrunken polymer dropped significantly. In Figure 6.15 the dependence of the limiting current on the temperature, varying from 10 to 55 °C is shown. As one can see, in collapsed gel, the steady state current drops almost to zero and the reproducibility of the limiting current is much worse than that for swollen gels. The relative standard deviation, *rsd*, of limiting currents after the phase transition was 37% (for swollen gels the *rsd* is less than 5%) which can be the consequence of inhomogeneous distribution of an electroactive probe in the collapsed polymeric phase or inhomogeneity of the collapsed polymeric phase.

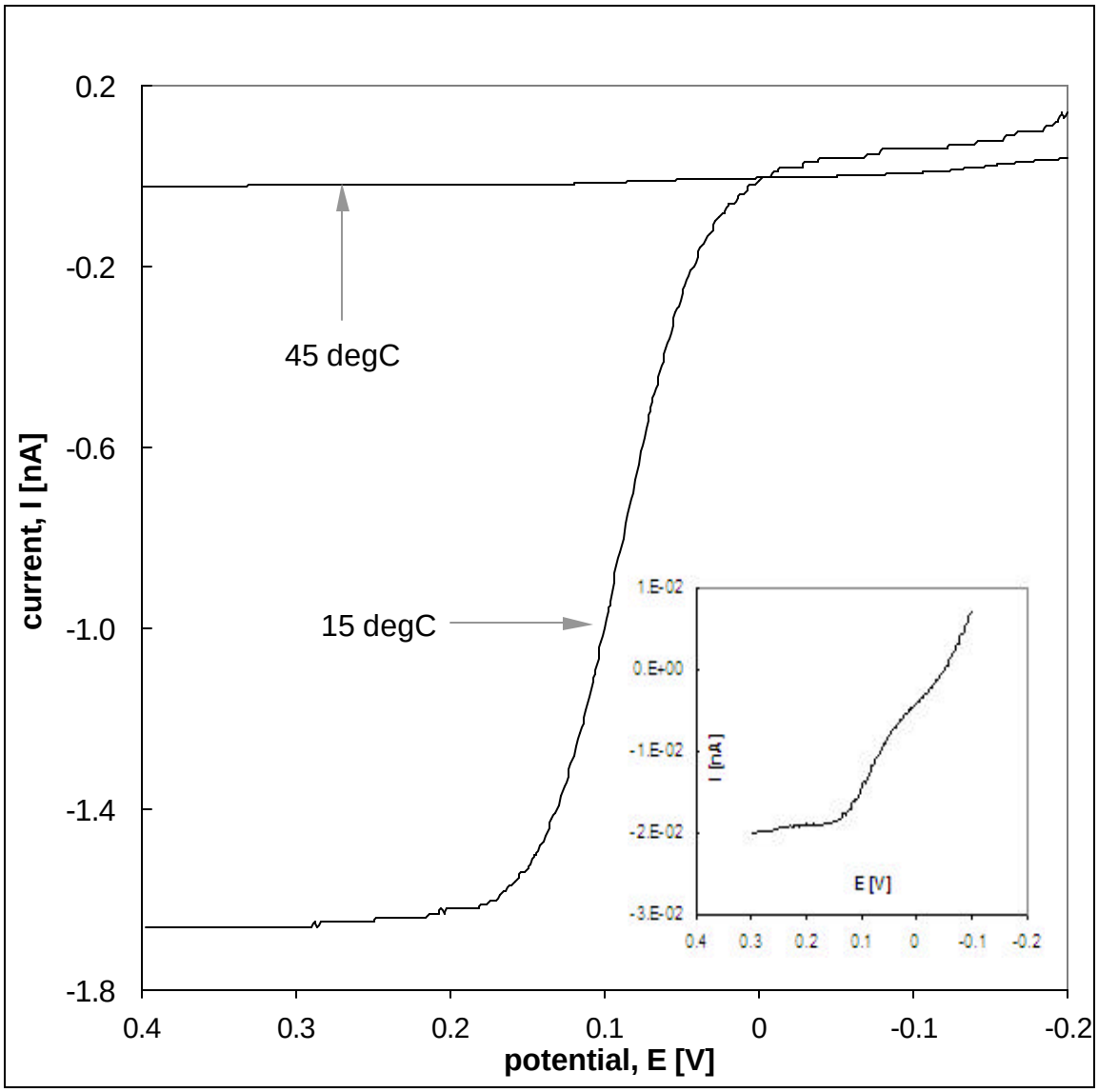

Figure 6.14. Steady-state voltammograms of oxidation of 2 mM $Fc(MeOH)_2$ in 4% NIPA-13 nm Au at 15 °C and 45 °C. (Inset: enlarged voltammogram at 45 °C).

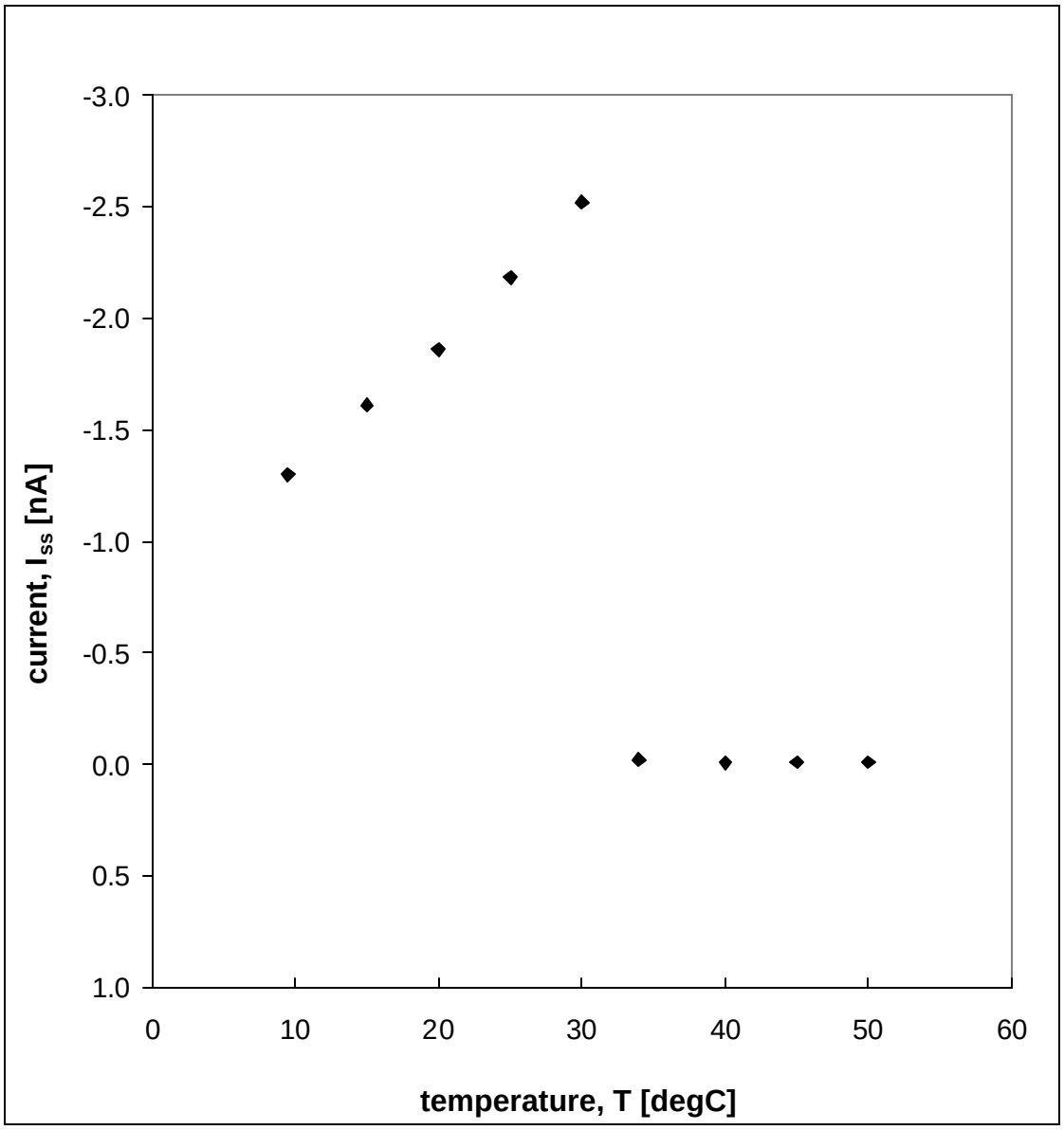

Figure 6.15. Dependence of steady state current of $Fc(MeOH)_2$ on temperature in 4% NIPA modified with 13 nm Au.

This decrease in the values of limiting current suggests that concentration and/or diffusion coefficients of $Fc(MeOH)_2$ in gels after volume phase transition decreases significantly (see Equation 1.7.7). For all gels the volume change was between 90 and 93%. The volume of expelled solution was independent of the presence of gold nanoparticles or concentration of $LiClO_4$; however, it decreased when the concentration of polymer matrix in the gel increased. The color of this solution implied that $Fc(MeOH)_2$ is present in this expelled solution. All expelled solutions were separated from the collapsed gels and steady-state voltammetry was performed. Equation 1.7.7 along with the values of the steady state oxidation currents and the value of the diffusion coefficient of $Fc(MeOH)_2$ in aqueous solution, were used to calculate concentrations of $Fc(MeOH)_2$ probe in expelled solutions. Since we do not know what fraction of $LiClO_4$ is retained in collapsed gels, we used the D value for $Fc(MeOH)_2$ in aqueous solution without the electrolyte ($D = 6.35 \cdot 10^{-6}$ cm^2/s). We found that the estimated concentration of electroactive probe in solutions expelled from all gel samples was 13-36% lower than the initial concentration of the probe (2 mM). These concentrations are independent of the presence of gold nanoparticles, however they decrease when the concentration of NIPA polymer increased. Average concentrations of $Fc(MeOH)_2$ in solutions expelled from neat and gold modified gels are presented in Table 6.7.

Table 6.7

Concentration of $Fc(MeOH)_2$ in solution expelled from NIPA gels. Initial concentration of $Fc(MeOH)_2$ was 2 mM in 0 – 100 mM $LiClO_4$

% polymer	**[$Fc(MeOH)_2$], [mM]**
2	1.69
3	1.57
4	1.47
5	1.38
6	1.31

Results in Table 6.7 also show that the higher the concentration of the polymeric matrix the higher fraction of electroactive probe remains in collapsed gel after volume phase transition. This can be attributed to hydrophobic interactions and/or van derWaals interactions between $Fc(MeOH)_2$ and the NIPA polymeric network. [207]

$Fc(MeOH)_2$ in aqueous solution has an absorption band in the UV-vis range with a maximum absorbance at 430 nm. We used UV-vis spectroscopy to study the distribution of $Fc(MeOH)_2$ between the collapsed polymer phase and the released solution and to determine changes of its concentration as a result of the volume phase transition. The calibration plot was prepared using standard $Fc(MeOH)_2$ aqueous solution with the concentration range from 1 to 3 mM. Several spectra with sample calibration curve are shown in Figure 6.16. Neat NIPA and NIPA hydrogels containing 2.7 and 18 nm Au with various polymer concentrations (3 and 5%) were prepared. Each gel contained 2 mM $Fc(MeOH)_2$ and no $LiClO_4$. After the gel collapsed, the solution expelled from the gel was collected and the absorbance of that solution was measured. The concentrations of $Fc(MeOH)_2$ was determined based on the calibration plot and it was in good agreement with the ones calculated from the values of steady state currents.

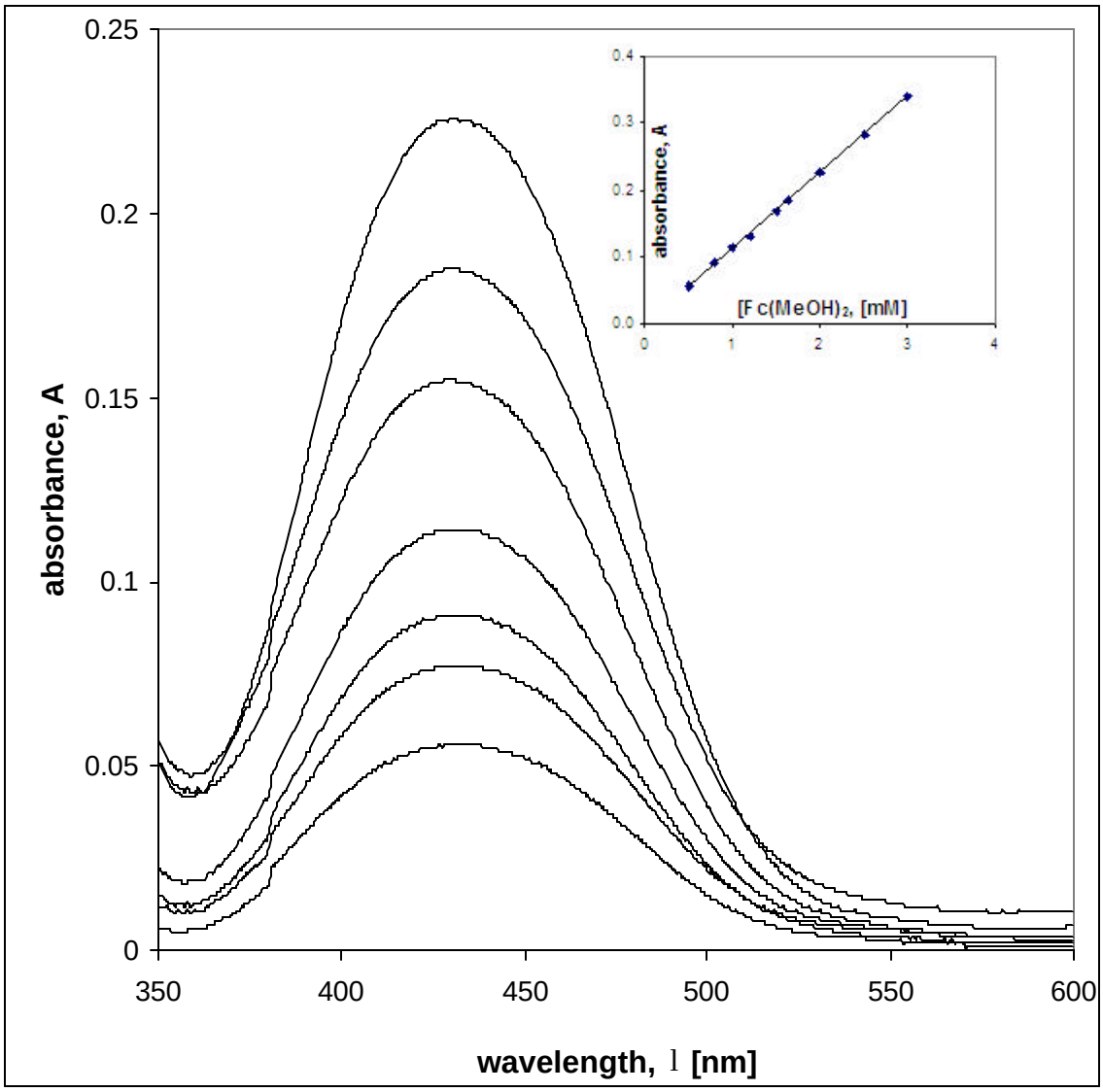

Figure 6.16. UV-vis spectra of $Fc(MeOH)_2$ in aqueous solution (Inset: Calibration curve).

The concentrations of $Fc(MeOH)_2$ in expelled solutions and the volumes of these solutions (~ 93% of initial volume) were used to determine distribution of $Fc(MeOH)_2$ probe between expelled solutions and collapsed gels. The mole fraction of electroactive probe calculated as $n_{\exp.sol.}^{Fc(MeOH)_2} / n_{in.sol.}^{Fc(MeOH)_2}$ and $n_{coll.gel.}^{Fc(MeOH)_2} / n_{in.sol.}^{Fc(MeOH)_2}$ is presented in Table 6.8. Since we have not noticed any significant effect from the gold nanoparticles, the values were averaged for neat gel and gels containing 2.7, 13 and 18 nm Au. As one can see the mole fraction of $Fc(MeOH)_2$ in collapsed gels is up to 4 times lower than in aqueous solutions. The volume of collapsed gel is up to 15 times smaller than expelled solution. With the assumption that the density of polymeric phase is close to that of aqueous solution, we estimated the concentration of probe in collapsed gel to be up to 6 times larger than that in the original swollen gel and up to 9 times higher than that in released liquid. This large difference indicates strong interaction between molecules of $Fc(MeOH)_2$ and the NIPA polymeric network. These might be due to hydrophobic interactions and/or van der Waals interactions. Much larger concentration of $Fc(MeOH)_2$ in collapsed gel compared to swollen gel means that the drop in the values of steady state current after the volume phase transition must be due to changes in diffusion coefficients. The estimated value of average diffusion coefficients, *D*, of $Fc(MeOH)_2$ in collapsed gels is $7.4 \cdot 10^{-9}$ cm^2/s and it is approximately 600 times lower than those in corresponding swollen gels.

Table 6.8

Average mole fraction of $Fc(MeOH)_2$ in expelled solutions and collapsed NIPA polymers

% gel	mole fraction	
	expelled solution	collapsed gel
2	0.80	0.20
3	0.74	0.26
4	0.69	0.31
5	0.65	0.35
6	0.60	0.40

The collapsed neat polymers and polymers containing 2.7, 13 and 18 nm gold nanoparticles were reswollen in water. The volume of water added was equal to the volume of the collected expelled solution so that the final volume of reswollen gel was identical with the initial one. We applied steady state voltammetry and the sample relationship of steady state limiting currents in reswollen NIPA gel modified with 13 nm Au and containing initial concentration of 0 – 100 mM $LiClO_4$, are shown in Figure 6.17. As one can see the values of steady state currents increase when the concentration of polymer in reswollen gels increases. It further confirms that more probe is retained in the matrix. Also for all analyzed samples the steady state currents were higher for the gels without supporting electrolyte. For the lowest, initial concentration of $LiClO_4$ in gels we observed small decrease in the values of the currents but then they increased with the increase of initial concentration of electrolyte. Table 6.9 shows estimated concentrations of $Fc(MeOH)_2$ in reswollen gels. Since we don't know what fraction of supporting electrolyte is retained in the matrix, we used the diffusion coefficients for 2 –6 % neat NIPA gels swollen in water without $LiClO_4$.

These results show that even after volume phase transition and reswelling, the probe retained in the gel is still electroactive. The average concentrations of $Fc(MeOH)_2$ in solution expelled from the collapsed gels (see Table 6.7) and reswollen gels (see Table 6.9) when added together yield the initial concentration of probe in gel before the volume phase transition. It means that the entire $Fc(MeOH)_2$ retained in polymer is available even after the volume phase transition. This fact is of big importance in sensing applications and drug delivery systems.

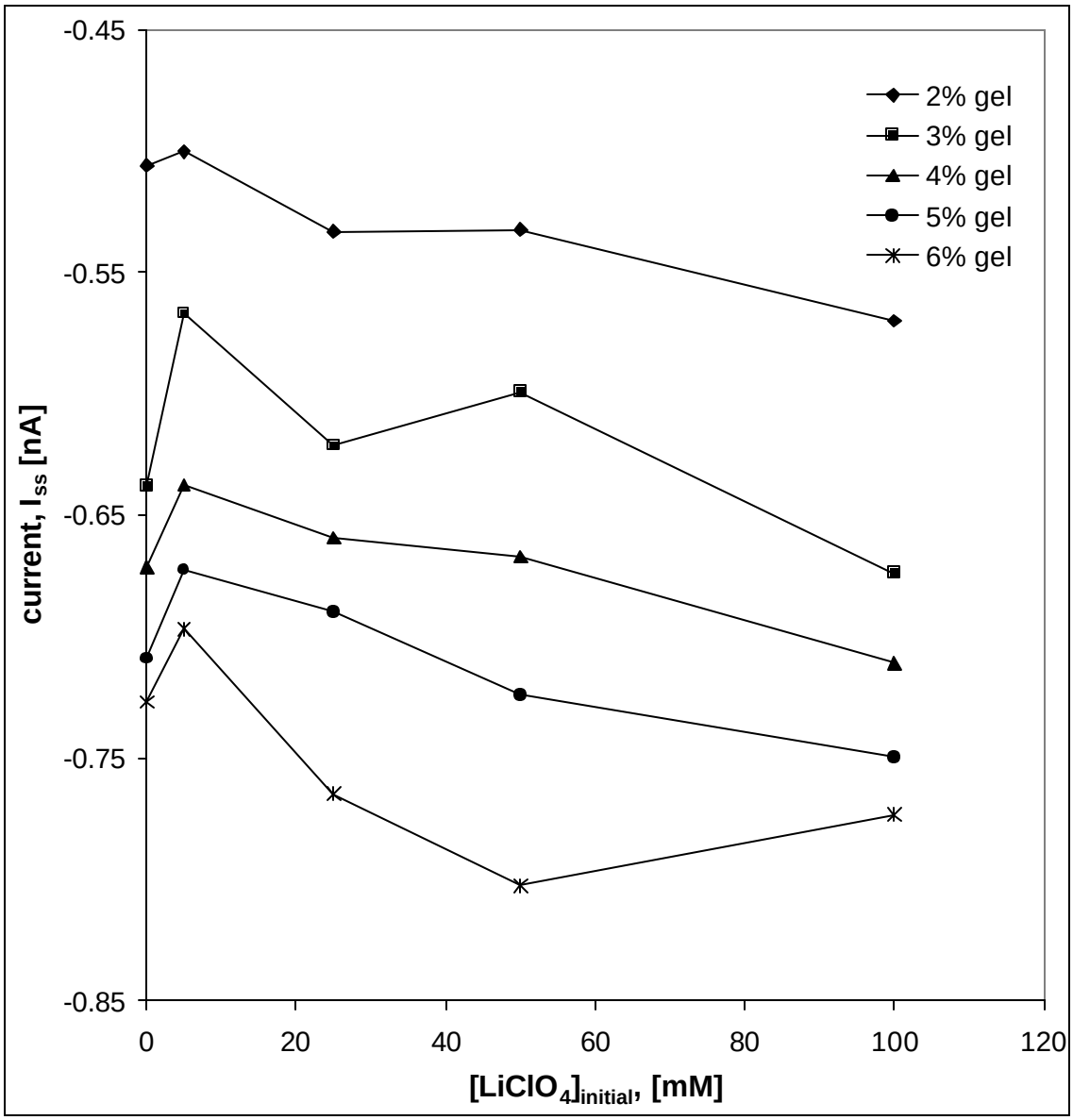

Figure 6.18. Steady state response of the oxidation of $Fc(MeOH)_2$ retained in reswollen 4% gels containing initially 0 – 100 mM $LiClO_4$.

Table 6.9

Estimated average concentration of $Fc(MeOH)_2$ in reswollen NIPA gels

% gel	**[$Fc(MeOH)_2$], [mM]**
2	0.38
3	0.50
4	0.55
5	0.61
6	0.65

VII. Discussion and Summary

Colloidal gold nanoparticles of 2.7, 13 and 18 nm in diameter were synthesized by chemical reduction of tetrachloroaurate, [$AuCl_4^-$], ions with sodium citrate and sodium borohydride $NaBH_4$. These colloid suspensions were used as a solvent for free radical polymerization of thermoresponsive *N*-isopropylacrylamide crosslinked hydrogel. The washing procedure based on collapsing-swelling cycles repeated several times showed that gold nanoparticles were not washed out with the impurities and they remained immobilized in polymeric matrix. Once the washing was completed the gel was dried, ground to a fine powder and as that used for the further analysis.

The preliminary characterization of gold-modified NIPA gels included UV-vis spectroscopy, transmission electron microscopy, TEM, analysis and determination of potential window of these new materials. The wavelengths of maximum absorbance for gold nanoparticles in aqueous sols were identical with literature values, that confirmed that the particles synthesized in this work had expected dimensions. We found that surface plasmon resonance for gold in NIPA gels is slightly shifted toward longer wavelengths comparing to the neat colloidal suspension. This can be explained by change of the dielectric constant of surrounding medium. However, the presence of polymeric matrix does not affect the properties of gold nanoparticles to absorb visible light. UV-vis analysis was used to monitor the stability of the gold in sols and gels. The wavelengths of maximum absorbance did not change significantly during the period of our studies. These new gel materials were stable over time (approximately 14 weeks). TEM images showed spherical, monodispersed particles with relatively narrow size distribution in both media, water and NIPA gel. Gold modified NIPA gels undergo a

discontinuous volume phase transition at temperature of 32.2 ± 0.4 °C and this temperature did not change with various concentrations of polymer. It was also independent of the presence of gold nanoparticles. This means that gold nanoparticles do not affect the hydrophilic/hydrophobic properties of the NIPA gel. It also means that gold does not participate in a crosslinkage of the polymer structure. The potential window was determined and it was between + 1.0 and – 1.0 V. In this potential range the colloidal gold in aqueous sol, in NIPA gel and the neat gel were electrochemically inactive. That means that there should not be any interference from gold or NIPA gel in our further experiments with electroactive probes.

Transport properties of gold modified NIPA gels were determined in terms of diffusion of 1,1'-ferrocenedimethanol, $Fc(MeOH)_2$, selected as an electroactive probe. This probe was introduced into the matrix thanks to the fact that even after dehydration the dry gel can be reswollen in many solutions or solvents. Steady state voltammetry on Pt-microdisk electrode was used to obtain oxidation currents of the probe in different media. All voltammograms were well defined and reproducible. The anodic response was not affected by the presence of gold or polymeric matrix. However, the diffusion coefficients calculated from the values of steady state currents were up to 30% lower than the one in aqueous solution. Also we found that the diffusion was faster for samples with gold. We believe that gold nanoparticles can additionally separate the polymeric chains what increases the free to diffuse volume. Other explanation is that presence of gold can reduce the hydration of NIPA chains.

To explain this decrease of D values for $Fc(MeOH_2)$ in gels we considered several possibilities. To make sure that the concentration of electroactive probe does not change

during the sample preparation we used chronoamperometry technique. Diffusion coefficients determined from the slope of the normalized current, I_t/I_{ss}, vs. $t^{-1/2}$ are concentration independent and they were in good agreement with the ones found from steady state voltammetry. However, these experiments were not reproducible, the relative standard deviation was almost 30%.

This decrease in diffusion coefficients of the probe in gels was not due to different viscosities of water and gel. Macroscopic viscosity of NIPA gel is always much larger. Using Stokes-Einstein equation one should find that diffusion coefficients in gels are 6 orders of magnitude smaller than in water whereas the values obtained in our experiments are all very close. Energies of activation for diffusion of $Fc(MeOH)_2$ in aqueous solution and in gels were found to be similar, 18.7 and 20.5 – 22.2 kJ/mol, respectively which suggests that the microscopic viscosity of gel and water must be also similar.

The "obstruction" and "hydration" effects were used to explain decrease in *D* values for $Fc(MeOH)_2$ in gels. Significant effect from water molecules that form hydration layers along the polymers was found. The values of hydration coefficient, *H*, were 4.0 and 4.4 for gold modified polymers and neat gels, respectively, which is larger than 1.667 for unhydrated polymer.

Effect of supporting electrolyte, $LiClO_4$, on diffusion of $Fc(MeOH)_2$ was determined. The preliminary studies showed that the presence of 100 mM electrolyte increased hydrophilicity of the gels, which results in the increase of the temperature of volume phase transition of the gels. Concentrations of electrolyte higher than 25 mM causes agglomeration of gold nanoparticles in sol. In gels gold particles were stable even at high concentration of electrolyte, up to 100 mM $LiClO_4$, that suggests no coagulation

between particles. This means that NIPA gel stabilizes gold nanoparticles better than Na_3-citrate. These observations were confirmed by UV-vis spectroscopy. Diffusion coefficients of electroactive probe in aqueous solutions containing different concentration of supporting electrolyte were determined from the values of steady state currents for the oxidation of $Fc(MeOH)_2$. As predicted by Stokes-Einstein equation, the diffusion coefficients decrease when the ionic strength of the system increases, which is connected to the increase in viscosity. Studies of diffusion of $Fc(MeOH)_2$ in neat and Au-modified gels in the presence of supporting electrolyte showed behavior similar to the one in aqueous solution. Generally the diffusion coefficients of electroactive probe in NIPA and NIPA-Au gels decrease when the concentrations of electrolyte increase at constant concentration of NIPA and NIPA-Au gels. The small decrease of the diffusion coefficient in polymeric gels compared to the solution without polymeric network can be explained by the "obstruction effect" and the "hydration effect". As one can see, the trend in the change of diffusion coefficient values of $Fc(MeOH)_2$ in both types of gel, neat and gold modified, was also similar. These similarities indicate that the electrochemical characteristics of the prepared gel are independent of the gold particles size.

After the gel collapsed up to 97% of solvent was expelled from the samples and the volume of expelled solution decreased for higher initial concentrations of polymer in the samples. Concentration of $Fc(MeOH)_2$ in all expelled solutions was calculated based on the values of steady state currents using D value for $Fc(MeOH)_2$ in aqueous solution. These concentrations were found to be 13 – 36% lower than initial concentration of electroactive probe. The concentrations of the probe in expelled solution determined

from steady state voltammetry were in good agreement with the results obtained from UV-vis spectroscopy. The values of steady state currents measured at Pt microelectrode in collapsed gels dropped almost to zero. This decrease was explained in terms of dramatic drop in diffusion coefficient, since the concentration of the probe in collapsed gel was up to 10 times larger. The diffusion coefficient of 1,1'-ferrocenedimethanol probe was estimated to be 600 times lower than in swollen phase.

In our experiments we showed that steady state voltammetry at Pt microelectrode can be successfully applied to determine the diffusion coefficients of electroactive probe in thermosensitive polymeric gels modified with colloidal gold nanoparticles. The knowledge of transport properties of these new materials is crucial for their potential applications as drug delivery systems. We also found that gold nanoparticles remain in the gel even after several shrinking-swelling steps. This is important for applications in the field of renewable sensors and biosensors.

REFERENCES

1. Daniel M.C., Astruc D.: *Chem. Rev.,* **2004**, 104, 293-346

2. Perez-Luna V., Aslan K., Betala P.: *Encyclopedia of Nanoscience And Nanotechnology,* Ed. H. S. Nalwa, Volume 2, 27-49

3. M. T. Franklin, K. J. Klabunde, in *High Energy Process in Organometallic Chemistry* (Ed.: K. S. Suslik), *Am. Chem. Soc.*, Washington D. C., **1987**, 246-259

4. Wesier H.B.: *"Inorganic Colloidal Chemistry"*, Wiley, New York, **1933**

5. Faraday M.: *Phil. Trans. Roy. Soc.* **1857**, 147, 145-181

6. Graham T.: *Phil. Trans. Roy. Soc.* **1861**, 151, 183-190

7. Ostwald W.: *Colloid-Zeitschrift,* **1907**, 1, 291-331

8. Wichterle O., Lim D.: *Nature*, **1960,** 185, 117-118

9. Dagani R.: *E&EN*, **1997**, June 9, 26-37

10. Dusek K., Patterson D.J.: *J. Poly. Sci. A-2,* **1968,** 6, 1209-1216

11. Flory P. J.: *J. Chem. Phys.*, **1949,** 17, 223-240

12. Kreibig U., Vollmer M.: *"Optical Properties of Metal Clusters"*, Springer (in Materials Science), (**1995**)

13. Shan J., Chen J., Nuopponen M., Viitala T., Jiang H., Peltonen J., Kauppinen E., Tenhu H.: *Lamgmuir,* **2006**, 22, 794-801

14. Buffat D.A., Bonel J.P.: *Phys. Rev. A,* **1976**, 13, 2289

15. Brust M., Kiely C.J.: *Colloids Surf. A: Physicochem. Eng. Asp.*, **2002**, 202, 175-186

16. Schmidt G., Baumle M., Geerkens M., Heim I., Osemann C., Sawitowski T.: *Chem. Soc. Rev.,* **1999**, 28, 179-185

17. Mulvaney P.: *Langmuir*, **1996**, 12, 788-800

18. Schmidt G.: *Chem. Rev.,* **1992**, 92, 1709-1727

19. Fukumi K., Chayahara A., Kadono K., Sakaguchi T., Horino Y., Miya M., Fujii K., Hayakawa J., Satou M.: *J. Appl. Phys.* **1994**, 75, 3075-3080

20. Elghanian R., Storhoff J.J., Mucic R.C., Letsinger R.L., Mirkin C.A.: *Science* **1997**, 277, 1078-1081

21. Andres R.P., Bielefeld J.D., Henderson J.I., Janes D.B., Kolagunta V.R., Kubiak C.P., Mahoney W.J., Osifchin R.G.: *Science*, **1996**, 273, 1690-1693

22. Brust M., Walker M., Bethell D., Schiffrin D.J., Whyman R.: *J. Chem. Soc. Chem. Commun*., **1994**, 801-802

23. Mirkin, C. A.; Letsinger, R. L.; Mucic, R. C.; Storhoff, J. J. *Nature* **1996**, *382*, 607-609

24. Grabar, K. C.; Smith, P. C.; Musick, M. D.; Davis, J. A.; Walter, D. G.; Jackson, M. A.; Guthrie, A. P.; Natan, M. J. *J. Am. Chem. Soc.* **1996**, *118*, 1148-1152

25. Larpent C., Brisse-Lemenn F., Patin H.: *New J. Chem.*, **1991**, *15*, 361-366

26. Boutonnet M., Kizling J., Touroude R., Maire G., Stenius p.: *Pure Appl. Catal.*, **1986**, 20, 163-177

27. Lewis L.N.: *J. Am. Chem. Soc*., **1990**, 112, 5998-6004

28. Haruta M. Kobayashi T. Yamada N.: *Chem. Lett.*, **1987**, 405-406

29. Yuan Y., Asakura K., Wan H., Tsai K., Iwasawa Y.: *Chem. Lett.*, **1996**, 9, 755-756

30. Kozlova P., Kozlov I., Sugiyama S., Matsui Y. Asakura K., Iwasawa Y.: *J. Catal.*, **1999**, 181, 37-48

31. Kulicke W.M., Nottelmann H.: "Polymers in Aqueous Media" – *Performance Through Association*, Glass, J. E., ed., American Chemical Society, Washington, D.C., pp.15-44, (**1989**)

32. Park H., Park K.: "Hydrogels and Biodegradable Polymers for Bioapplications", Ottenbrite, R. M., Huang, S. J., Park, K., eds., American Chemical Society, Washington, D.C., pp. 1-10, (**1996**)

33. Stauffer D., Coniglio A., Adam M.: *Adv. Polymer Sci*., **1982**, 44, 103-158

34. Park K., Shalaby W.S.W., Park H.: "Biodegradable Hydrogels for Drug Delivery", Technomic Publishing Company, Inc., Basel, pp. 1-12, 35-66, (**1993**)

35. Grosberg A.Y., Nechaev S.K.: *Macromolecules*, **1991**, 24, 2789-2793

36. Peppas N.A., Mikos A.G.: "Hydrogels in Medicine and Pharmacy"- *Fundamentals*, Peppas, N. A., ed., vol I, CRC Press, Inc., Florida, pp. 1-25, (**1986**)

37. Liu Q., Hedberg E.L., Liu Z., Bahulekar R., Meszlenyi R.K., Mikos A.G.: *Biomaterials*, **2000**, 21, 2163-2169

38. Barbieri R., Quaglia M., Delfini M., Brosio E.: *Polymer*, **1998**, 39, 1059-1066

39. Stammen J.A., Williams S., Ku D.N., Guldberg R.E.: *Biomaterials*, 2001, **22**, 799-806

40. Young R.J., Lovell P.A., "Introduction to Polymers", 2nd ed, Chapman & Hall, London, pp. 241-306, (**1991)**

41. Brazel C.S., Peppas N.A.: *Polymer*, **1999**, 40, 3383-3398

42. Zhang J., Peppas N.A.: *J. Biomater. Sci. Polymer Edn.*, **2002**, 13, 511-525

43. Tanaka T., Fillmore D.J., Sun S.T., Nishio I., Swislow G., Shah A.: *Phys. Rev. Lett.*, **1980**, 45, 1636-1639

44. Otake K., Inomato H., Konno M., Saito S.: *Macromolecules*, **1990**, 23, 283-289

45. Hirokawa Y., Tanaka T.: *J. Chem. Phys.*, **1984**, 81, 6379-6380

46. Hoffman A.S., Afrassiabi A., Dong L.C.: *J. Controlled Release*, **1986**, 4, 213-222

47. Annaka M., Motokawa K., Sasaki S., Kawasaki H., Maeda H., Amo Y., Tominaga Y.: *J. Chem. Phys.* **2000,** 14, 5980-5985

48. Barker I.C., Cowie J.M.G., Huckerby T.N., Shaw D.A., Soutar I, Swanson L.: *Macromolecules* **2003,** 36, 7765-7770

49. Reese C.E., Baltusavich M.E., Keim J.P., Asher S.A.: *Anal. Chem.*, **2001,** 73, 5038-5042

50. Inomata H., Nagahama K., Saito S.: *Macromolecules*, **1994**, 27, 6459-6464

51. Lowe J.S., Chowdhry B.Z, Parsonage J., Snowden M.J.: *Polymer*, **1998**, 39, 1207-1212

52. Akashi M., Nakano S., Kishida A.: *J. Polym. Sci. A*, **1996**, 34, 301-303

53. Suzuki A., Tanaka T.: *Nature*, **1990**, 346, 345-547

54. Zhu M.Q., Wang L.Q., Exarhos G.J., Li A.D.Q.: *J. Am. Chem. Soc.*, **2004**, 126, 2656-2657

55. Sershen S.R., Westcott S.L., West J.L., Halas N.J.: *J. Appl. Phys. B,* **2001**, 73, 379-381

56. Lones C.D., Lyon A.L.: *J. Am. Chem. Soc.,* **2003**, 125, 460-465

57. Casolaro M., Bottari S., Ito Y.: *Biomacromolecules,* **2006**, ASAP article

58. Hirotsu S.: *J. Phys. Soc. Jpn.,* **1987**, 56, 233-242

59. Amiya T., Hirokawa Y., Hirose Y., Li Y., Tanaka T.: *J. Chem. Phys.,* **1987**, 86, 2375-2379

60. Peppas N.A., Khare A.R.: *Adv. Drug Deliv. Rev.*, **1993**, 11, 1-35

61. Khare A.R., Peppas N.A.: *Biomaterials*, **1995**, 16, 559-567

62. Kim J.H., Lee R.T.: *Chem. Mater.,* **2004**, 16, 3647-3651

63. Brannon-Peppas L., Peppas N. A.: "Medical Plastics and Biomaterials Magazine", pp. 34-46, (**1997**)

64. Hedrick R.M., Mowry D.T., *Soil Sci.*, **1952**, 73, 427-441

65. Rosiak J.M., *J. Controlled Release*, **1994**, 31, 9-19

66. Wuelfing W.P., Gross S.M., Miles D.T., Murray R.W.: *J. Am. Chem. Soc.,* **1998**, 120, 12696-12697

67. Leff D.V., Ohara P.C., Heath J.R., Gelbart W.M.J.: *Phys. Chem.,* **1995**, 99, 7036-7041

68. Lee J., Sundar V.C., Heine J.R., Bawendi M.G., Jensen K.F.: *Adv. Mater.,* **2000**, 12, 1102-1105

69. Nath N., Chilkoti A.: *J. Am. Chem. Soc.*, **2001**, 123, 8197-8202

70. Manganey C., Ferrage F., Aujard I., Marchi-Artzner V., Jullien L., Ouari O., Rekai E.D., Laschewsky A., Vikholm I., Sadowski J.: *J. Am. Chem. Soc.*, **2002**, 124, 5811-5821

71. *Metal Vapour Synthesis* (Eds.: J. R. Blackborow, D. Young), Springer Verlag, New York 1979

72. Henglein A., Meisel D.: *Langmuir,* **1998**, 14, 7392-7396

73. Shimizu T., Teranishi T., Hasegawa S., Miyake M.: *J. Phys. Chem. B,* **2003**, 107, 2719-2724

74. a) Scaffardi L.B., Pellegri N., de Sanctis O., Tocho J.O.: *Nanotechnology*, **2005**, 16, 158-163

b) Mohamed M.B., Ahmadi T.S., Link S., Braun M., El-Sayed M.A.:*Chem. Phys. Lett.*, **2001**, 343, 55-63

75. Niidome Y., Hori A., Sato T., Yamada S.: *Chem. Lett.*, **2000**, 310-311

76. Takami A., Kurita H., Koda S.: *J. Phys. Chem. B*, **1999**, 103, 1226-1232

77. Turkevitch, J.; Stevenson, P. C.; Hillier, J.: *Discuss. Faraday Soc*. **1951**, 11, 55-75

78. Grabar K.C., Allison K.J., Baker B. E., Bright R. M., Brown K.R., Freeman R. G., Fox A. P., Keating C. D., Musick M. D., Natan M. J.: *Langmuir* **1999,** 12, 2353-2361

79. Grabar K.C., Freeman R. G., Hommer M. B., Natan M. J.: *Anal. Chem.* **1995,** 67, 735-743

80. Ingram R.S., Hostetler M.J., Murray R.W., Schaaff T.G., Khoury J.T., Whetten R.L., Bigioni T.P., Guthrie D.K., First P.N.: *J. Am. Chem.Soc.*, **1997**, 119, 9279-9280

81. Frens, G.: *Nature: Phys. Sci.* **1973**, *241*, 20-22

82. Hayat M.A., Ed., *"Colloidal Gold: Principles, Methods, and Applications", Vols. 1,2 and 3.* Academic Press, San Diego, **1989**

83. He J.A., Valluzzi K.Y., Dolukhanyan C.S., Kumar J., Tripatrhy S.K., Samuelson L., Balogh L, Tomalia D.A.; *Chem. Mater.*, **1999**, 11, 3268-3274

84. Bharathi S., Lev O.: *Chem. Commun*., **1997**, 23, 2303-2304

85. Elliot D.J., Furlong D.N., Grieser F., Mulvaney P., Giersig M.: *Coll. Surf. A*, **1997**, 129-130, 141-150

86. Brown K.B., Walter D.G., Natan M.J.: *Chem. Mater.*, **2000**, 12, 306-313

87. Brown K.B., Lyon L.A., Fox P.A., Reiss B.D., Natan M.J.: *Chem. Mater.*, **2000**, 12, 314-323

88. Goia D.V., Matijevic E.: *Coll. Surf. A*, **1999**, 146, 139-15

89. Gorelikov I., Field L.M., Kumacheva E.: *J. Am. Chem Soc.*, **2004**, 15938-15939

90. Hirai H.: *J. Macromol. Sci.-Chem. A*, **1979**, 13, 633-649

91. Han L., Luo J., Kariuki N.N., Maye M.M., Jones V.W., Zhong C.J.: *Chem. Mater.,* **2002**, 124, 13988-13989

92. Rowe M.P., Plass K.E., Kim K., Kurdak C., Zellers E.T., Matzger A.J.: *Chem. Mater.* **2004,** 16, 3513-3517

93. Hostetler M.J., Wingate J.E., Zhong C.J, Harris J.E., Vachet R.W., Clark M.R., Londono J.D., Green S.J., Stokes J.J., Wignale G.D., Glish G.L., Porter M.D., Evans N.D., Murray R.W.: *Langmuir,* **1998**, 14, 17-30

94. Hostetler M.J., Green S.J., Stokes, J.J., Murray R.W.: *J. Am. Chem. Soc.* **1996**, 118, 4212-4213

95. Ingram R.S., Hostetler M.J., Murray R.W.: *J. Am. Chem. Soc.* **1997**, 119, 9175-9178

96. Templeton A.C., Wuelfing W. P., Murray R. W.: *Acc. Chem. Res.* **2000**, 33, 27-36

97. Templeton, A. C.; Hostetler, M. J.; Kraft, C. T.; Murray, R.W.: *J. Am. Chem. Soc.* **1998**, 120, 1906-1911. (b) Hostetler, M. J.; Templeton, A. C.; Murray, R. W.: *Langmuir* **1999**, 15, 3782-3789

98. Terril R.H., Postlethwaite T.A., Chen C., Poon C., Terzis A., Chen A., Hutchison J.E., Clark M.R., Wignall G.: *J. Am. Chem. Soc.*, **1995**, 117, 12537-12548

99. Schaaff T.G., Knight G., Shafigullin M.N., Borkman R.F., Whetten R.L.: *J. Phys. Chem. B,* **1998**, 102, 10643-10646

100. Brust M., Fink J., Bethell D., Schriffrin D.J., Kiely C.: *J. Chem. Soc., Chem. Commun.,* **1995**, 16, 1655-1656

101. Johnson S.R., Evans S.D., Mahon S.W., Ulman A.: *Langmuir*, **1997**, 13, 51-57

102. Chen S., Murray R.W.: *Langmuir*, **1999**, 15, 682-689

103. Buining P.A., Humbel B.M., Philipse A.P., Verkleij A.J.: *Langmuir,* **1997**, 13, 3921-3926

104. Hostetler M.J., Templeton A.C., Murray R.W.: *Langmuir,* **1999**, 15, 3782-3789

105. Schmid G., Klein N., Korste L., Kreibig U, Schönauer D.: *Polyhedron* **1988**, *7*, 605-608

106. Green S.J., Stokes J.J., Hostetler M.J., Pietron J., Murray R.W.: *J. Phys. Chem. B,* **1997**, 101, 2663-2668

107. Tzhayik O., Sawant P., Efrima S., Kovalev E., Klug J.T.: *Langmuir*, **2002**, 18, 3364-3369

108. Porter L.A., Jr., Ji D., Westcott S.L., Graupe M., Czernuszewicz R.S., Halas N.J., Lee T.R.: *Langmuir*, **1998**, 14, 7378-7386

109. Yonezawa T., Yasui K., Kimizuka N.: *Langmuir*, **2001**, 17, 271-273

110. Manna A., Chen P.-L., Akiyama H., Wei T.-X., Tamada K., Knoll W.: *Chem. Mater.*, **2003**, 15, 20-28

111. Resch, R.; Baur, C.; Bugacov, A.; Koel, B. E.; Echternach, P. M.; Madhukar, A.; Montoya, N.; Requicha, A. A. G.; Will, P.: *J. Phys. Chem. B* **1999**, *103*, 3647-3650

112. Félidj, N.; Aubard, J.; Lévi, G.; Krenn, J. R.; Hohenau, A.; Schider, G.; Leitner, A.; Aussenegg, F. R.: *Appl. Phys. Lett.* **2003**, *82*, 3095-3097

113. Balasubramanian, R.; Kim, B.; Tripp, S. L.; Wang, X.; Lieberman, M.; Wei, A.: *Langmuir* **2002**, *18*, 3676-3681

114. Spatz J.P., Mossmer S., Moller M.: *Chem.-Eur.J.* **1996**, *12*, 1552-1555

115. Spatz J.P., Mossmer S., Moller M.: *Angew. Chem., Int. Ed. Engl*. **1996**, *35*, 1510-1512

116. *Immuno-Gold Electron Microscopy in Virus Diagnosis and Research*; Hyatt, A. D., Eaton, B. T., Eds.; CRC Press: Boca Raton, FL, 1993.

117. Spatz J.P., Roescher A., Moller M.: *Adv. Mater*. **1996**, *8*, 337-340

118. Bronstein L.M., Chernyshov D.M., Timofeeva G.I., Dubrovina L.V., Valetsky P.M., Obolonkova E.S., Khokhlov A.R.: *Langmuir* **2000**, *16*, 3626-3632

119. Sohn B.-H., Seo B.-W., Yoo S.-I.: *J. Mater. Chem.* **2002**, *12*, 1730-1734

120. Youk J.H., Park M.K., Locklin J., Advincula R., Yang J., Mays J.: *Langmuir* **2002**, *18*, 2455-2458

121. Otsuka H., Akiyama Y., Nagasaki Y., Kataoka K.: *J. Am. Chem. Soc*. **2001**, *123*, 8226-8230

122. Lowe A.B., Sumerlin B.S., Donovan M.S., McCormick C.L.: *J. Am. Chem. Soc.*, **2002**, 124, 11562-11563

123. Walker C.H., St. John J.V., Wisian-Neilson P.: . *Am. Chem. Soc.*, **2001,** 123, 3846-3847

124. Watkins J.J., McCarthy T.J., *Chem. Mater.*, **1995**, 7, 1991-1994

125. Sayo K., Deki S., Hayashi S.: *Eur. Phys. J. D,* **1999**, 9, 429-432

126. Jordan R., West N., Ulman A., Chou Y-M. Nuyken O.: *Macromolecules,* **2001**, 34, 1606-1611

127. Mandal T.K., Fleming M.S., Walt D.R.: *Nano Lett.,* **2002**, 2, 3-7

128. Ohno K., Koh K., Tsujii Y., Fukuda T.: *Macromolecules,* **2002**, 35, 8989-8993

129. Williams M.E., Masui H., Long J.W., Malik J., Murray R.W.J.: J. *Am. Chem. Soc.*, **1997**, 119, 11510-11515

130. Lowe A.B., Brent S., Sumerlin S., Donovan S., McCormick C.L.: *J. Am. Chem. Soc.,* **2002**, 124, 11562-11563

131. Teranishi T., Kiyokawa I., Miyake M.: *Adv. Mater.,* **1998**, 10, 596-599

132. Corbierre M.K., Cameron N.S., Sutton M., Mochrie S.G.J., Lurio L.B., Ruhm A., Lennox R.B., *J. Am. Chem. Soc.,* **2001**, 123, 10411-10412

133. a) Wang C., Flynn N.T., Langer R.: *Adv. Mater.,* **2004**, 16, 1074-1079

b) Wang C., Flynn N.T., Langer R.: *Mat. Res. Soc. Symp. Proc.,* **2004**, 820, 333-338

134. Pardo-Yissar V., Gabai R., Shipway A.N., Bourenko T., Willner I.: *Adv. Mater.,* **2001**, 13, 1320-1323

135. Keoshkerian B., Georges M.K., Qinlan M., Veregin R.P.N., Goodbroad B.: *Macromolecules,* **1998**, 31, 7559–7561

136. Wang J.S., Matyjaszewski K.: *Macromolecules,* **1995**, 23, 7901-7910

137. Chiefari Y., Chong Y.K., Ercole K., Krstina J., Jeffery J., Le T.P.T.: *Macromolecules,* **1998**, 31, 5559–5562

138. Convertine A.J., Ayres N., Scales C.W., Lowe A.B., McCornik C.: *Biomacromolecules,* **2004**, 5, 1177-1180

139. Donovan M. S., Lowe, A.B., Sumerlin B.S., McCormick C.L.: *Macromolecules* **2002**, 35, 4123-4123

140. Hawker C.J., Bosman A.W., Harth E.: *Chem. Rev*. **2001**, 101, 3661-3688

141. Stenzel M.H., Barner-Kowollik C., Davis T.P., Dalton H.: *Macromol. Biosci.,* **2004**, 4, 445-453

142. Mandal T.K., Fleming M.S., Walt D.R.: *Chem. Mater.,* **2000**, 12, 3481-3487

143. Watson K.J., Zhu J., Nguyen S.T., Mirkin C.A.: *J. Am. Chem. Soc.,* **1999**, 121, 462-463

144. Nuss S., Botcher H., Wurm H., Hallensleben M.L.: *Angew. Chem. Int. Ed.,* **2001**, 40, 4016-4018

145. Raula J., Shan J., Nuopponen M., Niskanen A., Jiang H, Kauppinen E.I., Tenhu H.: *Langmuir,* **2003**, 19, 3499-3504

146. Kim D.J., Kang S.M., Kong B., Kim W.J., Paik H., Choi H., Choi I.S.: *Macromol. Chem. Phys.,* **2005**, 206, 1941-1946

147. Mie G.: *Annalen der Physik*, **1908**, 25, 377-445

148. D. L. FeldheimJ. C. A. Foss, *Metal nanoparticles : synthesis, characterization, and applications*. 2002, Marcel Dekker, Inc.

149. Storhoff J.J, et al.: *Am Chem Soc*, **2000**, 122 (19), 4640-4650

150. Mackowski D.W., Mishchenko M.I.: J. *Opt. Soc. Am. A*, **1996,** 13, 2266-2278

151. Johnston R.L.: *Atomic andMolecular Clusters;* Taylor & Francis: London, **2002**

152. Srivastava S., Frankamp B.L., Rotello V.M.: *Chem. Mater.,* **2005**, 17, 487-490

153. Anija M., Thomas J., Singh N., Nair A.S., Tom R.T., Pradeep T., Philip R.: *Chem. Phys. Lett.,* **2003**, 380, 223-229

154. Sun W., Dai Q., Worden J.G., Huo Q.: *J. Phys. Chem. B,* **2005**, 109, 20854-20857

155. Suzuki D., Kawaguchi H.: *Langmuir,* **2005**, 21, 8175-8179

156. Feil H., Bae Y.H., Feijan J., Kim S.W.: *Macromolecules* **1993**, 26, 2496-2500

157. Katchalsky A., Lifson S., Eisenberg H.: *J. Polym. Sci.,* **1951**, 7, 571-574

158. Kawasaki H., Sasaki S., Maeda H.: *J. Phys. Chem. B,* **1997**, 101, 5089-5093

159. Lee J.W., Kim S.Y., Kim S.S., Lee Y.M., Lee K.H., Kim S.J.: *J. Appl. Polym. Sci.,* **1999**, 73, 113-120

160. Bae Y.H., Okano T., Kim S.W.: *J. Controlled Release,* **1989**, 9, 271-279

161. Bae Y.H., Okano T., Hsu R., Kim S.W.: *Makromol. Chem. Rapid Commun.* **1987**, 8, 481-485

162. Snowden M.J., Murray M.J., Chowdary B.Z.: *Chem. Ind.* **1996**, 14, 531-534

163. Hoffman A.: *J. Controlled Release* **1987**, 6, 297-305

164. Tanaka T., Fillmore D.J.: *J. Chem. Phys.* **1979**, 70, 1214-1218

165. Tanaka T., Hocker L.O., Benedek G.B.: *J. Chem. Phys.*, **1973**, 59, 5151-5159

166. Pelton R.H., Chibante P.: *Colloid Surf.*, **1986**, 20, 247-256

167. Daly E., Saunders B.: *Langmuir*, **2000**, 16, 5546-5552

168. Shibayama M., Uesaka M., Shiwa Y.: *J. Chem. Phys.* **1996**, 105, 4350-4357

169. Li Y., Tanaka T.J.: *J. Chem. Phys.*, **1989**, 90, 5161-5166

170. Hirose H., Shibayama M.: *Macromolecules*, **1998**, 31(16), 5336 –5342

171. Shibayama M., Tanaka T., Han C.C.: *J. Chem. Phys.*, **1992**, 97, 6829-6841

172. Shibayama M., Suetoh Y., Nomura S.: *Macromolecules*, **1996**, 29, 6966-6968

173. Binkert T., Oberreich J., Meewes M., Nyffenegger R., Ricka J.: *Macromolecules*, **1991**, 24, 5806-5810

174. Shan J., Chen J., Nuopponen M., Tenhu H.: *Langmuir*, **2004**, 20, 4671-4676

175. Hirsch L.R., Jackson J.B., Lee A., Halas N.J., West J.L.: *Anal. Chem.*, **2003**, 75, 2377-2381

176. Peppas N.A., Huang Y., Torres-Lugo M., Ward J.H., Zhang J.: *Annu. Rev. Biomed. Eng.*, **2000**, 2, 9-29

177. Holtz J.H., Asher S.A.: *Nature*, **1997**, 389, 829-832

178. Matsui J., Akamatsu K., Hara N., Miyoshi D., Nawafune H., Tamaki K., Sugimoto N.: *Anal. Chem.*, **2005**, 77, 4282 –4285,

179. Matsui J., Akamatsu K., Nishiguchi S., Miyoshi D., Nawafune H., Tamaki K., Sugimoto N.: *Anal. Chem.*, **2004**, 76, 1310-1315

180. Sershen S.R., Westcott S.L., Halas N.J., West J.L.: *J. Biomed. Mat. Res.*, **2000**, 51, 293-298

181. Cannon D.M., Kuo T.C., Bohn P.W., Sweedler J.V.: *Anal. Chem.*, **2003**, 75, 2224-2230

182. Zhao B., Moore J.S.: *Langmuir*, **2001**, 17, 4758-4763

183. Zhu M.Q., Wang L.Q., Exarhos G.J., Li A.D.Q.: *J. Am. Chem. Soc.*, **2004**, 126, 2656-2657

184. Kanazawa H., Kashiwase K., Yamamoto Y., Matsushima A., Kikuchi Y., Sakurari Y., Okano T.: *Anal. Chem.*, **1997**, 69, 823-830

185. Li C., Gunari N., Fischer K., Janshoff A., Schmidt M.: *Angew. Chem. Int. Ed.*, **2004**, 43, 1101-1104

186. Tatistcheff H.B., Fritsch-Faules I., Wrighton M.S.: *J. Phys. Chem*., **1993**, 97, 2732-2739

187. Bard A.J., Faulkner L.R.: *Electrochemical Methods: Fundamentals and Applications*, 2nd Ed., John Wiley & Sons, Inc. **2001**

188. Scoog D.A., Holler F.J., Nieman T.A.: *Principles of Instrumental Analysis*, Saunders College Publishing, Ed. 5th

189. Ciszkowska M., Donten M., Stojek Z.: *Anal. Chem.*, **1994**, 66, 4112-4115

190. Aoki K., Osteryoung J.: *J. Electroanal. Chem.*, **1981**, 122, 19-35

191. Shoup D., Szabo A.: *J. Elecroanal. Chem.*, **1982**, 140, 237-245

192. Denuault G., Mirkin V.M., Bard J.A.: *J. Elecroanal. Chem.*, **1991**, 308, 27-38

193. Hyk W., Ciszkowska M.: *J. Phys. Chem*., **1999**, 103, 6466-6474

194. Fan F.R.F.: *J. Phys. Chem. B*, **1998**, 102, 9777-9782

195. Shan J., Nuopponen M., Jiang H., Kauppinen E., Tenhu H.: *Macromolecules*, **2003**, 36, 4533-4542

196. Jones C.D., Lyon A.: *J. Am. Chem. Soc.*, **2003**, 125, 460-465

197. Wang X., Wu C.: *Macromolecules*, **1999**, 32, 4299-4301

198. Kawasaki H., Sasaki S., Maeda H.: *Langmuir*, **1998**, 14, 773-776

199. Mylonas Y., Stailcos G., Lianos P.: *Langmuir*, **1999**, 15, 7172-7175

200. Li D., Zhang Y., Jiang J., Li J.: *J. Col. Iterf. Scie.*, **2003**, 264, 109-113

201. Kooij E.S., Brouwer E.A.M., Wormeester H., Poelsema B.: *Langmuir*, **2002**, 18, 7677-7682

202. Jimenez V.L., Georganopoulou D.G., White R.J., Harper A.S., Mills A.J., Lee D., Murray R.W.: *Langmuir*, **2004**, 20, 6864-6870

203. Petrovic S.C., Zhang W., Ciszkowska M.: *Anal. Chem.*, **2000,** 72, 3449-3454

204. Bloemer M.J., Haus J.W., Ashley P.R.: *J. Opt. Soc. Am. B*, **1990**, 7, 790-795

205. Zhang W., Ma C., Ciszkowska M.: *J. Phys. Chem. B,* **2001**, *105,* 3435-3440.

206. Zhang W., Gaberman I., Ciszkowska M.: *Electroanalysis,* **2003**, *15,* 409-413

207. Goia D.V., Matijevic E.: *Colloids and Surfaces*, **1999**, *146,* 139-152

208. Frens F.: *Nature,* **1973**, *241*, 20-22

209. Anderson M.L., Morris C.A.: *Langmuir,* **1999,** *15*, 774-779

210. Brown K.B.: *Chem. Mater.,* **2000**, 12, 306-313

211. Akamatsu K., Deki S.: *J. Mater. Chem.,* **1997**, *7*, 1773-1777

212. Dokoutchaev A., James J.T., Koene S.C., Pathak S., Prakash G.K.S., Thompson M.E.: *Chem. Mater.,* **1999,** *11,* 2389-2399

213. Kazimierska E., Ciszkowska M.: *Electroanalysis*, **2005**, 17, 1384-1395

214. Jacob S.R., Hong Q., Coles B.A., Compton R. G.: *J. Phys. Chem. B,* **1999**, 103, 2963-2969

215. Wang J.H.: *J. Amer. Chem. Soc.*, **1947**, 76, 4755-4763

216. Lee H.B., Jhon M.S., Andrade J.D.: *J. Colloid Interface Sci.,* **1975**, 51, 225-231

217. Cheever E., Blum F.D., Foster K.R., Mackay R.A.: *J. Colloid Interface Sci.,* **1985**, 104, 121-129

218. Duval P.F., Porion P., Damme V.H.: *J. Phys. Chem. B,* **1999**, 103, 5730-5735

219. Von Meerwall E., Mahoney D., Iannacchine G.: *J. Colloid Interface Sci.,* **1990**, 139, 437-445